Low Energy Consequences of Some Non-standard Higgs Models

David Ian Thompson
Department of Physics and Astronomy

Presented as a thesis for the degree of Ph.D.

Abstract

Little Higgs models offer an innovative solution of the naturalness problem of the Standard Model. These models contain new particles which cancel the quadratic divergences in the Higgs mass caused by the top, gauge and Higgs loops. These new particles contribute to loop induced interactions of the Higgs boson. The loop induced decays of the Higgs $H \to gg$ and $H \to \gamma\gamma$ are examined in two Little Higgs models - the Littlest Higgs Model and the Schmaltz Model. The production of Higgs pairs from gluon fusion, which proceeds via heavy quark loops, is also examined in these models.

Another idea considered is the multiple point principle (MPP) applied to the two Higgs doublet extension of the Standard Model. The MPP stipulates that the coupling constants will be tuned to allow the existence of a maximal number of degenerate vacua. This principle is shown to lead to a Peccei-Quinn type symmetry which naturally suppresses phenomenologically dangerous flavour changing neutral currents. Quasi-fixed points of the renormalization group are then used to derive predictions for the Higgs masses and couplings.

Acknowledgement

I'd like to thank my supervisor, Colin Froggatt, for all his support and patience over the last few years. Special thanks also go to Andrew Davis who taught me quantum field theory and to David Sutherland for his help and advice.

I'm also grateful to all the rest of the staff who have helped me out over the years. In particular, David Miller, John Campbell, Roman Nevzorov and Kit Wong.

A mention also for those who shared my fate as PPT graduate students during my time in the group. The old (Peter Allan, Greig Cowan, Jack Cheyne, Ian Allison) and the new (Peter Athron, Luo Rui, Dan Guise, Iain Kendall). They... well... they were there.

I'm grateful to my collaborators Thomas Binoth and Stefan Karg. I enjoyed working with them very much.

Thanks go to all my friends. Too many to mention them all, but couldn't go without mentioning Niall and Kipper who put up with me as a flatmate.

Thanks also to my family - Mum, Dad, Amanda, Dawn and Danny - for all their love and support.

And, most of all, thanks to my wonderful wife Helen for her love, help and encouragement.

Declaration

I declare that none of the material presented in this thesis has previously been presented for a degree at this or any other university.

The material in chapters 1, 2 and 3 is mainly composed of background material drawn from references as stated. However, I found some mistakes in the literature and these are pointed out in chapter 2. Chapter 3 also contains some original work where mixing angles and couplings are calculated. Chapters 4, 5, 6 and 7 are my work except where stated otherwise. The work in chapter 5 was performed in collaboration with Stefan Karg and Thomas Binoth and the work in chapters 6 and 7 was performed in collaboration with Colin Froggatt, Roman Nevzorov and Holger Nielsen and is published in the paper [1].

Contents

1 Introduction **7**
- 1.1 Little Higgs Models . . . 7
  - 1.1.1 The Hierarchy Problem . . . 7
  - 1.1.2 Little Higgs Models . . . 9
  - 1.1.3 Survey Of Little Higgs Models . . . 15
- 1.2 The Multiple Point Principle . . . 16
  - 1.2.1 The Multiple Point Principle . . . 16
  - 1.2.2 Two Higgs-doublet Models . . . 17

2 The Littlest Higgs Model **19**
- 2.1 Overview of the Littlest Higgs Model . . . 19
- 2.2 Scalar Kinetic Terms . . . 20
- 2.3 Fermion-Scalar Interactions . . . 22
- 2.4 Electroweak Symmetry Breaking . . . 23
  - 2.4.1 Gauge boson masses and mixing . . . 26
  - 2.4.2 The top sector . . . 27
- 2.5 Higgs Couplings . . . 28
  - 2.5.1 W-Higgs Couplings . . . 28
  - 2.5.2 Top-Higgs Couplings . . . 29
  - 2.5.3 Scalar Trilinear Couplings . . . 30
- 2.6 Muon Decay and the Fermi Constant . . . 32
- 2.7 Electroweak Precision Constraints . . . 34

3 The Schmaltz Model **36**
- 3.1 Overview of the Schmaltz Model . . . 36
- 3.2 Scalar Kinetic Terms . . . 37
- 3.3 Fermion-Scalar Interactions . . . 38
  - 3.3.1 Model I . . . 38
  - 3.3.2 Model II . . . 40
  - 3.3.3 The Top Sector . . . 40
- 3.4 Electroweak Symmetry Breaking . . . 41
  - 3.4.1 Gauge Boson Masses And Mixing . . . 43
  - 3.4.2 The Top Sector . . . 44
- 3.5 Higgs Couplings . . . 45
  - 3.5.1 W-Higgs Couplings . . . 45
  - 3.5.2 Top-Higgs Couplings . . . 46
- 3.6 Muon Decay and the Fermi Constant . . . 47
- 3.7 Electroweak Precision Constraints . . . 48

4 Loop Induced Decays of Little Higgs **49**
4.1 Loop Induced Decays in the Littlest Higgs Model 53
4.1.1 Higgs Decay To Gluons 55
4.1.2 Higgs Decay To Photons 58
4.2 Loop Induced Decays in the Schmaltz Model 61
4.2.1 Higgs Decay To Gluons 62
4.2.2 Higgs Decays To Photons 65
4.3 Prospects For Observation 66

5 Two Higgs Production Via Gluon Fusion **70**
5.1 Higgs Pair Production 70
5.2 The Program: General Outline 71
5.3 Tensor Integral Reduction Algorithm 73
5.4 Spinor Helicity Methods 76
5.4.1 Introduction And Notation 76
5.4.2 Spinor Representation Of Polarization Vectors 77
5.5 The Standard Model Case 79
5.6 The Littlest Higgs Model Case 81
5.7 The Schmaltz Model Case 88
5.8 Prospects For Observation 91

6 The 2HDM and the Multiple Point Principle **95**
6.1 The Scalar Potential 95
6.2 Yukawa Couplings 98

7 2HDM Phenomenology **102**
7.1 Quasi-Fixed Point in 2HDM 102
7.2 Yukawa Couplings 102
7.2.1 QFP Solutions At Low-Moderate $\tan\beta$ 102
7.2.2 QFP Solutions At Large $\tan\beta$ 106
7.3 Higgs Self Couplings 108
7.4 Higgs Masses 111
7.5 Higgs Couplings 116

8 Summary and Conclusions **122**

List of Figures

1.1 Higgs with a top loop. 8
1.2 Higgs with a gauge boson loop. 8
1.3 Higgs with loop from quartic self-coupling. 8
1.4 Quadratically divergent gauge loop contributing to Φ_i potential. 12
1.5 Logarithmically divergent gauge loop contributing to Φ_i potential. . . . 13
1.6 Diagrams contributing to quadratically divergent Higgs mass. 14

2.1 Integrating out the W leads to an effective four fermion vertex. 33

4.1 The Higgs can decay to a pair of gluons via a quark loop. 49
4.2 Higgs decay to photons 49
4.3 The scalar loop function 52
4.4 The fermion loop function $F_1/2$ and its asymptotic value. 52
4.5 The vector loop function F_1. 53
4.6 Little Higgs enhancement vs f (gluons) 56
4.7 Little Higgs enhancement vs x (gluons) 56
4.8 Little Higgs enhancement vs c_t (gluons) 57
4.9 Little Higgs enhancement vs M_H (gluons) 57
4.10 Little Higgs enhancement vs f (photons) 59
4.11 Little Higgs enhancement vs x (photons) 59
4.12 Little Higgs enhancement vs c (photons) 60
4.13 Little Higgs enhancement vs M_H (photons) 60
4.14 Little Higgs enhancement vs c_t (photons) 61
4.15 Schmaltz model enhancement vs $\tan\beta$ (gluons) 63
4.16 Schmaltz model enhancement vs f (gluons) 64
4.17 Schmaltz model enhancement vs k (gluons) 64
4.18 Schmaltz model enhancement vs M_H (gluons) 65
4.19 Schmaltz model enhancement vs $\tan\beta$ (photons) 66
4.20 Schmaltz model enhancement vs f (gluons) 67
4.21 Schmaltz model enhancement vs k (gluons) 67
4.22 Schmaltz model enhancement vs M_H (gluons) 68

5.1 Higgs pair production via gluon fusion, triangle topology. 70
5.2 Higgs pair production via gluon fusion, box topology. 70
5.3 A generic loop diagram with m external legs 73
5.4 A triangle loop diagram 74
5.5 SM cross section vs Higgs mass for $PP \to HH$ 80
5.6 SM cross section vs factorisation scale for $PP \to HH$ 80
5.7 Box topology 81

5.8 Triangle topology . . . 82
5.9 Box topology with tTH couplings . . . 82
5.10 Triangle topology with dimension 5 vertex . . . 82
5.11 Triangle topology with intermediate Φ scalar . . . 83
5.12 LH $PP \to HH$ cross section vs M_H . . . 84
5.13 LH enhancement of cross section vs M_H . . . 85
5.14 LH $PP \to HH$ cross section vs f . . . 85
5.15 LH enhancement of cross section vs f . . . 86
5.16 LH $PP \to HH$ cross section vs k . . . 86
5.17 LH $PP \to HH$ enhancement vs k . . . 87
5.18 LH $PP \to HH$ cross section vs x . . . 87
5.19 LH $PP \to HH$ enhancement vs x . . . 88
5.20 Schmaltz $PP \to HH$ cross section vs M_H . . . 89
5.21 Schmaltz $PP \to HH$ enhancement vs M_H . . . 90
5.22 Schmaltz $PP \to HH$ cross section vs f . . . 90
5.23 Schmaltz $PP \to HH$ enhancement vs f . . . 91
5.24 Schmaltz $PP \to HH$ cross section vs $\tan\beta$ . . . 92
5.25 Schmaltz $PP \to HH$ enhancement vs $\tan\beta$ . . . 92
5.26 Schmaltz $PP \to HH$ cross section vs k . . . 93
5.27 Schmaltz $PP \to HH$ enhancement vs k . . . 93

7.1 Running top Yukawa with high MPP scale . . . 104
7.2 Running top with mid size MPP scale . . . 105
7.3 Running λ_1 with high MPP scale . . . 112
7.4 Running λ_2 with high MPP scale . . . 112
7.5 Running λ_3 with high MPP scale . . . 113
7.6 Running λ_4 with high MPP scale . . . 113
7.7 Running $\tilde{\lambda}$ with high MPP scale . . . 114
7.8 Scalar mass spectrum for large top Yukawa . . . 115
7.9 Scalar mass spectrum for medium top Yukawa . . . 116
7.10 Higgs-gauge coupling with high MPP scale . . . 117
7.11 Higgs-top coupling with high MPP scale . . . 118
7.12 Higgs-gauge coupling with medium top Yukawa . . . 119
7.13 Higgs-top coupling with medium top Yukawa . . . 119
7.14 Scalar mass spectrum with low MPP scale . . . 120
7.15 Higgs-Z couplings with low MPP scale . . . 121
7.16 Higgs-top couplings with low MPP scale . . . 121

List of Tables

2.1 Scalar-fermion Couplings 30
2.2 Scalar Trilinear Couplings 31

3.1 Gauge Boson Mass Eigenvalues 42
3.2 Top-Higgs Couplings 46

7.1 Lower bounds on $\tan\beta$ 105
7.2 Values of R_i satisfying equation (7.35) 109

Chapter 1

Introduction

1.1 Little Higgs Models

1.1.1 The Hierarchy Problem

Despite the tremendous success of the standard model (SM) when confronted with the experimental evidence assembled to date, one crucial element of the it, the Higgs boson, remains undetected. The Higgs boson is a vital component of the SM since it provides the mechanism for electroweak symmetry breaking (EWSB).

The potential of the Higgs field is minimised for a non-zero field value, leading to a vacuum expectation value (vev) which is not invariant under the $SU(2)_W \otimes U(1)_Y$ gauge transformations of the electroweak group. Masses for the electroweak W and Z gauge bosons, as well as for the fermions, are generated through their couplings to the Higgs (the Higgs mechanism).

The Higgs mechanism with a single Higgs doublet provides a conceptually simple mechanism for EWSB with a minimal new particle content. Despite this simplicity there is reason to believe that a single elementary Higgs doublet is not the true cause of EWSB since, as shall be shown, it implies a delicate and unnatural fine tuning of independent parameters of the theory.

The current experimental lower bound on the SM Higgs mass from direct searches is $M_H > 114.4$ GeV at 95% C.L.[2]. There is also an upper bound, the triviality bound, which is obtained by insisting that the Higgs quartic coupling remains finite when evolved with the renormalisation group for scales below the Planck scale (assuming no new physics below the Planck scale, $\approx 10^{19}$ GeV). This leads to the limit $M_H \lesssim 200$ GeV [3].

Another approach to obtaining an upper bound on the Higgs mass is to demand that the amplitude for WW scattering be compatible with perturbative unitarity. In this case the upper bound found is $M_H \lesssim 1.2$ TeV [3]. In addition, combining the electroweak precision fits and direct search limits from the LEP experiments favour a light Higgs with $M_H \lesssim 182$ GeV at the 95% C.L. [4].

The mass of the Higgs is modified from its bare value due to corrections from loop diagrams. The SM particles which have the strongest couplings with the Higgs, and therefore lead to the largest corrections to the Higgs mass parameter, are the top quark, the weak gauge bosons and the Higgs itself (see figures 1.1,1.2,1.3). The contributions

from other SM particles are much smaller than these and may be neglected for the purposes of the present discussion.

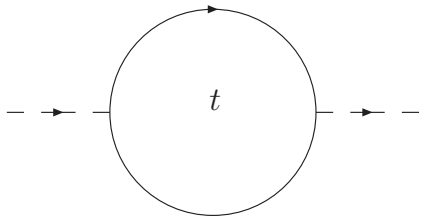

Figure 1.1: Higgs with a top loop.

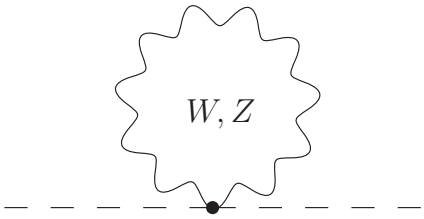

Figure 1.2: Higgs with a gauge boson loop.

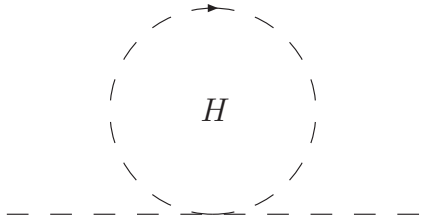

Figure 1.3: Higgs with loop from quartic self-coupling.

Regarding the SM as an effective theory with a cut off of order Λ, the largest corrections to the Higgs mass are found to vary quadratically with Λ. The top loop contribution is

$$-\frac{3}{8\pi^2}\lambda_t^2\Lambda^2, \tag{1.1}$$

the gauge boson loop contributes

$$\frac{1}{16\pi^2}g^2\Lambda^2, \tag{1.2}$$

and the contribution from the Higgs loop is

$$\frac{1}{16\pi^2}\lambda\Lambda^2, \tag{1.3}$$

where λ_t is the top quark Yukawa coupling, g is the $SU(2)$ gauge coupling and λ is the Higgs quadratic self-coupling. The observed mass of the Higgs is obtained from combining the bare mass m_{0H} with the loop induced corrections

$$M_H^2 = m_{0H}^2 - \frac{3}{8\pi^2}\lambda_t^2\Lambda^2 + \frac{1}{16\pi^2}g^2\Lambda^2 + \frac{1}{16\pi^2}\lambda\Lambda^2 \tag{1.4}$$

If the SM is valid all the way up to the Planck scale so that $\Lambda = \mathcal{O}(10^{19})$ GeV, the corrections to the Higgs mass are huge. This means that if the observed mass of the Higgs is to be of order 100 GeV the bare mass must be extremely fine tuned to cancel the contributions from the loop corrections.

Another way of saying this is that if a hierarchy is introduced between the electroweak scale and the cut off of the theory, this hierarchy will not be preserved when radiative corrections are taken into account. This instability of the electroweak scale to radiative corrections is known as the hierarchy problem.

The hierarchy problem motivates the search for new physics beyond the SM. However, new physics is constrained by the electroweak precision constraints (EWPCs). The new physics must enter at a high enough scale to avoid violating the EWPCs, yet without introducing an unnatural hierarchy between the new physics scale and the weak scale. This requirement can tell us something about the form the new physics might take.

If there is a Higgs boson, new particles might be expected to enter which eliminate the divergencies associated with at least the top and gauge boson loops, and possibly the Higgs loops too. Eliminating these most dangerous contributions to the Higgs mass means the scale of the new physics can be pushed above the requirements of the EWPCs without introducing fine tuning.

In practice, this means introducing particles with quantum numbers related to those of the top quark, the weak gauge bosons and the Higgs whose couplings to the Higgs are such that their contributions to its mass cancel the quadratic divergences due to their SM cousins. These new particles should be related to the SM particles by some symmetry, otherwise the fine tuning is just shifted onto their couplings.

Supersymmetric theories fit this bill. In these theories there are top squarks and gauginos which are related to their SM counterparts by supersymmetry. Supersymmetry guarantees that they have the same couplings as SM particles but opposite statistics, meaning there is a relative minus sign between the contributions from loop processes of particles and their supersymmetric partners which causes them to cancel.

In the last few years a new class of theories which meet the above criteria has been developed. In these theories the Higgs is naturally light which has inspired the name "Little Higgs" theories. The next section details the main ideas of Little Higgs models: pseudo-Goldstone bosons and collective symmetry breaking.

1.1.2 Little Higgs Models

Little Higgs models are an attempt to meet the challenge posed by the hierarchy problem. The challenge is to construct a theory of EWSB consistent with the EWPCs and in which the Higgs is naturally light.

Goldstone's theorem states that for each spontaneously broken continuous global symmetry, the theory must contain a massless particle. By also adding into the Lagrangian terms which explicitly break the global symmetry a potential for these Goldstone bosons can be generated radiatively, making them *pseudo*-Goldstone bosons. If the global symmetry breaking terms are proportional to a small coupling constant the terms generated by the radiative corrections will also be proportional to this constant which allows the radiative corrections to be kept under control.

An example of this is provided by the pions, which are light pseudo-Goldstone bosons associated with chiral symmetry breaking in QCD. This inspires the intriguing possibility that the Higgs may be a composite particle bound by a new strong force, that it is a pseudo-Goldstone boson of a spontaneously broken symmetry associated with this strong force, and that it acquires a potential through radiative corrections.

For example, consider the spontaneous breaking of a global $SU(3)$ symmetry to $SU(2)$ via a scalar triplet Φ which aquires a vev f. Through an $SU(3)$ transformation it is always possible to write the vev of the Φ field in the form

$$\langle \Phi \rangle = \begin{pmatrix} 0 \\ 0 \\ f \end{pmatrix}. \tag{1.5}$$

The spontaneous breaking of $SU(3)$ to $SU(2)$ results in $8 - 3 = 5$ Goldstone bosons (one for each broken symmetry generator). Small fluctuations around this vacuum may be parameterised by a non-linear sigma model (nlsm), which is obtained by integrating out the heavy radial mode. In this scheme Φ is written in the form

$$\Phi = e^{i\Theta/f} \begin{pmatrix} 0 \\ 0 \\ f \end{pmatrix} \tag{1.6}$$

where Θ is a matrix containing the Goldstone bosons which comprise a complex $SU(2)$ doublet h and a real $SU(2)$ singlet η,

$$\Theta = \frac{\eta}{\sqrt{2}} + \left(\begin{array}{cc|c} 0 & 0 & \\ 0 & 0 & \mathrm{h} \\ \hline & h^\dagger & 0 \end{array}\right) \tag{1.7}$$

The nlsm is an effective theory which is valid below some scale $\Lambda \approx 4\pi f$, since this is the scale at which it becomes inconsistent with perturbative unitarity.

To generate a potential it is necessary to add terms which break the global $SU(3)$ symmetry explicitly. In general, the Lagrangian may be written

$$\mathcal{L} = \mathcal{L}_0 + \varepsilon \mathcal{L}_1 \tag{1.8}$$

where $\mathcal{L}_0$ preserves the global $SU(3)$ symmetry, $\mathcal{L}_1$ explicitly breaks it and ε is a coupling constant. The term $\mathcal{L}_1$ might be, for example, the top Yukawa or the Higgs gauge interaction term. This will generate a contribution to the Higgs mass of order $\varepsilon^2 \Lambda^2 / 16\pi^2$. How large is this?

In general, new physics will contribute to higher dimensional operators such as $H^\dagger \tau^a H W^a_{\mu\nu} B^{\mu\nu} / \Lambda^2$ (where $W^a_{\mu\nu}$ is the $SU(2)$ gauge boson field strength tensor and $B^{\mu\nu}$ is the $U_Y(1)$ gauge boson field strength tensor) which must be suppressed by a scale

$\Lambda \approx 10$ TeV [5]. It is therefore challanging to build models where strongly coupled new physics enters below 10 TeV. If, then, the new physics doesn't enter until ≈ 10 TeV, and recall ε is supposed to be the top Yukawa coupling or the $SU(2)$ gauge coupling so this doesn't lead to much suppression, the Higgs mass generated via loop corrections will be of order 1 TeV or higher (at least, without some source of fine tuning) which is unacceptable.

Little Higgs models allow the successful implementation of the pseudo-Goldstone boson idea by adding the new ingredient of collective symmetry breaking. A Little Higgs theory introduces two global symmetries, $G_1 \otimes G_2$, such that the presence of either of these symmetries is enough to guarantee that the Higgs remains a Goldstone boson and so remains massless.

Schematically, two interaction terms are added to the Lagrangian,

$$\mathcal{L} = \mathcal{L}_0 + \varepsilon_1 \mathcal{L}_1 + \varepsilon_2 \mathcal{L}_2. \tag{1.9}$$

Here, the $\mathcal{L}_i$ are supposed to represent, for example, a pair of gauge coupling terms, or a pair of Yukawa coupling terms. The structure of these terms is such that if only one of the $\mathcal{L}_i$ is present, the Lagrangian is invariant under one of the global symmetries G_i and the Higgs is massless. Both these terms must be present to break all the global symmetries protecting the Higgs mass.

Since the Higgs mass is guaranteed to be zero whenever either of the ε_i is zero, contributions to the Higgs mass must be proportional to both ε_1 and ε_2. In particular, quadratically divergent contributions to the Higgs mass arise only at the two-loop level giving contributions of order $\varepsilon_1^2 \varepsilon_2^2 \Lambda^2/(16\pi^2)^2$ which are small enough for $\Lambda = \mathcal{O}(10)$ TeV.

To see a concrete implementation of these ideas consider a toy model [6] with a pair of scalar $SU(3)$ triplets, Φ_1 and Φ_2, with aligned vevs $\langle \Phi_i \rangle^T = (0, 0, f)$ taken to be equal for simplicity. Also, enlarge the SM $SU(2)$ gauge group to $SU(3)$ (i.e. embed the SM $SU(2)$ gauge group within an $SU(3)$ gauge group) and let both these scalar fields be charged under this $SU(3)$. In the absence of gauge and Yukawa terms this theory has an $SU(3)^2$ global symmetry which is spontaneously broken down to $SU(2)^2$ via the scalar vevs. The fields Φ_i may be parameterized

$$\begin{aligned} \Phi_1 &= e^{i\Theta'/f} e^{i\Theta/f} \begin{pmatrix} 0 \\ 0 \\ f \end{pmatrix} \\ \Phi_2 &= e^{i\Theta'/f} e^{-i\Theta/f} \begin{pmatrix} 0 \\ 0 \\ f \end{pmatrix} \end{aligned} \tag{1.10}$$

where Θ' is the "diagonal" part of the $SU(3)^2$ symmetry which acts on both Φ_i fields in the same sense and Θ is the "axial" part of the $SU(3)^2$ symmetry which acts on them in the opposite sense. The diagonal part of the $SU(3)^2$ symmetry can be rotated away via an $SU(3)$ gauge transformation giving a mass of order f to the gauge bosons associated with the broken generators of the $SU(3)$ gauge symmetry. The remaining Goldstone bosons are therefore parameterized

$$\begin{aligned}\Phi_1 &= e^{i\Theta/f}\begin{pmatrix}0\\0\\f\end{pmatrix}\\ \Phi_2 &= e^{-i\Theta/f}\begin{pmatrix}0\\0\\f\end{pmatrix}.\end{aligned} \tag{1.11}$$

The $SU(3)$ gauge couplings of the Φ_i fields are

$$\sum_i |(\partial_\mu + igA^a_\mu T^a)\Phi_i|^2. \tag{1.12}$$

Here, T^a are the $SU(3)$ generators and A^a_μ are the gauge fields.

Note that if either of these scalar triplets did not couple to the gauge fields, the model would have 2 $SU(3)$ *global* symmetries, one of which acts on one of the scalar fields and the gauge fields, the other acts on the other scalar fields. In this case the Higgs field would be an exactly massless Goldstone boson. It is only if both couple to the gauge fields that all the global symmetries protecting the Higgs mass are broken.

This means that diagrams like figure 1.4 do not contribute to the Higgs mass. This must be the case since this diagram appears in the theory where one of the Φ fields does not couple to the gauge fields. In other words, it leaves one of the $SU(3)$ global symmetries protecting the Higgs mass unbroken.

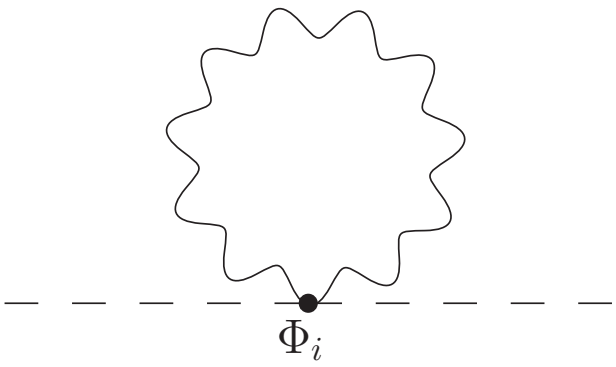

Figure 1.4: Quadratically divergent gauge loop contributing to Φ_i potential.

These diagrams produce the term

$$\frac{g^2\Lambda^2}{16\pi^2}(\Phi_1^\dagger\Phi_1 + \Phi_2^\dagger\Phi_2) \tag{1.13}$$

which is just a constant, as can be seen by substituting in the Φ fields of equation (1.11).

Only diagrams which contain gauge couplings to both Φ fields can generate a mass term for the Higgs. A quadratically divergent term can thus be generated only at two loops. However, the diagram which generates the leading gauge boson contribution to

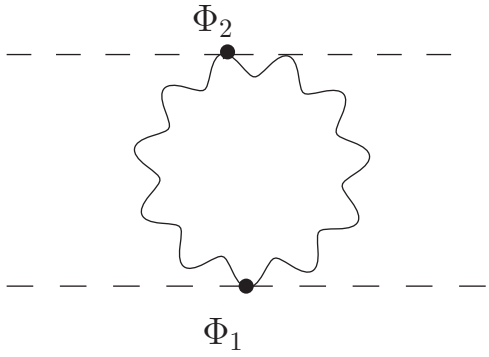

Figure 1.5: Logarithmically divergent gauge loop contributing to Φ_i potential.

the Higgs potential is in fact the one-loop logarithmically divergent diagram of figure 1.5. These contribute

$$\frac{g^4}{16\pi^2}|\Phi_1^\dagger\Phi_2|^2\log(\frac{\Lambda^2}{f^2}) = \frac{g^4 f^2}{16\pi^2}\log(\frac{\Lambda^2}{f^2})h^\dagger h \tag{1.14}$$

which is small enough to be an acceptable Higgs mass.

A similar game can be played with the top Yukawa couplings. To introduce the notation used for fermions consider the top quark. The left handed component is written t, whilst t^c will denote $\varepsilon\, t_R^*$ where ε is the antisymmetric tensor and t_R is the right handed component. Then the fermionic mass term is $t_R^\dagger t_L + \text{h.c.} = t^c.t + \text{h.c.}$ where $t^c.t = t.t^c \equiv t^c\varepsilon\, t$.

The left handed SM fermions transform as weak $SU(2)$ doublets. It is necessary to enlarge these to $SU(3)$ triplets. The top Yukawa coupling is replaced by the terms

$$\frac{\lambda}{\sqrt{2}}(t_1^c\Phi_1^\dagger + t_2^c\Phi_2^\dagger)\begin{pmatrix} t \\ b \\ T \end{pmatrix} + \text{h.c.} \tag{1.15}$$

where t and T are left handed up type quarks, and t_i^c are right handed up type quarks. The Yukawa couplings for these terms are assumed equal in this toy model for simplicity.

If either of these two terms is removed there will be an $SU(3)$ global symmetry protecting the mass of the Higgs. As in the gauge sector, both these terms are necessary in order to break enough of the global symmetry to generate a mass for the Higgs. The one loop quadratically divergent diagrams again contribute only an overall constant to the potential with the leading contribution to the Higgs mass coming from the one loop logarithmically divergent diagram.

So far contributions to the potential have been discussed in terms of $SU(3)$ fields such as the Φ_i. It is also useful to examine them from the point of view of the SM Higgs field to better understand how contributions to the Higgs mass are cancelled.

Let's examine the cancellation in the top sector. Expanding the Φ_i fields in equation (1.15) to order h^2/f^2 generates some mass terms of order f for the fermions as well as

interactions between the fermions and the Higgs. Performing a rotation on the right handed fields,

$$\begin{pmatrix} t^c \\ T^c \end{pmatrix} = \frac{1}{\sqrt{2}} \begin{pmatrix} 1 & -1 \\ 1 & 1 \end{pmatrix} \begin{pmatrix} t_1^c \\ t_2^c \end{pmatrix} \tag{1.16}$$

leads to the diagonalized top sector Lagrangian

$$\mathcal{L}_{\text{top}} = \lambda f(1 - \frac{h^\dagger h}{2f^2})T^c T + \lambda t^c h^\dagger \begin{pmatrix} t \\ b \end{pmatrix} + \text{h.c.} \tag{1.17}$$

One of the up type quarks has a mass of scale f and a dimension 5 interaction with a pair of Higgs, the other is the SM top quark with its standard Yukawa coupling.

These couplings give rise to the diagrams portrayed in figure 1.6 where a mass insertion has been performed in the diagrams involving the heavy partner of the top.

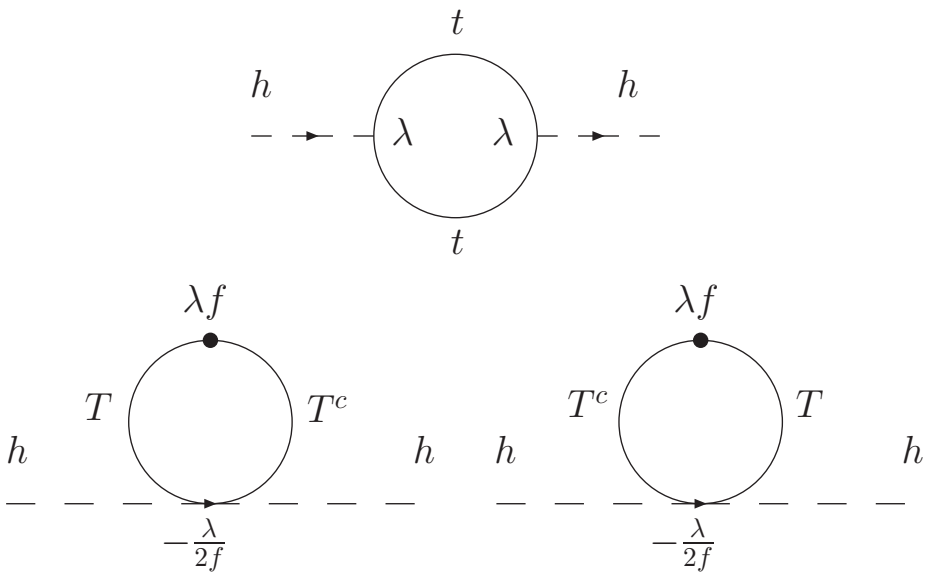

Figure 1.6: Diagrams contributing to quadratically divergent Higgs mass.

The two diagrams involving the heavy partner of the top quark are proportional to $-\lambda/2f \times \lambda f = -\lambda^2/2$ whilst the diagram involving the top quark is proportional to λ^2. These three diagrams therefore sum to zero leading to no quadratically divergent contribution to the Higgs mass at the one loop level.

It is interesting to note that, unlike supersymmetry, the cancellations occur between particles of the same spin. The diagrams which cancel the top loop get a relative minus sign, not because they have different spin statistics, but because they are generated by a dimension 5 operator with a negative coupling constant.

A realistic model which is very similar in structure to this toy model is considered in Chapter 3.

1.1.3 Survey Of Little Higgs Models

Originally, Little Higgs models were inspired by the dimensional deconstruction technique [7] applied in 5 dimensional theories where the Higgs is the fifth component of a gauge field. This is where the phenomenon of collective symmetry breaking, the crucial ingredient of Little Higgs theories, was first identified. Although first identified in this context, the collective symmetry breaking mechanism can be applied to regular 4 dimensional theories and this is what is done in most Little Higgs models.

The Little Higgs models in the literature can be divided into 2 classes, *product group* models and *simple group* models, based on the structure of their gauge and Yukawa sectors.

Product group models have a global symmetry group G which is broken to a subgroup H by the vev of a scalar field. Also, two or more gauge groups are embedded within the global symmetry group G and these gauge groups are broken down to the SM electroweak group by the condensate. Each of these gauge groups leaves invariant some global subgroup of G which protects the Higgs mass so that no single gauge coupling alone can generate a mass for the Higgs.

Most Little Higgs models are of this type. These include the "Littlest Higgs" [8] based on $SU(5)/SO(5)$, the so-called "moose" models [9],[10], a model based on $SU(6)/Sp(6)$ [11], an $SU(9)/SU(8)$ model [12], and variations on the Littlest Higgs with an added custodial $SU(2)$ [13],[14].

Product group models have in common new free parameters in the gauge sector because of the new independent gauge groups. They also allow for economical extensions of the fermion sector. For example, the Littlest Higgs contains only one new fermion, a heavy top-like quark which cancels the quadratically divergent contribution to the Higgs mass from the SM top.

Simple group models are based on an extension of the SM $SU(2)\otimes U(1)$ gauge group to $SU(N)\otimes U(1)$. They also feature more than one set of sigma model fields, since this is necessary to implement the collective symmetry breaking. Little Higgs models of this type are the "simplest" Little Higgs or "Schmaltz model" [15] featuring a $SU(3)\otimes U(1)$ gauge group and a model based on an $SU(4)\otimes U(1)$ gauge group [16]. The toy model of the previous section is also a product group model presented in [6].

Simple group models do not have free parameters in the gauge sector. The gauge couplings are determined by the necessity to reproduce the SM gauge couplings after breaking down to the SM gauge group. On the other hand, the various sigma model fields can in general have different vevs introducing more parameters and it is necessary to extend all SM fermion weak doublets to N-plets of $SU(N)$.

Supersymmetric models usually are chosen to have an R-parity under which SM particles are even and supersymmetric partners are odd. This means that supersymmetric partners can only be produced in pairs which weakens experimental constraints on these models. For product group Little Higgs models it is possible to define an analogous discrete symmetry called T-parity under which SM particles are T-even and the new particles are T-odd. This T-parity forbids the new heavy gauge bosons from contributing to EWPCs at tree level which significantly weakens the experimental constraints on these models. [17],[18].

It is worth bearing in mind that Little Higgs theories are only effective theories which require a UV completion at around the 10 TeV scale. A UV completion of the Littlest Higgs is presented in [19] in which the Higgs is a composite particle. This model contains new strong interactions and softly broken supersymmetry which both enter at $\mathcal{O}(10)$ TeV. There is also a UV completion of the Schmaltz model in which the collective symmetry breaking mechanism is iterated twice to create a theory which is weakly coupled below $\mathcal{O}(100)$ TeV [20].

There are a number of good reviews in the literature which give an overview of Little Higgs models [6],[21],[22],[23].

The Littlest Higgs and the Schmaltz models are the simplest examples of product group and simple group models respectively. It thus makes sense to study these as prototypes for their respective classes. The Littlest Higgs model is developed in some detail in chapter 2 whilst the Schmaltz model is developed in chapter 3.

In chapter 4 the loop induced decays of the Higgs to pairs of gluons or photons are examined in both these models, whilst chapter 5 looks at Higgs pair production from gluon fusion via quark loops. These processes are of particular interest in Little Higgs models because they contain the crucial couplings of the Higgs with t and T quarks which are dictated by the necessity of cancelling quadratic divergences in the Higgs mass, and are thus robust predictions of the respective models.

Also investigated in this thesis is Higgs physics within another conceptual framework, that of the multiple point principle.

1.2 The Multiple Point Principle

1.2.1 The Multiple Point Principle

In addition to Little Higgs models, this thesis also contains work on the multiple point principle (MPP) [24], [25], [26]. The MPP postulates that the universe tunes parameters such that there exist a maximal number of different vacua with the same energy density.

To understand the motivation for the MPP, consider the analogy of the temperature of an ice and water mixture. If a mixture of water and ice exist in equilibrium (at atmospheric pressure) the system is "tuned" to be at zero degrees celsius. There are a wide range of values for the extensive variables (such as total energy and number of molecules) for which the system will be forced to exist in a mixture of phases. When this is the case, the intensive variables (such as temperature and pressure) will be tuned to the values they have at the phase transition.

In this analogy the coupling constants of the theory play the role of intensive variables. If the existence of some extensive variables are assumed, with values which are fixed for space-time as a whole, they could force the universe to exist in a mixture of phases. If this is the case the coupling constants will be tuned to the values which allow a large number of phases with the same energy density to coexist.

In order for a mixture of phases to be likely it should be required for a wide range of extensive variables. This is the case if the range of extensive variables which allow the existence of only a single phase is small. Going back to the water and ice analogy this

would correspond to a large latent heat of fusion. The corresponding requirement in the quantum field theory is that the vevs of the fields in the different vacua should be widely separated in energy.

In this thesis, the multiple point principle is simply taken as an ansatz and its consequences investigated.

The MPP has previously been applied to the SM [26]. In this case, the existence of another vacuum is assumed with energy density $V_{\rm eff}(\langle\phi_{\rm new}\rangle)$ equal to that of the vacuum we are currently in. Here $V_{\rm eff}$ is the effective potential and $\langle\phi_{\rm new}\rangle$ is the Higgs vacuum expectation value in the new minimum which is taken to be of order the Planck scale. With these assumptions it is possible to derive predictions for the Higgs and the top pole masses, $M_t = 173 \pm 4$ GeV and $M_H = 135 \pm 9$ GeV, which are compatible with current experimental data.

The MPP has also been applied to a supergravity model [29] where it provides an explanation for the small deviation of the cosmological constant from zero.

In this thesis the consequences of applying the MPP to the two Higgs doublet model (2HDM) will be considered.

1.2.2 Two Higgs-doublet Models

Although a single Higgs doublet is the simplest way of obtaining EWSB, the scalar sector has yet to be directly probed by experiments and may well be more complicated. It is therefore important to examine how it might be extended. The two Higgs doublet model (2HDM) enlarges the scalar sector by adding an extra Higgs doublet. For $n = 1, 2$ the Higgs doublets may be written as

$$H_n = \begin{pmatrix} \chi_n^+ \\ (H_n^0 + iA_n^0)/\sqrt{2} \end{pmatrix} \tag{1.18}$$

The most general (tree level) potential for the two Higgs doublets which satisfies gauge invariance, renormalisability and CP invariance is

$$\begin{aligned} V(H_1, H_2) \;=\; & m_1^2 H_1^\dagger H_1 + m_2^2 H_2^\dagger H_2 - [m_3^2 H_1^\dagger H_2 + \text{h.c.}] + \frac{1}{2}\lambda_1 (H_1^\dagger H_1)^2 + \frac{1}{2}\lambda_2 (H_2^\dagger H_2)^2 \\ & + \lambda_3 (H_1^\dagger H_1)(H_2^\dagger H_2) + \lambda_4 |H_1^\dagger H_2|^2 + [\frac{1}{2}\lambda_5 (H_1^\dagger H_2)^2 + \lambda_6 (H_1^\dagger H_1)(H_1^\dagger H_2) \\ & + \lambda_7 (H_2^\dagger H_2)(H_2^\dagger H_1) + \text{h.c.}] \end{aligned} \tag{1.19}$$

where the couplings λ_1-λ_6 are required to be real by CP invariance. The parameters are assumed to be such that minimising this potential causes the Higgs doublets to gain vevs triggering EWSB. After EWSB, a linear combination of the charged scalars and a linear combination of the CP odd scalars are eaten by the $W^\pm$ and Z gauge bosons respectively. This leaves one charged scalar, one neutral CP odd scalar and a pair of CP even scalars.

In the most general case both Higgs doublets can couple to all the fermions. This means that the Cabibo-Kobayashi-Maskawa (CKM) matrix [27],[28] which diagonalises the fermion masses will not in general diagonalise their coupling with the Higgs bosons. This is a problem because it induces flavour changing neutral currents (FCNCs) which

are very strongly constrained by experiment. For instance, bounds from $K^0 - \bar{K}^0$ mixing and CP violation in K meson decay imply that the effective Lagrangian term inducing these processes must be suppressed by some scale of order $\geq 10^4$ TeV.

The undesireable couplings can be avoided by the introduction of a $U(1)$ symmetry (Peccei-Quinn symmetry). This symmetry requires that the couplings λ_6 and λ_7 vanish, each fermion couples to only one Higgs doublet and all fermions with the same electric charge couple to the same Higgs doublet. The symmetry also requires that m_3^2 is zero, but this is not required to suppress FCNCs at the tree level. If these conditions are met the Weinberg theorem (which states that tree level FCNCs are not generated in the Higgs sector if all fermions with the same electric charge couple to the same Higgs doublet) applies [30] and tree level FCNCs are absent from the theory.

In chapter 6 the MPP is applied to the 2HDM resulting in an approximate Peccei-Quinn type symmetry. Then, in chapter 7, the implications of the MPP for scalar masses and couplings are investigated.

Chapter 2

The Littlest Higgs Model

2.1 Overview of the Littlest Higgs Model

The Littlest Higgs model [8] is an economic extension of the SM in which the Higgs is a pseudo-Goldstone boson which remains naturally light due to the Little Higgs mechanism. It is based on an $SU(5)$ global symmetry with a locally gauged subgroup, $G_1 \otimes G_2 = [SU(2)_1 \otimes U(1)_1] \otimes [SU(2)_2 \otimes U(1)_2]$.

At a scale Λ_S a 5×5 symmetric matrix of scalar fields gains a vev f where f is of the order a TeV and naive dimensional analysis [31] suggests that $\Lambda_S \sim 4\pi f$. This vev spontaneously breaks $SU(5)$ to $SO(5)$ and simultaneously breaks the gauge symmetry $G_1 \otimes G_2$ down to its diagonal subgroup which is the SM electroweak group $SU(2)_L \otimes U(1)_Y$.

The breaking of the global symmetry leads to a set of Goldstone bosons. Some of these become the longitudinal components of the gauge bosons associated with the broken generators of $G_1 \otimes G_2$ leading to these gauge bosons aquiring masses of order f. A complex doublet (the Little Higgs) and a complex triplet remain.

The couplings of the Little Higgs and complex triplet to fermions and gauge bosons break the $SO(5)$ global symmetries leading to the generation of a Coleman-Weinberg potential [32]. This Coleman-Weinberg potential has the form required to give a vev to the Little Higgs and induce EWSB. At least two of the couplings to gauge bosons or fermions are required in order to break enough of the global symmetry to contribute to the mass of the Little Higgs, which means that only logarithmic dependence on the cut off is allowed at the one loop level and quadratic cut off dependence is only present at two loops or higher keeping the Higgs mass naturally small.

In this chapter certain aspects of the low energy effective field theory of the Littlest Higgs Model are worked out in detail, including some corrections to some mixing angles and the Feynman rules in the literature. The interactions of the scalars with gauge bosons are examined, followed by their interactions with fermions. Next the electroweak symmetry breaking is examined along with its consequences in terms of the masses of the heaviest particles. The modification to the standard model relation between the Higgs vev and the Fermi constant is considered, since this will be important in subsequent work, and the chapter concludes with a short summary of the bounds on the parameters of the model from EWPCs.

2.2 Scalar Kinetic Terms

The Littlest Higgs model is based on an $SU(5)$ global symmetry which is broken to $SO(5)$ via the vev of a 5×5 symmetric matrix of scalar fields. This vev may be taken to be proportional to the unit matrix but it is conventional to use a different basis in which the vev is proportional to the matrix

$$\Sigma_0 = \begin{pmatrix} & & 1_{2\times 2} \\ & 1 & \\ 1_{2\times 2} & & \end{pmatrix}. \tag{2.1}$$

$SU(5)$ has $5^2-1 = 24$ generators while $SO(5)$ has $5\times(5-1)/2 = 10$ so, by Goldstone's theorem, there will be 14 massless Goldstone bosons associated with the spontaneous breakdown of the symmetry. Four of these will be removed by the Higgs mechanism when the $[SU(2)\otimes U(1)]^2$ is broken to its diagonal subgroup, the 10 remaining Goldstone bosons are parameterised by a non-linear sigma model field

$$\Sigma = e^{i\Pi/f}\Sigma_0 e^{i\Pi^T/f}. \tag{2.2}$$

Here the Goldstone boson matrix Π is

$$\Pi = \begin{pmatrix} 0_{2\times 2} & h^\dagger/\sqrt{2} & \phi^\dagger \\ h/\sqrt{2} & 0 & h^*/\sqrt{2} \\ \phi & h^T/\sqrt{2} & 0_{2\times 2} \end{pmatrix} \tag{2.3}$$

and

$$h = (h^+, h^0), \qquad \phi = \begin{pmatrix} \phi^{++} & \phi^+/\sqrt{2} \\ \phi^+/\sqrt{2} & \phi^0 \end{pmatrix} \tag{2.4}$$

where h is a complex doublet which plays the role of the SM Higgs and ϕ is a complex electroweak triplet.

The interactions of the scalars with gauge bosons, as well as the gauge boson masses, may be obtained from the scalar kinetic term. This is given by

$$\mathcal{L}_\Sigma = \frac{1}{8}f^2 \mathrm{Tr}|\mathcal{D}_\mu \Sigma|^2 \tag{2.5}$$

where the covariant derivative takes the form

$$\mathcal{D}_\mu\Sigma = \partial_\mu - i\sum_{j=1}^{2}(g_j(W_{\mu j}\Sigma + \Sigma W_{\mu j}^T) + g_j'(B_{\mu j}\Sigma + \Sigma B_{\mu j}^T)) \tag{2.6}$$

with the $SU(2)_j$ fields given by $W_j = W_{\mu j}^a Q_j^a$ and the $U(1)_j$ fields given by $B_j = B_{\mu j}Y_j$ where the generator matrices Q_i and Y_i are given by

$$Q_1^a = \begin{pmatrix} \sigma^a/2 & & \\ & & \\ & & 0_{3\times 3} \end{pmatrix}, \qquad Q_2^a = \begin{pmatrix} 0_{3\times 3} & & \\ & & \\ & & -\sigma^{a*}/2 \end{pmatrix} \tag{2.7}$$

$$Y_1 = \frac{1}{10}\mathrm{diag}(-3,-3,2,2,2), \qquad Y_2 = \frac{1}{10}\mathrm{diag}(-2,-2,-2,3,3). \tag{2.8}$$

The numerical constants are chosen such that the scalar kinetic terms are canonically normalised (i.e. the kinetic term for a scalar field ψ is $\frac{1}{2}\psi^\dagger\psi$) and σ^a are the Pauli matrices,

$$\sigma^1 = \begin{pmatrix} 0 & 1 \\ 1 & 0 \end{pmatrix}, \quad \sigma^2 = \begin{pmatrix} 0 & -i \\ i & 0 \end{pmatrix}, \quad \sigma^3 = \begin{pmatrix} 1 & 0 \\ 0 & -1 \end{pmatrix}. \tag{2.9}$$

Note that if the gauge couplings of G_1 are set to zero there is an $SU(3)$ global symmetry ($SU(3)_1$) embedded in the upper left 3×3 block of $SU(5)$. This $SU(3)$ global symmetry would be broken to $SU(2)$ by the vev Σ_0 and the Higgs would be a Goldstone boson corresponding to this breaking and would consequently be exactly massless. Similarly, if the gauge couplings of G_2 are set to zero there is a different $SU(3)$ symmetry ($SU(3)_2$) embedded in the bottom right block of $SU(5)$ which would also guarantee the masslessness of the Higgs. Only if the gauge couplings of both G_1 and G_2 are present is the Higgs no longer an exact Goldstone boson. It follows that gauge bosons may generate a Higgs mass radiatively only through processes involving both sets of gauge bosons.

Inserting the non-zero vev for the Σ field, (2.1), into expression (2.5) generates mass terms for the gauge bosons

$$\begin{aligned} \mathcal{L}_\Sigma \approx & \frac{1}{2}\frac{f^2}{8}(g_1^2 W_{1\mu}^a W_1^{a\mu} + g_2^2 W_{2\mu}^a W_2^{a\mu} - 2g_1 g_2 W_{1\mu}^a W_2^{a\mu}) \\ & + \frac{1}{2}\frac{f^2}{20}(g_1'^2 B_{1\mu}^a B_1^{a\mu} + g_2'^2 B_{2\mu}^a B_2^{a\mu} - 2g_1' g_2' B_{1\mu}^a B_2^{a\mu}) \end{aligned} \tag{2.10}$$

These mass terms may be diagonalised to find the pre-EWSB mass eigenstates by performing the transformations

$$\begin{pmatrix} W \\ W' \end{pmatrix} = \begin{pmatrix} s & c \\ -c & s \end{pmatrix} \begin{pmatrix} W_1 \\ W_2 \end{pmatrix}, \qquad \begin{pmatrix} B \\ B' \end{pmatrix} = \begin{pmatrix} s' & c' \\ -c' & s' \end{pmatrix} \begin{pmatrix} B_1 \\ B_2 \end{pmatrix} \tag{2.11}$$

where the mixing angles are given by

$$c = \frac{g_1}{\sqrt{g_1^2 + g_2^2}}, \qquad s = \frac{g_2}{\sqrt{g_1^2 + g_2^2}} \tag{2.12}$$

$$c' = \frac{g_1'}{\sqrt{g_1'^2 + g_2'^2}}, \qquad s' = \frac{g_2'}{\sqrt{g_1'^2 + g_2'^2}} \tag{2.13}$$

It might be better to relabel $s \leftrightarrow c$ and $s' \leftrightarrow c'$ but the above notation is that which is used in the literature (for example, [33]). Performing this transformation on the fields results in heavy gauge bosons W' and B' with masses

$$m_{W'} = \frac{1}{2} f \sqrt{g_1^2 + g_2^2} = \frac{g}{2sc} f \quad \text{and} \quad m_{B'} = \frac{1}{2\sqrt{5}} f \sqrt{g_1'^2 + g_2'^2} = \frac{g'}{2\sqrt{5}s'c'} f \tag{2.14}$$

and the SM gauge bosons W and B which are massless at this stage. The SM gauge boson couplings g and g' are given by

$$g = \frac{g_1 g_2}{\sqrt{g_1^2 + g_2^2}}, \qquad g' = \frac{g_1' g_2'}{\sqrt{g_1'^2 + g_2'^2}} \tag{2.15}$$

Later the Coleman-Weinberg potential for the scalar fields h and ϕ shall be required and to calculate this the gauge boson mass matrix in the presence of a general background field Σ, which we define to be $M^2_{V_iV_j}(\Sigma)$ where V_i and V_j run over all the $[SU(2)\otimes U(1)]^2$ gauge bosons, is required. This is obtained from expression (2.5) leading to the gauge boson mass terms

$$\mathcal{L}_\Sigma \approx \frac{1}{2}(M_V^2)_{ij}(\Sigma)V_{i\mu}V_j^\mu \tag{2.16}$$

where

$$M_V^2(\Sigma)_{ij} = \frac{1}{4}f^2 g_{V_i}g_{V_j}\mathrm{Tr}[(Q_{V_i}\Sigma + \Sigma Q_{V_i}^T)(Q_{V_j}\Sigma + \Sigma Q_{V_j}^T)^\dagger] \tag{2.17}$$

In the above expression g_{V_i} is the coupling associated with vector boson V_i and Q_{V_i} is the 5×5 generator matrix associated with V_i.

2.3 Fermion-Scalar Interactions

In order to obtain a large top Yukawa coupling without introducing a corresponding large quadratic divergence to the Higgs mass, the top sector interactions are defined such that each individual interaction retains enough of the global symmetry to guarantee the masslessness of the Higgs, as in the gauge boson sector.

In addition to the SM third family electroweak doublet $q_3 = (t_3, b_3)$ and the electroweak singlet $u_3'^c$ a new pair of electroweak singlet quarks $\tilde{t}$, $\tilde{t}^c$ are introduced, with quantum numbers $(\mathbf{3},\mathbf{1})_{Y_i}$ and $(\overline{\mathbf{3}},\mathbf{1})_{-Y_i}$ respectively. The top-sector Lagrangian is defined to be

$$\mathcal{L}_t = -\frac{1}{2}\lambda_1 f\epsilon_{ijk}\epsilon_{xy}\chi_i\Sigma_{jx}\Sigma_{ky}u_3'^c - \lambda_2 f\tilde{t}\tilde{t}'^c + \text{h.c.} \tag{2.18}$$

where $\{i,j,k\}$ are summed over 1,2,3 and $\{x,y\}$ over 4,5. Here ϵ_{ijk} and ϵ_{xy} are anti-symmetric tensors and

$$\chi = \begin{pmatrix} \sigma_2 q_3 \\ \tilde{t} \end{pmatrix} \tag{2.19}$$

This is the top-sector Lagrangian proposed in the original Littlest Higgs paper, [8], but with some different conventions. A factor of $\frac{1}{2}$ has been extracted from the definition of λ_1 for later convenience as in [33] and [23], and some of the quarks have been rephased as in [23] to ensure that the fermion masses will be real and non-negative.

The first term in $\mathcal{L}_t$ is invariant under $SU(3)_1$, which acts on the indices $\{i,j,k\}$, but violates $SU(3)_2$. The second term is a bare mass term for the new quark which is chosen to be of order f. It violates $SU(3)_1$ but preserves $SU(3)_2$ and so, by the same argument as that presented underneath equation (2.8), only processes involving both interactions may generate a mass for the Higgs.

The extra fermions $\tilde{t}$ and $\tilde{t}'^c$ are the only new fermions in the Littlest Higgs model. All SM fermions other than the top quark have small Yukawa couplings which don't lead to significant fine tuning of the Higgs mass with a cut off at around 10 TeV. This means there is no need to introduce any other new fermions to cancel their contributions.

Inserting the non-zero vev for the Σ field (2.1) into the top sector Lagrangian (2.18) leads to the pre-EWSB (i.e., non field dependent) top sector mass terms

$$\mathcal{L}_t \approx -\lambda_1 f \tilde{t} u_3'^c - \lambda_2 f \tilde{t}\tilde{t}'^c \tag{2.20}$$

To diagonalize the fermion mass matrix requires performing different transformations on the left and right handed fermion fields. The pre-EWSB mass eigenstates may be found by performing the transformations

$$\begin{pmatrix} u_3^c \\ \tilde{t}^c \end{pmatrix} = \begin{pmatrix} \frac{\lambda_2}{\sqrt{\lambda_1^2+\lambda_2^2}} & -\frac{\lambda_1}{\sqrt{\lambda_1^2+\lambda_2^2}} \\ \frac{\lambda_1}{\sqrt{\lambda_1^2+\lambda_2^2}} & \frac{\lambda_2}{\sqrt{\lambda_1^2+\lambda_2^2}} \end{pmatrix} \begin{pmatrix} u_3'^c \\ \tilde{t}'^c \end{pmatrix} \tag{2.21}$$

There is no need for any transformation on the left handed fields. The above transformation leads to

$$\mathcal{L}_t \approx -f\sqrt{\lambda_1^2+\lambda_2^2}\tilde{t}\tilde{t}^c \tag{2.22}$$

This means that before EWSB there is a single massive quark $\tilde{t}$ with mass $m_{\tilde{t}} = \sqrt{\lambda_1^2+\lambda_2^2}f$, whilst the SM top quark remains massless at this stage.

As in the gauge boson case the top sector masses in a general background Σ field shall be required in order to compute the fermion contribution to the effective potential. The top sector mass matrix is defined by

$$\mathcal{L}_t = -M_t(\Sigma)_{ij}\chi_i\chi_j^c \tag{2.23}$$

where $\chi_j^c = (b_3^c, u_3'^c, \tilde{t}'^c)$ and $M_t(\Sigma)$ is given by

$$[M_t(\Sigma)]_{i,j} = \frac{\lambda_1}{2} f \epsilon_{ikl}\epsilon_{wx}\Sigma_{kw}\Sigma_{lx}\delta_{j2} + \lambda_2 f \delta_{i3}\delta_{j3} \tag{2.24}$$

2.4 Electroweak Symmetry Breaking

The Coleman-Weinberg potential [32] describes the radiative corrections to the scalar potential thorough fermion and gauge boson loops. The dominant contribution comes from one-loop quadratic divergences. The contribution to this from gauge boson loops is [32]

$$V_g = \frac{3\Lambda^2}{32\pi^2}\mathrm{Tr}[M_V^2(\Sigma)] = \frac{3}{2}af^2\mathrm{Tr}[M_V^2(\Sigma)] \tag{2.25}$$

where a is a coefficient of $\mathcal{O}(1)$ since $\Lambda \approx 4\pi f$. This differs from the expressions in [8] and [33] by a factor of 3/2, with the factor of 3 coming from the contraction of the Lorentz indices. Perhaps they absorb this factor into the coefficient a but here it is kept explicitly. Substituting the gauge boson mass matrix defined in equation (2.17) into (2.25) gives

$$\begin{aligned} V_g &= \frac{3}{8}af^4\sum_j\{g_j^2\sum_a\left[\mathrm{Tr}[(Q_j\Sigma+\Sigma Q_j^T)(Q_j\Sigma+\Sigma Q_j^T)^\dagger]\right] \\ &\quad +\mathrm{Tr}\left[(Y_j\Sigma+\Sigma Y_j^T)(Y_j\Sigma+\Sigma Y_j^T)^\dagger\right]\}. \end{aligned} \tag{2.26}$$

Using the trace identities $\mathrm{Tr}[ABC] = \mathrm{Tr}[CAB]$ and $\mathrm{Tr}[(ABC)^T] = \mathrm{Tr}[ABC]$, as well as the relation $\Sigma\Sigma^* = 1_{5\times5}$, this can be shown to be

$$V_g = \frac{3a}{4} f^4 \sum_j \left(g_j^2 \sum_a \mathrm{Tr}[Q_j^a \Sigma Q_j^{a*} \Sigma^*] + g_j'^2 \mathrm{Tr}[Y_j \Sigma Y_j^* \Sigma^*] \right) \tag{2.27}$$

Expanding the Σ field in (2.27) up to quadratic order in ϕ and quartic order in h (using (2.2) and (2.3)) leads to the expression

$$\begin{aligned} V_g &= \frac{3a}{4}(g_1^2 + g_1'^2)\left[f^2 \mathrm{Tr}(\phi^\dagger\phi) - \frac{if}{2}(h\phi^\dagger h^T - h^*\phi h^\dagger) + \frac{1}{4}(hh^\dagger)^2 \right] \\ &\quad \frac{3a}{4}(g_2^2 + g_2'^2)\left[f^2 \mathrm{Tr}(\phi^\dagger\phi) + \frac{if}{2}(h\phi^\dagger h^T - h^*\phi h^\dagger) + \frac{1}{4}(hh^\dagger)^2 \right] \end{aligned} \tag{2.28}$$

The other quadratically divergent contribution to the effective potential comes from top-sector fermion loops. The contributions from other fermions are suppressed by their small Yukawa couplings and so may be neglected. The fermion contribution to the effective potential is

$$V_f = -\frac{3\Lambda^2}{8\pi^2} \mathrm{Tr}[M_t(\Sigma) M_t^\dagger(\Sigma)] \tag{2.29}$$

where the factor of 3 comes from the colour factor. Using expression (2.24) this gives

$$V_f = -\frac{3\Lambda^2}{8\pi^2} \frac{\lambda_1^2 f^2}{4} (\epsilon_{ikl}\epsilon_{wx}\Sigma_{kw}\Sigma_{lx}\delta_{j2} + \lambda_2 f \delta_{i3}\delta_{j3})(\epsilon_{imn}\epsilon_{yz}\Sigma_{my}\Sigma_{nz}\delta_{j2} + \lambda_2 f \delta_{i3}\delta_{j3}) \tag{2.30}$$

Dropping constant terms proportional to f^4 this gives

$$V_f = -3a' \frac{\lambda_1^2 f^4}{2} \epsilon_{ikl}\epsilon_{wx}\epsilon_{imn}\epsilon_{yz}\Sigma_{kw}\Sigma_{lx}\Sigma^*_{my}\Sigma^*_{nz} \tag{2.31}$$

Here a' is a constant of $\mathcal{O}(1)$. Substituting in the expression for Σ (2.2), and again retaining terms up to quadratic order in ϕ and quartic order in h, gives

$$V_f = 24a'\lambda_1^2 \left[f^2 \mathrm{Tr}(\phi^\dagger\phi) + \frac{if}{2}(h\phi^\dagger h^T - h^*\phi h^\dagger) + \frac{1}{4}(hh^\dagger)^2 \right] \tag{2.32}$$

It is interesting to note that the potential generated by the top loops is of the same form as that generated by the $SU(2)_1 \otimes U(1)_1$ gauge bosons. This should not be surprising since they both preserve the global symmetry $SU(3)$.

There are some discrepancies between the above work and some work in the literature. In the gauge boson sector there is the factor of 3/2 noted below equation (2.25). Also, there is an anomalous factor of -1 between expression (2.27) and equations (A20) and (A21) in reference [33]. This is probably due to confusion between the Lagrangian and the potential which differ by a factor of -1, but comparing their equations (A19) and (A24) it can be seen that this typo also is not present in their final answer.

There are also discrepancies in the fermionic contribution to the effective potential. Firstly there is again some confusion due to the relative minus sign between the Lagrangian and the effective potential. Equations (A22) and (A23) of reference [33]

describe the potential, not the Lagrangian. As in the gauge boson sector, this typo is resolved by equation (A24) where the fermion contribution enters with the correct sign.

Also, there is a difference of a factor of 6 between equation (2.31) and equation (A22) of reference ([33]). Comparing equations (2.32) and (A23) of [33] the discrepancy is reduced to a factor of 3, which can be explained by the omission of a colour factor. This will affect all coefficients of λ_1 in equation (A24) of reference [33].

As advertised, no mass term for the Higgs is present in the one-loop quadratically divergent effective potential. Higher order contributions will generate a Higgs mass with equally significant contributions from one loop logarithmically divergent and two loop quadratically divergent terms of order $f^2/16\pi^2$ [33]. The Higgs mass μ will be treated as a free parameter of order $f/4\pi$. Including contributions from both gauge boson and fermion loops, the effective potential has the form

$$V_{\text{eff}} = \lambda_{\phi^2} f^2 \text{Tr}(\phi^\dagger \phi) + i\lambda_{h\phi h} f(h\phi^\dagger h^T - h^* \phi h^\dagger) - \mu^2 h h^\dagger + \lambda_{h^4}(h h^\dagger)^2 \tag{2.33}$$

where the λ coefficients are given by

$$\begin{aligned}
\lambda_{\phi^2} &= \frac{3a}{4}\left[\frac{g^2}{c^2 s^2} + \frac{g'^2}{c'^2 s'^2}\right] + 24 a' \lambda_1^2 \\
\lambda_{h\phi h} &= -\frac{3a}{8}\left[\frac{(c^2 - s^2)g^2}{c^2 s^2} + \frac{(c'^2 - s'^2)g'^2}{c'^2 s'^2}\right] + 12 a' \lambda_1^2 \\
\lambda_{h^4} &= \frac{1}{4}\lambda_{\phi^2}.
\end{aligned} \tag{2.34}$$

The minimum of this potential can easily be found. For $\mu^2 > 0$ this results in the vevs $\langle h^0 \rangle = v/\sqrt{2}$ and $\langle i\phi^0 \rangle = v'$ where

$$\begin{aligned}
v^2 &= \frac{\mu^2}{\lambda_{h^4} - \lambda_{h\phi h}^2/\lambda_{\phi^2}} \\
v' &= \frac{\lambda_{h\phi h}}{2\lambda_{\phi^2}} \frac{v^2}{f}
\end{aligned} \tag{2.35}$$

Note that $v'/v = \mathcal{O}(v/f)$. This will be important as many quantities will be expanded as series in powers of v/f.

Expanding the fields around their vevs results in mixing in the scalar sector. Expressed in terms of the mass eigenstates [33] the scalar fields are

$$\begin{aligned}
h^0 &= \frac{c_o H - s_0 \Phi^0 + v}{\sqrt{2}} + i\frac{c_P G^0 - s_P \Phi^P}{\sqrt{2}} \\
\phi^0 &= \frac{s_P G^0 + c_P \Phi^P}{\sqrt{2}} - i\frac{s_0 H + c_0 \Phi^0 + \sqrt{2} v'}{\sqrt{2}} \\
h^+ &= c_+ G^+ - s_+ \Phi^+ \\
\phi^+ &= \frac{s_+ G^+ + c_+ \Phi^+}{i} \\
\phi^{++} &= \frac{\Phi^{++}}{i}.
\end{aligned} \tag{2.36}$$

Here H is the light neutral scalar, Φ^0 and Φ^P are the heavy neutral scalar and pseudoscalar and Φ^+, Φ^{++} are singly and doubly charged heavy scalars and G^0 and G^+ are the Goldstone bosons that are eaten by the SM W and Z gauge bosons. Up to order v^2/f^2 the mixing angles are given [33] by

$$\begin{aligned} s_P &= \frac{2\sqrt{2}v'}{\sqrt{v^2+8v'^2}} \simeq 2\sqrt{2}\frac{v'}{v} \\ c_P &= \frac{v}{\sqrt{v^2+8v'^2}} \simeq 1-4\frac{v'^2}{v^2} \\ s_+ &= \frac{2v'}{\sqrt{v^2+4v'^2}} \simeq 2\frac{v'}{v} \\ c_+ &= \frac{v}{\sqrt{v^2+4v'^2}} \simeq 1-2\frac{v'^2}{v^2} \\ s_0 &\simeq 2\sqrt{2}\frac{v'}{v} \\ c_0 &\simeq 1-4\frac{v'^2}{v^2} \end{aligned}$$

The mass of the Higgs is given by

$$M_H^2 \simeq 2(\lambda_{h^4} - \frac{\lambda_{h\phi h}^2}{\lambda_{\phi^2}}) = 2\mu^2 \tag{2.37}$$

and, to leading order, the Φ states all have the same mass,

$$M_\Phi^2 \simeq \lambda_{\phi^2} f^2 = \frac{2M_H^2}{1-x^2}\frac{f^2}{v^2} \tag{2.38}$$

2.4.1 Gauge boson masses and mixing

The EWSB generates vevs for the scalar fields, and these vevs generate mass terms for the gauge bosons. The gauge boson mass terms may be found by substituting the scalar vevs into expressions (2.16) and (2.17). The expression for the mass of the $W^\pm$ differs from the SM case at order v^2/f^2 as there is mixing amongst the scalars, mixing between the heavy and light gauge bosons, and other modifications due to the form of the couplings of the nlsm fields to the gauge bosons.

Only the charged gauge bosons are relevant to the work in this thesis so only these are examined here. In terms of the pre-EWSB mass eigenstates, and up to terms of order v^4/f^4 relative to f^2, the charged gauge boson mass terms are

$$\mathcal{L}_\Sigma = \frac{1}{2}\sum_{a=1,2} \begin{pmatrix} W^a, & W'^a \end{pmatrix} M_W^2 \begin{pmatrix} W^a \\ W'^a \end{pmatrix} \tag{2.39}$$

where

$$M_W^2 = \begin{pmatrix} a & -a(c^2-s^2)/2sc \\ -a(c^2-s^2)/2sc & -f^2g^2/4s^2c^2 - a \end{pmatrix} \tag{2.40}$$

and

$$a = \frac{1}{4}g^2v^2(1 + \frac{v^2}{f^2}(2\frac{fv'}{v^2} - \frac{2}{3})). \tag{2.41}$$

This mass matrix can be diagonalized by performing the transformation

$$\begin{pmatrix} W \\ W' \end{pmatrix} = \begin{pmatrix} 1 & \beta \\ -\beta & 1 \end{pmatrix} \begin{pmatrix} W_L \\ W_H \end{pmatrix} \tag{2.42}$$

where

$$\beta = \frac{1}{2}sc(c^2 - s^2)\frac{v^2}{f^2} \tag{2.43}$$

Performing this diagonalization gives the masses of the charged gauge bosons,

$$M^2_{W_L} = \frac{g^2v^2}{4}[1 - \frac{v^2}{f^2}(\frac{1}{6} + \frac{1}{4}(c^2 - s^2)^2 + \frac{4f^2v'^2}{v^4})] \tag{2.44}$$

and

$$M^2_{W_H} = \frac{f^2g^2}{4s^2c^2} - M^2_{W_L} \tag{2.45}$$

2.4.2 The top sector

The scalar vevs also generate mass terms for the fermions. The top sector mass terms are of particular interest due to the large coupling of the top quark to scalars. These mass terms are generated by substituting the scalar vevs into (2.23) and (2.24) which, in terms of the pre-EWSB mass eigenstates, gives

$$\mathcal{L}_t = -\begin{pmatrix} t_3, & \tilde{t} \end{pmatrix} M_t \begin{pmatrix} u_3^c \\ \tilde{t}^c \end{pmatrix} \tag{2.46}$$

where the mass matrix M_t is given, up to terms of order fv^3/f^3, by

$$M_t = \begin{pmatrix} \frac{\lambda_1\lambda_2 v}{\sqrt{\lambda_1^2+\lambda_2^2}}[1 + \frac{v^2}{f^2}(-\frac{1}{3} + \frac{fv'}{v^2})] & \frac{\lambda_1^2 v}{\sqrt{\lambda_1^2+\lambda_2^2}}[1 + \frac{v^2}{f^2}(-\frac{1}{3} + \frac{fv'}{v^2})] \\ -\frac{\lambda_1\lambda_2}{\sqrt{\lambda_1^2+\lambda_2^2}}\frac{v^2}{2f} & f\sqrt{\lambda_1^2+\lambda_2^2} - \frac{\lambda_1^2}{\sqrt{\lambda_1^2+\lambda_2^2}}\frac{v^2}{2f} \end{pmatrix} \tag{2.47}$$

This is in agreement with [33] after taking account of the quark rephasings to guarantee real and positive fermion masses. The top sector mass matrix can be diagonalized by performing the following transformations,

$$\begin{pmatrix} t_3 \\ \tilde{t} \end{pmatrix} = \begin{pmatrix} c_L & s_L \\ -s_L & c_L \end{pmatrix} \begin{pmatrix} t_L \\ T_L \end{pmatrix}$$
$$\begin{pmatrix} u_3^c \\ \tilde{t}^c \end{pmatrix} = \begin{pmatrix} c_R & s_R \\ -s_R & c_R \end{pmatrix} \begin{pmatrix} t_R^c \\ T_R^c \end{pmatrix} \tag{2.48}$$

where the mixing angles are

$$
\begin{aligned}
c_L &= 1 - \frac{1}{2}\frac{\lambda_1^4}{(\lambda_1^2+\lambda_2^2)^2}\frac{v^2}{f^2} \\
s_L &= \frac{\lambda_1^2}{\lambda_1^2+\lambda_2^2}\frac{v}{f}[1 + \frac{v^2}{f^2}(-\frac{5}{6} + \frac{fv'}{v^2} + \frac{\lambda_1^2}{\lambda_1^2+\lambda_2^2}(2 - \frac{3}{2}\frac{\lambda_1^2}{\lambda_1^2+\lambda_2^2}))] \\
c_R &= 1 \\
s_R &= \frac{1}{2}\frac{\lambda_1\lambda_2(\lambda_1^2+\lambda_2^2)}{(\lambda_1^2+\lambda_2^2)^2}\frac{v^2}{f^2}
\end{aligned}
$$

These rotations lead to the following masses for the t (light top) and T (heavy top) quarks

$$m_t = \frac{\lambda_1\lambda_2 v}{\sqrt{\lambda_1^2+\lambda_2^2}}[1 + \frac{v^2}{f^2}(\frac{fv'}{v^2} - \frac{1}{3} + \frac{1}{2}\frac{\lambda_1^2\lambda_2^2}{(\lambda_1^2+\lambda_2^2)^2}) + \mathcal{O}(\frac{v^3}{f^3})], \tag{2.49}$$

$$m_T = f\sqrt{\lambda_1^2+\lambda_2^2}[1 - \frac{v^2}{f^2}\frac{1}{2}\frac{\lambda_1^2\lambda_2^2}{(\lambda_1^2+\lambda_2^2)^2} + \mathcal{O}(\frac{v^3}{f^3})]. \tag{2.50}$$

The transformations which diagonalize the mass matrix do not agree with those given in appendix A of [33], and implicitly used elsewhere by those who take their Feynman rules from the tables in appendix B of the same paper. Note that the transformation of the left handed fields given in [33] are not unitary and so must be incorrect. The transformations of the right handed fields in [33] are unitary but also are incorrect.

2.5 Higgs Couplings

In later chapters it will be necessary to know the couplings of the Higgs to the charged gauge bosons and the top-sector quarks (other fermions' Higgs couplings are negligibly small).

2.5.1 W-Higgs Couplings

The coupling of the charged gauge bosons to the Higgs arises from the scalar kinetic term (2.5) with the covariant derivative (2.6). Keeping terms quadratic in ϕ and quartic in h leads to

$$
\begin{aligned}
\mathcal{L} &= \frac{f^2}{8}(g_1W_1 - g_2W_2)^2 + g_1g_2W_1W_2[\phi^*\phi + \frac{1}{2}h^*h \\
&\quad + \frac{1}{6f}(\phi h^{*2} + \phi^* h^2) - \frac{1}{4f^2}(\phi^*\phi h^* h + \frac{1}{3}(h^*h)^2)] + \text{h.o.t.}
\end{aligned} \tag{2.51}
$$

where "h.o.t." stands for "higher order terms". The Higgs coupling to W_L or W_H pairs is found by expressing the above Lagrangian in terms of the mass eigenstates of the fields (see equations (2.11), (2.36) and (2.42)). In this fashion the couplings $W_L^+W_L^-H$ and $W_H^+W_H^-H$ can be extracted,

$$\begin{aligned}\mathcal{L}_{WWH} &= \frac{g^2 v}{4}\left[1+\frac{v^2}{f^2}(-\frac{1}{3}-\frac{1}{2}(c^2-s^2)^2+4\frac{f^2 v'^2}{v^4})+\mathcal{O}(\frac{v^4}{f^4})\right]W_L^+ W_L^- H \\ &\quad -\frac{g^2 v}{2}[1+\mathcal{O}(\frac{v^2}{f^2})]W_H^+ W_H^- H. \end{aligned} \tag{2.52}$$

This Lagrangian may be rewritten in the form

$$\mathcal{L} = 2\frac{M_{W_L}^2}{v} y_{W_L} W_L^+ W_L^- H + 2\frac{M_{W_H}^2}{v} y_{W_H} W_H^+ W_H^- H \tag{2.53}$$

where

$$\begin{aligned} y_{W_L} &= 1+\frac{v^2}{f^2}[-\frac{1}{6}-\frac{1}{4}(c^2-s^2)^2] \\ y_{W_H} &= -s^2 c^2 \frac{v^2}{f^2}. \end{aligned} \tag{2.54}$$

Note that in the SM case $y_{W_L}=1$ and $y_{W_H}=0$ so the above couplings modify the SM at order v^2/f^2.

These couplings agree with those in [34] but, curiously, the W_L coupling does not agree with that given in Appendix B of their earlier paper [33].

2.5.2 Top-Higgs Couplings

The couplings of the quarks t and T to scalars arise from the top-sector Lagrangian (2.18). Expanding the Σ field and keeping terms up to quadratic order in ϕ^0 and cubic order in h^0 gives the Lagrangian

$$\begin{aligned}\mathcal{L} &= \sqrt{2}\lambda_1 t_3 (h^0 + \frac{i}{f}h^{0*}(h^0)^2)u_3'^c \\ &\quad -\lambda_1 f\tilde{t}(1-\frac{1}{f^2}h^{0*}h^0-\frac{2}{f^2}\phi^{0*}\phi^0)u_3'^c \\ &\quad -\lambda_2 f\tilde{t}\tilde{t}'^c. \end{aligned} \tag{2.55}$$

The coupling of the quarks to the Higgs can be extracted by expressing the fields in the above equation in terms of their mass eigenstates (see equations (2.21), (2.48) and (2.36)). This gives the couplings of the quarks to a single Higgs,

$$\begin{aligned}\mathcal{L} &= -\frac{\lambda_1\lambda_2}{\sqrt{\lambda_1^2+\lambda_2^2}}[1+\frac{v^2}{f^2}(-1-4\frac{f^2 v'^2}{v^4}+3\frac{f v'}{v^2}+\frac{3}{2}\frac{\lambda_1^2\lambda_2^2}{(\lambda_1^2+\lambda_2^2)^2})]t_L t_R^c H \\ &\quad +\frac{\lambda_1^2\lambda_2^2}{(\lambda_1^2+\lambda_2^2)^{\frac{3}{2}}}\frac{v}{f}T_L T_R^c H. \end{aligned} \tag{2.56}$$

This Lagrangian can be rewritten in the form,

$$\mathcal{L} = -\frac{m_t}{v} y_t \bar{t}tH - \frac{m_T}{v} y_T \bar{T}TH \tag{2.57}$$

where

$$\begin{aligned} y_t &= 1+\frac{v^2}{f^2}[-\frac{2}{3}+\frac{2fv'}{v^2}-\frac{4f^2v'^2}{v^4}+\frac{\lambda_1^2\lambda_2^2}{(\lambda_1^2+\lambda_2^2)^2}] \\ y_T &= -\frac{\lambda_1^2\lambda_2^2}{(\lambda_1^2+\lambda_2^2)^2}\frac{v^2}{f^2}. \end{aligned} \tag{2.58}$$

Again, this surprisingly agrees with the paper [34], despite the latest version of their earlier paper [33] having the wrong mixing matrix for the top sector.

The fact that [33] has the wrong mixing matrix for the top sector means that all the Feynman rules in appendix B which involve the t and T quarks are incorrect. The correct Feynman rules for the couplings of t and T to scalars, up to order v^2/f^2 and with the quark phase conventions defined in section 2.3, are given in table 2.1.

Table 2.1: Scalar-fermion Couplings

Vertex	Feynman Rule
$\bar{t}tH$	$\frac{-i\lambda_1\lambda_2}{\sqrt{\lambda_1^2+\lambda_2^2}}[1+\frac{v^2}{f^2}(-1-4\frac{f^2v'^2}{v^4}+3\frac{fv'}{v^2}+\frac{3}{2}\frac{\lambda_1^2\lambda_2^2}{(\lambda_1^2+\lambda_2^2)^2})]$
$\bar{T}TH$	$\frac{i\lambda_1^2\lambda_2^2}{(\lambda_1^2+\lambda_2^2)^{\frac{3}{2}}}\frac{v}{f}$
$\bar{t}TH$	$\frac{i\lambda_1^2}{\sqrt{\lambda_1^2+\lambda_2^2}}[1+\frac{v^2}{f^2}(-\frac{3}{2}-4\frac{f^2v'^2}{v^4}+3\frac{fv'}{v^2}+\frac{5}{2}\frac{\lambda_1^2}{\lambda_1^2+\lambda_2^2}-\frac{3}{2}\frac{\lambda_1^4}{(\lambda_1^2+\lambda_2^2)^2})]P_R$ $+\frac{i\lambda_1\lambda_2^3}{(\lambda_1^2+\lambda_2^2)^{\frac{3}{2}}}\frac{v}{f}P_L$
$\bar{T}tH$	$\frac{-i\lambda_1^2}{\sqrt{\lambda_1^2+\lambda_2^2}}[1+\frac{v^2}{f^2}(-\frac{3}{2}-4\frac{f^2v'^2}{v^4}+3\frac{fv'}{v^2}+\frac{5}{2}\frac{\lambda_1^2}{\lambda_1^2+\lambda_2^2}-\frac{3}{2}\frac{\lambda_1^4}{(\lambda_1^2+\lambda_2^2)^2})]P_L$ $+\frac{-i\lambda_1\lambda_2^3}{(\lambda_1^2+\lambda_2^2)^{\frac{3}{2}}}\frac{v}{f}P_R$
$\bar{t}tHH$	$\frac{2i\lambda_1\lambda_2}{\sqrt{\lambda_1^2+\lambda_2^2}}\frac{v}{f^2}[1-\frac{2fv'}{v^2}-\frac{1}{2}\frac{\lambda_1^2}{\lambda_1^2+\lambda_2^2}]$
$\bar{T}THH$	$\frac{i\lambda_1^2}{\sqrt{\lambda_1^2+\lambda_2^2}}\frac{1}{f}$
$\bar{t}t\Phi^0$	$\frac{-i\lambda_1\lambda_2}{\sqrt{\lambda_1^2+\lambda_2^2}}\frac{v}{\sqrt{2}f}[1-\frac{4fv'}{v^2}]$
$\bar{T}T\Phi^0$	$\frac{-i\lambda_1^4}{(\lambda_1^2+\lambda_2^2)^{\frac{3}{2}}}\frac{v^2}{f^2}[1-\frac{4fv'}{v^2}]$

Here, P_L and P_R are projection operators that project onto left and right handed fermion states respectively.

2.5.3 Scalar Trilinear Couplings

Another set of couplings which shall be needed in this thesis are the scalar trilinear couplings, specifically the Higgs trilear coupling and the coupling of a pair of Higgses

to a Φ. These arise from the Coleman-Weinberg (CW) potential, equation (2.33). The relevant trilinear couplings can be found by expressing the CW potential in terms of the physical eigenstates, given in equation (2.36). Up to leading order, this gives the Lagrangian

$$\mathcal{L} \simeq v(2\lambda_{h\phi h}\frac{fv'}{v^2} - \lambda_{h^4})HHH + \frac{f\lambda_{h\phi h}}{\sqrt{2}}HH\Phi \tag{2.59}$$

This Lagrangian can be rewritten in terms of the masses of the scalars given in equations (2.37) and (2.38) by using the equations for the scalar vevs (2.35) and the final relation in (2.34) to give

$$\mathcal{L} \simeq -\frac{m_H^2}{2v}HHH + \frac{\sqrt{2}M_\Phi^2}{v}\frac{v'}{v}HH\Phi \tag{2.60}$$

When corrections of order v^2/f^2 are taken into account the scalar trilinear couplings are found to be

Table 2.2: Scalar Trilinear Couplings

Vertex	Feynman Rule
HHH	$-i(3\frac{m_H^2}{v} - \frac{66M_\Phi^2 v'^2}{f^2 v})$
$HH\Phi$	$i(2\sqrt{2}\frac{M_\Phi^2}{f}\frac{fv'}{v^2} - 56\sqrt{2}\frac{M_\Phi^2}{f}\frac{f^3v'^3}{v^6}\frac{v^2}{f^2} + 29\frac{\sqrt{2}}{3}\frac{M_\Phi^2}{f}\frac{fv'}{v^2}\frac{v^2}{f^2}$

This is in agreement with the result in [35].

Also, in order to extract the couplings $\Phi^+\Phi - H$ and $\Phi^{++}\Phi^{--}H$, the higher order terms in the potential can be calculated from equations (2.25) and (2.29). These are

$$\Delta V = \lambda_{h\phi\phi h}h\phi^\dagger\phi h^\dagger + \lambda_{\phi^2\phi^2}(\mathrm{Tr}[\phi^\dagger\phi])^2 + \lambda_{\phi^4}\mathrm{Tr}[\phi^\dagger\phi\phi^\dagger\phi] \tag{2.61}$$

where

$$\begin{aligned}
\lambda_{h\phi\phi h} &= -\frac{4}{3}\lambda_{\phi^2} \\
\lambda_{\phi^2\phi^2} &= -48\lambda_1^2 \\
\lambda_{\phi^4} &= -a[\frac{g^2}{s^2c^2} + \frac{g'^2}{s'^2c'^2}] + 16a'\lambda_1^2
\end{aligned} \tag{2.62}$$

Expanding out this effective potential leads to the Lagrangian

$$\Delta\mathcal{L} = -2\frac{M_\Phi^2}{v}y_{\Phi^+}\Phi^+\Phi^-H - 2\frac{M_\Phi^2}{v}y_{\Phi^{++}}\Phi^{++}\Phi^{--}H \tag{2.63}$$

where

$$y_{\Phi^+} = \frac{v^2}{f^2}(-\frac{1}{3} + \frac{4v'^2f^2}{v^4}) \tag{2.64}$$

$$y_{\Phi^{++}} = \mathcal{O}(\frac{v^4}{f^4}, \frac{v^2}{16\pi^2f^2}) \tag{2.65}$$

as in reference [34].

2.6 Muon Decay and the Fermi Constant

In the SM the vacuum expectation value of the Higgs field can be obtained from the Fermi constant G_F. The Fermi constant is accurately known from measurements of the muon lifetime [2]. The muon decays by emitting a W^- and a ν_μ, with the W^- decaying to an e^- and $\bar{\nu}_e$. The vev of the Higgs can be obtained by integrating out the W and setting the coefficient of the four fermion operator (which depends on v through the mass of the W) to $G_F/\sqrt{2}$.

In the SM, the coupling of the $W^\pm$ to the first 2 families of leptons are described by the Lagrangian

$$\mathcal{L} = g(W^+_\alpha J^{+\,\alpha}_W + W^-_\alpha J^{-\,\alpha}_W) \tag{2.66}$$

where

$$\begin{aligned} {J^\alpha_W}^+ &= \frac{1}{\sqrt{2}}[\bar{\nu}_e\gamma^\alpha(\frac{1-\gamma^5}{2})e + \bar{\nu}_\mu\gamma^\alpha(\frac{1-\gamma^5}{2})\mu] \\ {J^\alpha_W}^- &= \frac{1}{\sqrt{2}}[\bar{e}\gamma^\alpha(\frac{1-\gamma^5}{2})\nu_e + \bar{\mu}\gamma^\alpha(\frac{1-\gamma^5}{2})\nu_\mu]. \end{aligned} \tag{2.67}$$

Taking the 4-momentum of the intermediate W to be q, we can write a four fermion effective Lagrangian term for processes where $q \ll M_W$. For the interaction of a muon and muon neutrino with an electron and electron neutrino the contribution of a single intermediate W is

$$\begin{aligned} \mathcal{L}_{\text{eff}} &\simeq \frac{1}{i}\frac{(ig)^2}{2}(\bar{\mu}\gamma^\alpha(\frac{1-\gamma^5}{2})\nu_\mu)\frac{-ig_{\alpha\beta}}{q^2-M_W^2}(\bar{\nu}_e\gamma^\beta(\frac{1-\gamma^5}{2})e) + \text{h.c.} \\ &\xrightarrow[q\to 0]{} -\frac{g^2}{8M_W^2}((\bar{\mu}\gamma^\alpha(1-\gamma^5)\nu_\mu)(\bar{\nu}_e\gamma_\alpha(1-\gamma^5)e) + \text{h.c.}) \\ &\equiv -\frac{G_F}{\sqrt{2}}((\bar{\mu}\gamma^\alpha(1-\gamma^5)\nu_\mu)(\bar{\nu}_e\gamma_\alpha(1-\gamma^5)e) + \text{h.c.}). \end{aligned} \tag{2.68}$$

This is illustrated in diagram 2.1.

The last line of equation (2.68) is to be understood to define the fermi constant, G_F. This leads to the (tree level) SM relation

$$\begin{aligned} G_F &= \sqrt{2}\frac{g^2}{8M_W^2} \\ &= \frac{1}{\sqrt{2}v^2}. \end{aligned} \tag{2.69}$$

Where the SM relation $M_W^2 = g^2v^2/4$ has been used in the last line. So we see that in the SM the vev of the Higgs field can be traded for the Fermi constant as defined in the decay of the muon.

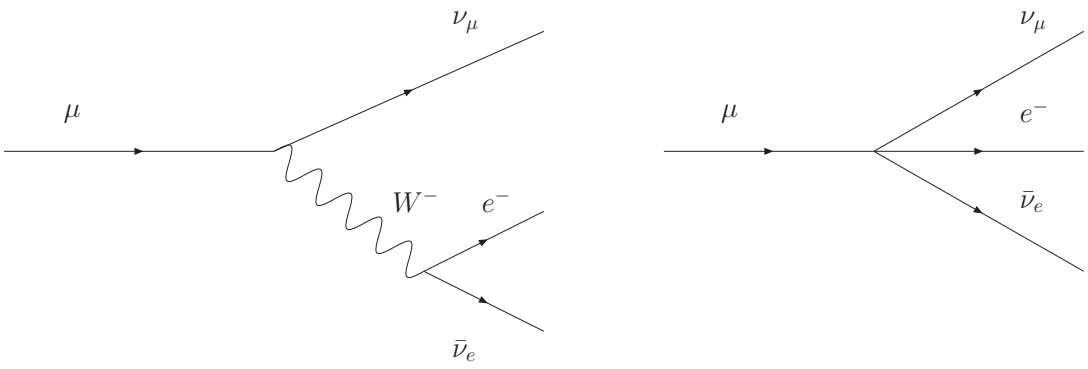

Figure 2.1: Integrating out the W leads to an effective four fermion vertex.

This simple relationship between v and G_F is modified in the Littlest Higgs model. The coupling of the W_L boson to the leptons is modified due to the mixing in the gauge boson sector. Also, the expression for M_{W_L} is modified. Furthermore, the heavy gauge boson W_H also contributes to the decay of the muon.

The Lagrangian of the Littlest Higgs model must be invariant under $[SU(2)_1 \otimes U(1)_1] \otimes [SU(2)_2 \otimes U(1)_2]$ gauge transformations. If the scalar couplings of the quarks discussed in the previous sections are to be gauge invariant the left handed SM fermion doublets must be taken to transform as doublets under $SU(2)_1$ and singlets under $SU(2)_2$. This means the Littlest Higgs counterpart of equation (2.66) is

$$\mathcal{L} = g_1(W_{1_\alpha}^{+} J_W^{+\alpha} + W_{1_\alpha}^{-} J_W^{-\alpha}). \tag{2.70}$$

Using equations (2.11), (2.12), (2.15) and (2.42) to rewrite $g_1 W_1$ in terms of g and the mass eigenstates W_L and W_H gives

$$\begin{aligned}\mathcal{L} &= g\left[\left((1-\frac{1}{2}c^2(c^2-s^2)\frac{v^2}{f^2})W_{L_\alpha}^{+} - \frac{c}{s}((1+\frac{1}{2}s^2(c^2-s^2)\frac{v^2}{f^2})W_{H_\alpha}^{+}\right) J_W^{+\alpha}\right. \\ &\quad \left. + \left((1-\frac{1}{2}c^2(c^2-s^2)\frac{v^2}{f^2})W_{L_\alpha}^{-} - \frac{c}{s}(1+\frac{1}{2}s^2(c^2-s^2)\frac{v^2}{f^2})W_{H_\alpha}^{-}\right) J_W^{-\alpha}\right] \end{aligned} \tag{2.71}$$

The contribution to the effective four fermion vertex arising from the interaction intermediated by a W_L is then

$$(\Delta\mathcal{L}_{\text{eff}})_{W_L} = \frac{-g^2}{8M_{W_L}^2}[1 - c^2(c^2-s^2)\frac{v^2}{f^2}](\bar{\mu}\gamma^\alpha(1-\gamma^5)\nu_\mu)(\bar{\nu}_e\gamma_\alpha(1-\gamma^5)e) \tag{2.72}$$

and, similarly, the contribution from the W_H intermediated interaction is

$$(\Delta\mathcal{L}_{\text{eff}})_{W_H} = \frac{-g^2}{8M_{W_H}^2}\frac{c^2}{s^2}[1 + s^2(c^2-s^2)\frac{v^2}{f^2}](\bar{\mu}\gamma^\alpha(1-\gamma^5)\nu_\mu)(\bar{\nu}_e\gamma_\alpha(1-\gamma^5)e). \tag{2.73}$$

Note that in the limit $c \to 0$, $s \to 1$ the normal four fermion effective theory is recovered.

Substituting in the formulae for the masses of the W_L and W_H, equations (2.44) and (2.45), and adding the 2 contributions together gives

$$\mathcal{L}_{\text{eff}} = \frac{-1}{2v^2}[1 + \frac{v^2}{f^2}(\frac{5}{12} - \frac{4f^2v'^2}{v^4})](\bar{\mu}\gamma^\alpha(1-\gamma^5)\nu_\mu)(\bar{\nu}_e\gamma_\alpha(1-\gamma^5)e). \tag{2.74}$$

As before we take this to be equal to $-G_F/\sqrt{2}$ giving the ralation

$$\frac{1}{\sqrt{2}v^2} = G_F y_{G_F}^2 \tag{2.75}$$

where

$$y_{G_F}^2 = 1 + \frac{v^2}{f^2}(\frac{4f^2v'^2}{v^4} - \frac{5}{12}), \tag{2.76}$$

in agreement with the result stated in [34].

2.7 Electroweak Precision Constraints

Before proceding any further a note on the impact of EWPCs on the Littlest Higgs model is in order. The parameter f is tightly constrained by the EWPCs. Analyses of the EWPCs in the Littlest Higgs model which include LEP2 data are to be found in references [36],[37], [38]. The strongest constraints come from operators generated through exchange of heavy vector bosons, with smaller contributions coming from the triplet vev [39].

The stringency of the constraints depend on how the fermions are taken to transform under the gauge groups. If the SM fermions are taken to transform only under $[SU(2)\otimes U(1)]_1$, reference [36] finds an extremely tight constraint, $f \gtrsim 5$ TeV at 99% C.L., and even then only in certain regions of the parameter space where $g_2 > g_1$, $g_2' > g_1'$. However, in some regions of parameter space the 1-loop corrections to the mass of the Z from the scalar ϕ partially cancel some of the tree level Little Higgs corrections to the ρ parameter which may have some effect in reducing this constraint [40].

The fermions may be taken to transform under $SU(2)_1 \otimes U(1)_1 \otimes U(1)_2$, subject to the constraint that the correct SM hypercharge quantum numbers are reproduced. In this case the constraint on f can be weakened to $f \gtrsim 2-3$ TeV [36].

Another intriguing possibility is to gauge only $SU(2)_1 \otimes SU(2)_2 \otimes U(1)_Y$ [41]. In this case the heavy B_H is not present which means a quadratic divergence in the Higgs mass due to B loops remains. However, due to the relatively small hypercharge coupling this does not lead to significant fine tuning. Since the B_H is the lightest of the new gauge bosons predicted in the Littlest Higgs model, getting rid of it allows a substantial weakening of the bounds on f from EWPCs with values as low as 1 TeV allowed [42].

One further way of evading the EWPCs is to introduce a discrete symmetry called T-parity (in analogy with R-parity in supersymmetric theories) under which all SM particles are even and the new heavy gauge bosons are odd [17], [18]. This allows a substantial reduction in the bounds on f because all heavy gauge bosons must be produced in pairs, eliminating their tree level contributions to EWPCs, as well as producing a dark matter candidate (generically the A_H). On the other hand, a consistent

implementation of T-parity requires the introduction of new extra fermions which make the model more complicated and spoil its "minimal" nature. The Littlest Higgs model with T-parity will not be considered in this thesis.

Chapter 3

The Schmaltz Model

3.1 Overview of the Schmaltz Model

In the Schmaltz model [16],[15],the SM electroweak gauge group, $SU(2)_L \otimes U(1)_Y$, is enlarged to $SU(3)_L \otimes U(1)_X$. The model contains two $SU(3)_L$ complex triplet scalar fields which, in the absence of gauge and Yukawa couplings, lead to two global $SU(3)$ symmetries, both of which must be broken if the Higgs is to gain a mass.

At some scale Λ_S the complex triplets aquire aligned vevs, f_1 and f_2, of order $\Lambda_S/4\pi$. These vevs break the approximate global $SU(3)^2$ symmetry down to $SU(2)^2$ leading to massless Goldstone bosons. At the same time, the $SU(3)_L \otimes U(1)_X$ gauge group is broken down to the SM $SU(2)_L \otimes U(1)_Y$.

The Goldstone bosons associated with the diagonal part of the broken global symmetry give mass via the Higgs mechanism to the gauge bosons associated with the $SU(3)$ symmetry breaking. The remaining Goldstone bosons comprise a complex $SU(2)$ doublet h, which plays the role of the SM Higgs, and a real singlet η.

The Schmaltz model implements the Little Higgs collective symmetry breaking mechanism to keep the Higgs naturally light. The Yukawa and gauge couplings explicitly break the global symmetries of the model, however each coupling taken individually preserves enough of the global symmetry to guarantee the masslessness of the Higgs. Only by including two or more of these couplings is the Higgs able to aquire a mass radiatively.

There are no one loop quadratically divergent diagrams which contain two or more different gauge or Yukawa couplings. This means that the Higgs can only aquire a logarithmically divergent mass at one loop, with quadradically divergent contributions only entering at two or more loops.

In this chapter elements of the low energy effective theory of the Schmaltz model are worked out, as for the Littlest Higgs Model in chapter 2. The method is more or less the same. First the contributions to the Coleman-Weinberg potential from the gauge and Yukawa sectors are computed, followed by an account of the EWSB and the masses and mixing of the fermions and gauge bosons. Next the corrections to the relation between the Higgs vev and the Fermi constant as measured in muon decay are computed, and the chapter closes with a brief overview of the EWPCs.

3.2 Scalar Kinetic Terms

The model contains two complex triplet scalar fields, Φ_1 and Φ_2, which aquire vevs f_1 and f_2 respectively. The Goldstone bosons can be parameterised in an nlsm. In the unitary gauge, where the gauge bosons associated with the longitudinal components of the heavy gauge bosons have been rotated away with a gauge transformation, the scalar fields take the form

$$\Phi_1 = e^{i\Theta\frac{f_2}{f_1}} \begin{pmatrix} 0 \\ 0 \\ f_1 \end{pmatrix}, \qquad \Phi_2 = e^{-i\Theta\frac{f_2}{f_1}} \begin{pmatrix} 0 \\ 0 \\ f_2 \end{pmatrix} \tag{3.1}$$

where

$$\Theta = \frac{1}{f}\left[\frac{\eta}{\sqrt{2}} + \begin{pmatrix} 0 & 0 & h^* \\ 0 & 0 & \\ & h^T & 0 \end{pmatrix}\right] \tag{3.2}$$

with $h = (h^+, h^0)^T$ and $f^2 = f_1^2 + f_2^2$.

Both these scalar fields are complex triplets under $SU(3)_L$ and have charge $-1/3$ under $U(1)_X$. The scalar kinetic term is

$$\mathcal{L}_\Phi = |\mathcal{D}_\mu \Phi_1|^2 + |\mathcal{D}_\mu \Phi_2|^2 \tag{3.3}$$

where the covariant derivative is given by

$$\mathcal{D}_\mu \Phi_i = (\partial_\mu + igA^a_\mu T^a - \frac{i}{3} g_x A^x_\mu)\Phi_i. \tag{3.4}$$

Prior to EWSB the scalar kinetic term leads to mass terms of order f for the gauge bosons associated with the broken part of the $SU(3)_L$ gauge symmetry. These are

$$\mathcal{L}_\Phi \approx \frac{g^2 f^2}{4} X'^+_\mu X'^{-\mu} + \frac{g^2 f^2}{4} Y'^0_\mu \bar{Y}'^{0\mu} + f^2 (A^8_\mu, A^x_\mu) \begin{pmatrix} \frac{g^2}{3} & \frac{g g_x}{\sqrt{3}} \\ \frac{g g_x}{\sqrt{3}} & \frac{g_x^2}{9} \end{pmatrix} \begin{pmatrix} A^8_\mu \\ A^x_\mu \end{pmatrix}. \tag{3.5}$$

Here $iX'^+ = 1/\sqrt{2}(A^4 + iA^5)$ and $-iY'^0 = 1/\sqrt{2}(A^6 + iA^7)$ form an $SU(2)_L$ doublet. There is mixing between the neutral gauge boson associated with the diagonal $SU(3)_L$ generator T^8 and the $U(1)_X$ gauge boson A^x. These mass terms are diagonalised by the transformation

$$\begin{pmatrix} A^8_\mu \\ A^x_\mu \end{pmatrix} = \frac{1}{\sqrt{3g^2 + g_x^2}} \begin{pmatrix} \sqrt{3}g & -g_x \\ g_x & \sqrt{3}g \end{pmatrix} \begin{pmatrix} \tilde{Z}'_\mu \\ B_\mu \end{pmatrix}. \tag{3.6}$$

Here, B_μ is the hypercharge gauge boson. The term in the covariant derivative which contains B_μ is

$$\mathcal{D}_\mu \Phi_i \approx -\frac{ig'}{2} \begin{pmatrix} 1 & 0 & 0 \\ 0 & 1 & 0 \\ 0 & 0 & 0 \end{pmatrix} B_\mu \Phi_i \tag{3.7}$$

showing that the $U(1)_Y$ gauge symmetry operates only on those components of $SU(3)$ triplets which transform under the unbroken $SU(2)$ subgroup. Here, the hypercharge gauge coupling g' is given by

$$g' = \frac{g_x}{\sqrt{1 + \frac{g_x^2}{3g^2}}}. \tag{3.8}$$

It is interesting to note that, unlike in the Littlest Higgs model, the gauge couplings of the Schmaltz model can be calculated in terms of the known $SU(2)_L \otimes U(1)_Y$ gauge couplings of the SM.

In order to determine the contribution to the Coleman-Weinberg potential from the gauge boson sector it is necessary to know the field dependent mass matrix of the gauge bosons. This originates from the scalar kinetic terms and is given by

$$\mathcal{L}_\Phi \approx \sum_{i=1,2} \mathrm{tr}[(gA_\mu^a T^a - \frac{1}{3} g_x A_\mu^x)^2 \Phi_i \Phi_i^\dagger]. \tag{3.9}$$

3.3 Fermion-Scalar Interactions

Since the $SU(2)_L$ of the SM is enlarged to $SU(3)_L$ in the Schmaltz model, it is necessary to extend all SM $SU(2)$ doublets to $SU(3)$ triplets. In particular, new left handed fermions are required to extend the SM quark and lepton doublets to $SU(3)$ triplets, and new right handed singlet states are required to write mass terms for the new fermions.

There is some freedom to choose how to extend the SM fermion doublets to $SU(3)$ triplets. Two models are discussed in the literature.

In model I each generation of fermions is extended to include a new heavy "neutrino" and a heavy up-type quark. This is attractive in that it preserves the symmetry between the generations, but it leaves the $SU(3)$ and $U(1)_X$ gauge groups anomalous [15], [43], [22].

In model II each generation receives a heavy "neutrino" but the quark assignments are more complicated, with the first two generations receiving down-type quarks and only the third generation receiving an up-type quark. This breaks the inter-generational symmetry but cancels the $SU(3)$ gauge anomalies [43] making the model easier to UV complete [20].

It is important that the third generation receives a heavy up-type quark, since this allows us to cancel the top quark contribution to the Higgs mass in the Coleman-Weinberg potential. However, the first two generations can receive a quark of either type since there are no large contributions to the Coleman-Weinberg potential which need to be cancelled.

3.3.1 Model I

In model I the SM lepton doublets are enlarged to $SU(3)$ triplets via the addition of a heavy neutrino-like field. Also, a right handed partner for the heavy neutrino

is required. The leptons of the mth generation (neglecting the right handed ν_m) are written as an $SU(3)$ triplet and a pair of singlet states as follows

$$L_m = \begin{pmatrix} -ie'^{-}_m \\ i\nu'_m \\ N'_m \end{pmatrix}, \quad e'^{\,c}_m, \quad N^c_m. \tag{3.10}$$

Also, each SM quark doublet gets extended to an $SU(3)$ triplet via the addition of an up-type quark, with a new right handed singlet state also present. Then the mth generation quarks are

$$Q_m = \begin{pmatrix} -id'_m \\ iu'_{1m} \\ u'_{2m} \end{pmatrix}, \quad u'^{\,c}_{1m}, \quad u'^{\,c}_{2m}, \quad b'^{\,c}_m \tag{3.11}$$

The phases of the fermions have been chosen to ensure the masses are real and positive.

The SM Yukawa couplings are reproduced by expanding out the Φ_i fields to leading order in h/f, if the scalar fermion couplings take the form

$$\mathcal{L}_{\text{Yuk}} = -\lambda_1^m u'^{\,c}_{1m}\Phi_1^\dagger Q_m - \lambda_2^m u'^{\,c}_{2m}\Phi_2^\dagger Q_m - \frac{\lambda_d^{mn}\Phi_1^i\Phi_2^j Q_m^k \epsilon^{ijk} d'^{\,c}_n}{\Lambda} \tag{3.12}$$

$$-\lambda_N^m N_m^c \Phi_2^\dagger L_m - \frac{\lambda_e^{mn}\Phi_1^i\Phi_2^j L_m^k \epsilon^{ijk} e'^{\,c}_n}{\Lambda} \tag{3.13}$$

where $\{m, n\}$ are generation indices running over $\{1, 2, 3\}$ and $\{i, j, k\}$ are $SU(3)$ indices also running over $\{1, 2, 3\}$.

Note that the assumption has been made that it is possible to find a basis for the fermions such that the scalar couplings for the up-type quarks and heavy neutrinos do not couple together fermions from different generations. In principle this is not forbidden but it is necessary to make some such assumption about the scalar couplings in order to suppress dangerous FCNCs. As a result of this assumption the up-type quarks only mix with other up-type quarks of the same generation and the same is true of the neutral leptons.

This implies that all the mixing between fermions of different generations comes from the charged lepton and down-type quark couplings. In particular, all the mixing that leads to the CKM matrix comes from the off diagonal terms of the 3×3 matrix λ_d^{mn}. Also, there will in general be a matrix V^l which encodes the flavour misalignment in the lepton sector which will appear in the coupling of leptons to gauge bosons. Neutrino masses, and a possible right handed ν^c, are not considered here. Consequently, the matrix V^l can be absorbed into the ν'_i and so will not appear in the lepton couplings to the light neutrinos except insofar as they have a small mixing with the N'_i.

The structure of the scalar-fermion couplings is different from that in the original paper, [15]. In [15] the Lagrangian for the up-type quarks takes the form

$$\mathcal{L} = -\lambda_1^{mn} u'^{\,c}_{1\,m}\Phi_1^\dagger Q_n - \lambda_2^{mn} u'^{\,c}_{2\,m}\Phi_2^\dagger Q_n \tag{3.14}$$

If it is assumed that λ_2 is proportional to the unit matrix, it is then possible to diagonalise the matrix λ_1 by unitary transformations of the $u'^{\,c}_{1m}$ and the Q_n. The unitary

matrix which describes the mixing of the Q_n then appears in the λ_2 term, but it commutes with the λ_2 matrix (since λ_2 is proportional to the unit matrix) and can be absorbed into a tranformation on the $u'^{\,c}_{2m}$. This makes both λ_1 and λ_2 diagonal with λ_2 proportional to the unit matrix.

The assumption that λ_2 is proportional to the unit matrix is a stronger assumption than that adopted in equation (3.12). To avoid flavour changing effects is enough to assume there exist some bases for the $u'^{\,c}_{1m}$, $u'^{\,c}_{2m}$ and Q_m such that both λ_1 and λ_2 are simultaneously diagonal. Some small amount of flavour changing may be permissible so there could be small off-diagonal terms in $\lambda_{1,2}$, but here it is assumed these are zero.

3.3.2 Model II

In model II the leptons and the third generation quarks are the same as in model I, but the first and second generations get a new down-type quark instead of a new up-type quark. This entails adding an extra down-type right handed singlet state and putting the left handed quarks into the $\bar{3}$ representation of $SU(3)$. The generation one and two fermions are then

$$Q_m = \begin{pmatrix} -iu'_m \\ -id'_{1m} \\ d'_{2m} \end{pmatrix}, \quad d'^{\,c}_{1m}, \quad d'^{\,c}_{2m}, \quad u'_m. \tag{3.15}$$

The quark-scalar couplings are then

$$\begin{aligned} \mathcal{L}_{\text{Yuk}} &= -\lambda_1^m d'^{\,c}_{1m} Q_m^T \Phi_1 - \lambda_2^m d'^{\,c}_{2m} Q_m^T \Phi_2 + \frac{\lambda_u^{mn} \Phi_1^{*i} \Phi_2^{*j} Q_m^k \epsilon^{ijk} u'^{\,c}_n}{\Lambda} && (3.16) \\ &\quad -\lambda_1^3 u'^{\,c}_{13} \Phi_1^\dagger Q_3 - \lambda_2^3 u'^{\,c}_{23} \Phi_2^\dagger Q_3 - \frac{\lambda_d^3 \Phi_1^i \Phi_2^j Q_3^k \epsilon^{ijk} d'^{\,c}_3}{\Lambda} && (3.17) \end{aligned}$$

where the generation indices $\{m, n\}$ run over $\{1, 2\}$ and the lepton-scalar couplings are the same as in model I. Here, as before, the phases and couplings of the quarks have been chosen such that the quark masses are real and positive and the SM Yukawa couplings are correctly reproduced when the Φ_i fields are expanded at leading order in h/f.

Couplings of this form guarantee that the light quarks in each generation only mix with heavy quarks of the same generation (i.e. they don't mix with heavy quarks of other generations). This assumption is made to make the theory safe from flavour changing effects which could contribute to $\bar{D}^0 - D$ mixing.

3.3.3 The Top Sector

Given the flavour structure of the scalar-fermion couplings, chosen to suppress flavour changing effects, the third generation up-type (top sector) quark mass terms are the same in both model I and model II. The top sector Lagrangian may be written

$$\mathcal{L}_t = -\lambda_1 t'^{\,c}_1 \Phi_1^\dagger Q_3 - \lambda_2 t'^{\,c}_2 \Phi_2^\dagger Q_3 \tag{3.18}$$

where for present purposes λ_i^3 is written as simply λ_i to ease notation and

$$Q_3 = \begin{pmatrix} -ib \\ it_1 \\ t_2 \end{pmatrix}. \tag{3.19}$$

Before EWSB the f vevs generate mass terms

$$\mathcal{L}_t \approx -\lambda_1 f_1 t_1'^c t_2 - \lambda_2 f_2 t_2'^c t_2. \tag{3.20}$$

This is diagonalized by performing the transformation,

$$\begin{pmatrix} t_1^c & t_2^c \end{pmatrix} = \begin{pmatrix} t_1'^c & t_2'^c \end{pmatrix} \begin{pmatrix} c & s \\ -s & c \end{pmatrix} \tag{3.21}$$

where $c = \lambda_2 f_2/m_T$, $s = \lambda_1 f_1/m_T$ and $m_T = \sqrt{\lambda_1^2 f_1^2 + \lambda_2^2 f_2^2}$. This leads to one heavy quark of mass m_T and one quark which remains massless before EWSB.

The field dependent mass matrix will be required in order to compute the fermion contribution to the effective potential. Neglecting all Yukawa couplings other than those in the top sector yields the Lagrangian

$$\mathcal{L}_t = -[M_t(\Phi_1, \Phi_2)]_{ij} Q_R^i Q_3^j \tag{3.22}$$

where the right handed third generation quarks have been gathered into the object

$$Q_R = \begin{pmatrix} b^c \\ t_1'^c \\ t_2'^c \end{pmatrix} \tag{3.23}$$

and the quark mass matrix is

$$M_t(\Phi_1, \Phi_2) = \begin{pmatrix} 0 & 0 & 0 \\ & \lambda_1 \Phi_1^\dagger & \\ & \lambda_2 \Phi_2^\dagger & \end{pmatrix} \tag{3.24}$$

3.4 Electroweak Symmetry Breaking

The interactions of the Higgs with fermions and gauge bosons generate an effective potential for the Higgs of the form

$$V_{\text{eff}} = \delta m^2 h^\dagger h + \delta\lambda (h^\dagger h)^2 \tag{3.25}$$

The fermion contribution to the effective potential is given by the formula

$$V_f = -\frac{3}{8\pi^2}\Lambda^2 \text{Tr}[M_t M_t^\dagger] + \frac{3}{16\pi^2}\text{Tr}[(M_t M_t^\dagger)^2 \log(\frac{\Lambda^2}{M_t M_t^\dagger})] \tag{3.26}$$

as in [15]. Note that [15] has a factor $3/16\pi^2$ in the first term of the above equation. This should be $3/8\pi^2$, and indeed this mistake is corrected on the next line of that paper. Using equation (3.24),

$$M_t M_t^\dagger = \begin{pmatrix} 0 & 0 & 0 \\ 0 & \lambda_1^2 f_1^2 & \lambda_1\lambda_2 \Phi_1^\dagger \Phi_2 \\ 0 & \lambda_1\lambda_2 \Phi_2^\dagger \Phi_1 & \lambda_2^2 f_2^2 \end{pmatrix} \tag{3.27}$$

The (non-zero) eigenvalues of this matrix give the squares of the field dependent masses of the top quarks. The eigenvalues are

$$m = \frac{1}{2}m_T^2 \left(1 \pm \sqrt{1 - \frac{4(\lambda_1^2\lambda_2^2 f_1^2 f_2^2 - \lambda_1^2\lambda_2^2|\Phi_1^\dagger\Phi_2|^2)}{m_T^4}}\right) \tag{3.28}$$

which, when expanded to fourth order in terms of h/f and η/f, are

$$m_{t,4}^2 = \lambda_t^2\langle h^\dagger h\rangle - \left[\frac{1}{3}\lambda_t^2\frac{f^2}{f_1^2 f_2^2} - \frac{\lambda_t^4}{m_T^2}\right]\langle h^\dagger h\rangle^2 \tag{3.29}$$

$$m_{T,4}^2 = m_T^2 - m_{t,4}^2 \tag{3.30}$$

where

$$\lambda_t = \lambda_1\lambda_2\frac{f}{m_T}. \tag{3.31}$$

Note that the quadratically divergent term in equation (3.26) contributes only a constant term to the effective potential, so there is no quadratically divergent contribution to the Higgs mass.

The field dependent masses of the gauge bosons are calculated from equation (3.9). The eigenvalues of the gauge boson mass matrix are given in [15] up to order h^4/f^2. These are given in table 3.1.

Table 3.1: Gauge Boson Mass Eigenvalues

Particle	Mass (to order h^4/f^2)
$W^\pm$	$\frac{g^2}{2}[1 + \frac{\langle h^\dagger h\rangle}{f^2}(1 - \frac{1}{3}\frac{f^4}{f_1^2 f_2^2})]\langle h^\dagger h\rangle$
$X^\pm$	$\frac{g^2 f^2}{2} - m_{W^\pm,4}^2$
Y^0	$\frac{g^2 f^2}{2}$
Z	$\frac{g^2}{2}(1+t^2)[1 + \frac{\langle h^\dagger h\rangle}{f^2}(1 - \frac{1}{3}\frac{f^4}{f_1^2 f_2^2} - \frac{1}{4}(1-t^2)^2)]\langle h^\dagger h\rangle$
Z'	$\frac{g^2 f^2}{2}\frac{4}{3-t^2} - m_{Z,4}^2$
B	0

Here, $t = \tan\theta_W = g'/g$ where θ_W is the weak mixing angle. Denoting the squared gauge boson mass matrix in the diagonal basis as M_V^2, the contribution of gauge boson loops to the effective potential is [15]

$$V_g = \frac{3}{32\pi^2}\Lambda^2\mathrm{Tr}[M_V^2] - \frac{3}{64\pi^2}\mathrm{Tr}[M_V^4\log(\frac{\Lambda^2}{M_V^2})]. \tag{3.32}$$

Note that, again, the quadratically divergent term contributes only a constant to the effective potential and there is no quadratically divergent contribution to the Higgs mass. Substituting the field dependent masses of the fermions and gauge bosons into equations (3.26) and (3.32) gives [15]

$$\delta m^2 = -\frac{3}{8\pi^2}[\lambda_t^2 m_T^2\log(\frac{\Lambda^2}{m_T^2}) - \frac{g^2}{4}m_X^2\log(\frac{\Lambda^2}{m_X^2}) - \frac{g^2}{8}(1+t^2)m_{Z'}^2\log(\frac{\Lambda^2}{m_{Z'}^2})] \tag{3.33}$$

and

$$\begin{aligned}\delta\lambda &= -\frac{\delta m^2}{3}\frac{f^2}{f_1^2 f_2^2} + \frac{3}{16\pi^2}\times \\ &\quad [\lambda_t^4(\log\left(\frac{m_T^2}{m_t^2}\right) - \frac{1}{2}) - \frac{g^4}{8}(\log\left(\frac{m_X^2}{m_W^2}\right) - \frac{1}{2}) - \frac{g^4}{16}(1+t^2)^2(\log\left(\frac{m_{Z'}^2}{m_Z^2}\right) - \frac{1}{2})].\end{aligned} \tag{3.34}$$

This generates a Higgs mass which is too large, $M_H = \mathcal{O}(1\text{TeV})$ for a typical set of parameters. This undesireably large Higgs mass can be remedied by including a tree level potential term,

$$\begin{aligned}V_{\text{tree}} &= \mu^2\Phi_1^\dagger\Phi_2 + \text{h.c.} \\ &= \mu^2\frac{f^2}{f_1 f_2}(h^\dagger h + \frac{1}{2}\eta^2) - \frac{1}{12}\mu^2\frac{f^4}{f_1^3 f_2^3}(h^\dagger h)^2 + \text{h.o.t.}.\end{aligned} \tag{3.35}$$

This introduces a partial cancellation of the Higgs mass term. Some tuning is needed between μ^2 and δm^2. However, this tuning is not too severe because, without the μ^2 term, there exists a global $U(1)$ symmetry under which Φ_1 and Φ_2 have opposite charges. The μ^2 term is the only term in the theory which breaks this symmetry so it is stable against radiative corrections and therefore does not constitute a reintroduction of the hierarchy problem. In addition to lowering the Higgs mass, the μ^2 term also generates a mass for the singlet scalar η.

3.4.1 Gauge Boson Masses And Mixing

The Higgs potential takes the required form for EWSB to occur. The Higgs mass is a free parameter since μ^2 is arbitrary. The Higgs will develop a vev, $\langle h^\dagger h\rangle = v^2/2$, generating mass terms for the fermions and gauge bosons.

The Higgs vev introduces mixing between the gauge bosons. Later on the mixing angles of the charged gauge bosons will be needed in order to calculate their couplings to the Higgs. The heavy $X'^{\pm}$ gauge boson mixes with the light $W'^{\pm}$ with a mass term of order v^3/f. In the charged gauge boson sector the mass terms, up to terms of order v^4/f^4, are

$$\mathcal{L}_W = \frac{1}{2}\begin{pmatrix} W'^- , & X'^- \end{pmatrix} M_{W^\pm}\begin{pmatrix} W'^+ \\ X'^+ \end{pmatrix} \tag{3.36}$$

where $W'^+ = (A^1 + iA^2)/\sqrt{2}$, $X'^\pm$ is defined below equation (3.5) and the matrix $M_{W^\pm}$ is

$$M_{W^\pm} = \begin{pmatrix} \frac{g^2 f^2}{2}[1 - \frac{1}{2}\frac{v^2}{f^2} + \frac{1}{12}(1 - \frac{1}{3}\frac{f^4}{f_1^2 f_2^2})\frac{v^4}{f^4}] & -\frac{g^2 v^2}{6\sqrt{2}}\frac{f_1^2 - f_2^2}{f_1 f_2}\frac{v}{f} \\ -\frac{g^2 v^2}{6\sqrt{2}}\frac{f_1^2 - f_2^2}{f_1 f_2}\frac{v}{f} & \frac{g^2 v^2}{4}(1 - \frac{1}{6}(1 - \frac{1}{3}\frac{f^4}{f_1^2 f_2^2})\frac{v^2}{f^2}) \end{pmatrix}. \tag{3.37}$$

The mass terms may be diagonalised by performing the transformation

$$\begin{pmatrix} X'^+ \\ W'^+ \end{pmatrix} = \begin{pmatrix} 1 & -\frac{1}{3\sqrt{2}}\frac{f_1^2 - f_2^2}{f_1 f_2}\frac{v^3}{f^3} \\ \frac{1}{3\sqrt{2}}\frac{f_1^2 - f_2^2}{f_1 f_2}\frac{v^3}{f^3} & 1 \end{pmatrix}\begin{pmatrix} X^+ \\ W^+ \end{pmatrix}. \tag{3.38}$$

This leads to a light $W^{\pm}$ and a heavy $X^{\pm}$ with masses (up to order v^4/f^2)

$$M^2_{W^{\pm},4} = \frac{g^2v^2}{4}[1+\frac{v^2}{2f^2}(1-\frac{1}{3}\frac{f^4}{f_1^2f_2^2})] \tag{3.39}$$

$$M^2_{X^{\pm},4} = \frac{g^2f^2}{2} - M_{W^{\pm},4}. \tag{3.40}$$

3.4.2 The Top Sector

The Higgs vev also generates mass terms for the fermions. Of particular interest are the third generation up-type quarks (the top sector) since these have the strongest coupling to the Higgs. After substituting in the Higgs vev, the top sector mass terms, up to terms of order v^4/f^3, are

$$\mathcal{L} \approx \left(\begin{array}{cc} t_1'^c & t_2'^c \end{array} \right) \left(\begin{array}{cc} \frac{\lambda_1 f_2}{\sqrt{2}}\frac{v}{f}(1-\frac{1}{12}\frac{f_2^2}{f_1^2}\frac{v^2}{f^2}) & \lambda_1 f_1(1-\frac{1}{4}\frac{f_2^2}{f_1^2}\frac{v^2}{f^2}+\frac{1}{96}\frac{f_2^4}{f_1^4}\frac{v^4}{f^4}) \\ -\frac{\lambda_2 f_1}{\sqrt{2}}\frac{v}{f}(1-\frac{1}{12}\frac{f_1^2}{f_2^2}\frac{v^2}{f^2}) & \lambda_2 f_2(1-\frac{1}{4}\frac{f_1^2}{f_2^2}\frac{v^2}{f^2}+\frac{1}{96}\frac{f_1^4}{f_2^4}\frac{v^4}{f^4}) \end{array} \right) \left(\begin{array}{c} t_1 \\ t_2 \end{array} \right). \tag{3.41}$$

These mass terms may be diagonalized by separate transformations on the left and right handed fermions. The pre-EWSB mass eigenstates may be found by expressing the right handed fields in terms of t_1^c and t_2^c, defined in equation 3.21. The post-EWSB mass eigenstates (up to order v^4/f^3) are found by performing the tranformations

$$\left(\begin{array}{c} t \\ T \end{array} \right) = \left(\begin{array}{cc} C_L & -S_L \\ S_L & C_L \end{array} \right) \left(\begin{array}{c} t_1 \\ t_2 \end{array} \right) \tag{3.42}$$

and

$$\left(\begin{array}{cc} t^c & T^c \end{array} \right) = \left(\begin{array}{cc} t_1^c & t_2^c \end{array} \right) \left(\begin{array}{cc} C_R & -S_R \\ S_R & C_R \end{array} \right) \tag{3.43}$$

where

$$C_R = 1-\frac{1}{2}c^2s^2(c^2-s^2)^2\frac{f^8}{16f_1^4f_2^4}\frac{v^4}{f^4} \tag{3.44}$$

$$S_R = cs(c^2-s^2)[\frac{f^4}{4f_1^2f_2^2}\frac{v^2}{f^2}+(\frac{1}{4}c^2s^2-\frac{1}{96})\frac{f^8}{f_1^4f_2^4}\frac{v^4}{f^4}] \tag{3.45}$$

$$\begin{aligned} C_L = {} & 1-\frac{1}{4}(s^2\frac{f_2}{f_1}-c^2\frac{f_1}{f_2})^2\frac{v^2}{f^2}+[-\frac{1}{2}(s^2\frac{f_2}{f_1}-c^2\frac{f_1}{f_2})^2(s^2\frac{f_2^2}{f_1^2}+c^2\frac{f_1^2}{f_2^2}) \\ & +\frac{11}{32}(s^2\frac{f_2}{f_1}-c^2\frac{f_1}{f_2})^4+\frac{1}{6}(s^2\frac{f_2}{f_1}-c^2\frac{f_1}{f_2})(s^2\frac{f_2^3}{f_1^3}-c^2\frac{f_1^3}{f_2^3})]\frac{v^4}{f^4} \end{aligned} \tag{3.46}$$

$$\begin{aligned} S_L = {} & \frac{1}{\sqrt{2}}(s^2\frac{f_2}{f_1}-c^2\frac{f_1}{f_2})\frac{v}{f}+\frac{1}{\sqrt{2}}[(s^2\frac{f_2^2}{f_1^2}+c^2\frac{f_1^2}{f_2^2})(s^2\frac{f_2}{f_1}-c^2\frac{f_1}{f_2}) \\ & -\frac{3}{4}(s^2\frac{f_2}{f_1}-c^2\frac{f_1}{f_2})^3-\frac{1}{3}(s^2\frac{f_2^3}{f_2^3}-c^2\frac{f_1^3}{f_2^3})]\frac{v^3}{f^3}. \end{aligned} \tag{3.47}$$

Here, c and s are as defined below equation (3.21). Performing these transformations allows the calculation of the masses of the t and T quarks, denoted M_t and M_T, up to order v^4/f^3.

$$M_t = \lambda_t \frac{v}{\sqrt{2}}[1 + \frac{1}{4}(\lambda_t^2 \frac{f^2}{m_T^2} - \frac{1}{3}\frac{f^4}{f_1^2 f_2^2})\frac{v^2}{f^2}] \tag{3.48}$$

and

$$M_T = m_T(1 - \frac{1}{4}\lambda_t^2 \frac{f^2}{m_T^2}\frac{v^2}{f^2} + (\frac{\lambda_t^2}{24}\frac{f^4}{f_1^2 f_2^2}\frac{f^2}{m_T^2} - \frac{5\lambda_t^4}{32}\frac{f^4}{m_T^4})\frac{v^4}{f^4}) \tag{3.49}$$

where m_T is defined below equation (3.21).

3.5 Higgs Couplings

It will be necessary in subsequent chapters to know the couplings of the Higgs to the $W^\pm$ and $X^\pm$ gauge bosons and to the t and T quarks.

3.5.1 W-Higgs Couplings

The W^+W^-H and X^+X^-H couplings arise from the scalar kinetic term, equation (3.9). The Φ fields are expanded in terms of h and the subsitution $h^T = (0, (v+H)/\sqrt{2})$ is made. Keeping terms linear in H, this leads to

$$\begin{aligned} \mathcal{L}_{WWH} &= \frac{g^2 f^2}{2}[\frac{v}{f}(1 + (1 - \frac{1}{3}\frac{f^4}{f_1^2 f_2^2})\frac{v^2}{f^2})(W'^+W'^- - X'^+X'^-)H & (3.50)\\ &\quad + \frac{v^2}{\sqrt{2}f^2}\frac{f_2^2 - f_1^2}{f_1 f_2}(X'^-W'^+ + W'^-X'^+)H]. & (3.51)\end{aligned}$$

In order to extract the couplings of the Higgs to the charged gauge boson mass eigenstates it is necessary to perform the rotation of equation (3.38). This leads to the couplings

$$\mathcal{L}_{WWH} \approx 2\frac{M_{W^\pm}^2}{v} y_{W^\pm} W^+W^-H + 2\frac{M_{X^\pm}^2}{v} y_{X^\pm} X^+X^-H \tag{3.52}$$

where

$$\begin{aligned} y_{W^\pm} &= 1 + \frac{1}{2}(1 - \frac{1}{3}\frac{f^4}{f_1^2 f_2^2})\frac{v^2}{f^2} & (3.53)\\ y_{X^\pm} &= -\frac{1}{2}\frac{v^2}{f^2}. & (3.54)\end{aligned}$$

Note that the SM couplings are reproduced in the limit $v/f \to 0$, i.e. $f \to \infty$.

3.5.2 Top-Higgs Couplings

The coupling of the t and T quarks to Higgses arises from the Yukawa-like terms in equation (3.18). In order to express the couplings in terms of the mass eigenstates of the particles it is necessary to perform the transformations defined in equations (3.21), (3.42) and (3.43). Also the substitution $h^T \to (0, (v+H)/\sqrt{2})$ is made. The couplings of the top quarks to the Higgses which are relevant to the later chapters of this thesis are given, to order v^2/f^2, in table 3.2.

Table 3.2: Top-Higgs Couplings

Vertex	Feynman Rule
$\bar{t}tH$	$-\frac{i\lambda_t}{\sqrt{2}}[1+\frac{1}{4}(3\lambda_t^2\frac{f^2}{m_T^2}-\frac{f^4}{f_1^2f_2^2})\frac{v^2}{f^2}]$
$\bar{T}TH$	$\frac{i}{2}\lambda_t^2\frac{f}{m_T}\frac{v}{f}$
$\bar{t}TH$	$-i\frac{\lambda_1\lambda_2 f(\lambda_1^2f_1^4-\lambda_2^2f_2^4)}{2f_1f_2m_T^3}\frac{v}{f}P_L$ $-i[\frac{(\lambda_2^2-\lambda_1^2)f_1f_2}{\sqrt{2}fm_T}-\frac{\lambda_1^2\lambda_2^2f^3(2(\lambda_1^2f_1^4-\lambda_2^2f_2^4)+(\lambda_1^2-\lambda_2^2)f_1^2f_2^2)}{4\sqrt{2}f_1f_2m_T^5}\frac{v^2}{f^2}]P_R$
$\bar{T}tH$	$i\frac{\lambda_1\lambda_2 f(\lambda_1^2f_1^4-\lambda_2^2f_2^4)}{2f_1f_2m_T^3}\frac{v}{f}P_R$ $+i[\frac{(\lambda_2^2-\lambda_1^2)f_1f_2}{\sqrt{2}fm_T}-\frac{\lambda_1^2\lambda_2^2f^3(2(\lambda_1^2f_1^4-\lambda_2^2f_2^4)+(\lambda_1^2-\lambda_2^2)f_1^2f_2^2)}{4\sqrt{2}f_1f_2m_T^5}\frac{v^2}{f^2}]P_L$
$\bar{t}tHH$	$\frac{i\lambda_1\lambda_2(\lambda_1^2f_1^6+\lambda_2^2f_2^6)}{2\sqrt{2}f_1^2f_2^2m_T^3}\frac{v}{f}$
$\bar{T}THH$	$\frac{i(\lambda_1^2f_2^2+\lambda_2^2f_1^2)}{2f^2m_T}$

In table 3.2, P_L and P_R are the left and right projection operators respectively.

In particular, the flavour diagonal couplings of t and T quarks to a single Higgs can be written up to order v^2/f^2 in the form

$$\mathcal{L}_{\mathrm{ttH}} \approx -\frac{M_t}{v}y_t\bar{t}tH - \frac{M_T}{v}y_T\bar{T}TH \tag{3.55}$$

where

$$y_t = 1+(\frac{1}{2}\lambda_t^2\frac{f^2}{m_T^2}-\frac{1}{6}\frac{f^4}{f_1^2f_2^2})\frac{v^2}{f^2} \tag{3.56}$$

$$y_T = -\frac{1}{2}\lambda_t^2\frac{f^2}{m_T^2}\frac{v^2}{f^2}. \tag{3.57}$$

3.6 Muon Decay and the Fermi Constant

In the SM the vev of the Higgs field, v, can be calculated via the relation

$$G_F = \frac{1}{\sqrt{2}v^2} \tag{3.58}$$

where G_F is the Fermi constant as measured in muon decay (see section 2.6). In the Schmaltz model this relation is modified, because the mass of the $W^{\pm}$ is modified and because of mixing between the neutral leptons of each generation. The heavy X^- gauge boson might be expected to play a role since it can mediate muon decay, but it turns out not to have any effect at order v^2/f^2. The interactions of leptons with the gauge bosons arises from the leptons' kinetic terms,

$$\mathcal{L}_{\text{lept}} = \sum_{k=1}^{3} \bar{L}_k i\mathcal{D}_\alpha \gamma^\alpha L_k \tag{3.59}$$

where L_k is the $SU(3)$ lepton triplet for the kth generation, as in equation (3.10), and the covariant derivative $\mathcal{D}_\alpha$ is as defined in equation (3.4).

The neutral lepton 'Yukawa' couplings do not couple fermions of different generations so mixing only occurs within each generation. The neutral lepton mass terms will have a similar structure to the top quark mass terms, but with λ_1 set to 0. The mixing matrix will then be like the top mixing matrix, but with $c = 1$ and $s = 0$. Then the mass eigenstates would be ν_k and N_k where

$$\begin{pmatrix} \nu_k \\ N_k \end{pmatrix} = \begin{pmatrix} 1 - \frac{1}{4}\frac{f_1^2}{f_2^2}\frac{v^2}{f^2} & \frac{1}{\sqrt{2}}\frac{f_1}{f_2}\frac{v}{f} \\ -\frac{1}{\sqrt{2}}\frac{f_1}{f_2}\frac{v}{f} & 1 - \frac{1}{4}\frac{f_1^2}{f_2^2}\frac{v^2}{f^2} \end{pmatrix} \begin{pmatrix} \nu'_k \\ N'_k \end{pmatrix} \tag{3.60}$$

Note that the mixing angles are the same for all generations.

This coupling of leptons to charged gauge bosons may be extracted from the Lagrangian (3.59)

$$\Delta\mathcal{L} = \frac{g}{\sqrt{2}}[(\bar{e}_m \gamma^\alpha \nu'_m) W'^-_\alpha - V^{l\dagger}_{nm}(\bar{e}_m \gamma^\alpha N'_n) X'^-_\alpha + \text{h.c.}] \tag{3.61}$$

where V^l is the equivalent of the CKM matrix for the leptons and e_m (without a primed index) are the mass eigenstates of the charged leptons. Including the mixing betwen neutral leptons gives

$$\begin{aligned} \Delta\mathcal{L} &= \frac{g}{\sqrt{2}}[(\bar{e}_m \gamma^\alpha [(1-\delta_\nu^2)\nu_m - V^{l\dagger}_{nm} N_n]) W'^-_\alpha & (3.62) \\ &\quad -(\bar{e}_m \gamma^\alpha [V^{l\dagger}_{nm}(1-\delta_\nu^2) N'_n + \delta_\nu \nu_m]) X'^-_\alpha + \text{h.c.}] & (3.63) \end{aligned}$$

where

$$\delta_\nu = \frac{1}{\sqrt{2}}\frac{f_1}{f_2}\frac{v}{f}. \tag{3.64}$$

The aim here is to calculate order v^2/f^2 corrections to the SM relation between the Higgs vev and the Fermi constant. The mixing between W' and X' is of order v^3/f^3 (see equation (3.38)), so it is irrelevant at this order. The contribution to muon decay

from the X mediated interaction is proportional to δ_ν^2/M_X^2 and so is also irrelevant at this order. The only contribution is from the W mediated interaction, which gives

$$\mathcal{L}_{\text{eff}} = -\frac{g^2}{8M_{W^\pm}}(1-\delta_\nu^2)(\bar{\mu}\gamma^\alpha(1-\gamma^5)\nu_\mu)(\bar{\nu}_e\gamma_\alpha(1-\gamma^5)e). \tag{3.65}$$

Plugging in the mass of the $W^\pm$ from equation (3.39) and setting the coefficient of this operator equal to $-G_F/\sqrt{2}$ gives the relation

$$\frac{1}{\sqrt{2}v^2} = G_F y_{G_F}^2 \tag{3.66}$$

where

$$y_{G_F}^2 = 1 + \frac{1}{2}(1 - \frac{1}{3}\frac{f^4}{f_1^2 f_2^2} + \frac{f_1^2}{f_2^2})\frac{v^2}{f^2}. \tag{3.67}$$

3.7 Electroweak Precision Constraints

Bounds on the scale f from the EWPCs were reported in the original Schmaltz model paper, [15]. Bounds from the mass shift of the Z due to mixing with the heavy Z' and from 4 fermion operators associated with Z' exchange (for example, $(\bar{e}\gamma^\mu\gamma^5 e)^2$) imply that $f \gtrsim 2$ TeV at 95% c.l. for both model I and model II.

The original paper also notes stringent constraints from atomic parity violation measured in the 'weak charge' of Caesium. In model I these constraints are very tight, $f \gtrsim 3.9$ TeV at 95% c.l. In model II the constraint is not so severe with $f \gtrsim 1.7$ TeV at 95% confidence.

A constraint on the mass of the W' boson is derived in [38]. The W' must be heavier than 1.8 TeV at 95% C.L.. This implies a tighter constraint on f, requiring $f > 4$ TeV at 95%C.L..

The mass of the Z' is given by

$$m_{Z'}^2 = \frac{2g^2}{3-t^2}(f_1^2 + f_2^2) \tag{3.68}$$

and the mass of the heavy Top is

$$M_T = \sqrt{\lambda_1^2 f_1^2 + \lambda_2^2 f_2^2}. \tag{3.69}$$

It is possible to increase the mass of the Z' to avoid EWPCs whilst keeping m_T light by going to a region of parameter space where one of the f_i is much larger than the other (dominating the Z' mass). Then the corresponding Yukawa coupling, λ_i can be made much smaller than the other (reducing the impact of a large f_i on the heavy Top mass). This helps to keep δm^2 small (equation (3.33)) which leads to a lighter Higgs.

Chapter 4

Loop Induced Decays of Little Higgs

The Higgs particle can couple to pairs of gluons or photons via loop processes. Figure 4.1 shows how a loop involving a massive coloured particle induces a Higgs decay to gluons, while figure 4.2 shows how a loop involving a massive charged particle induces a Higgs decay to photons.

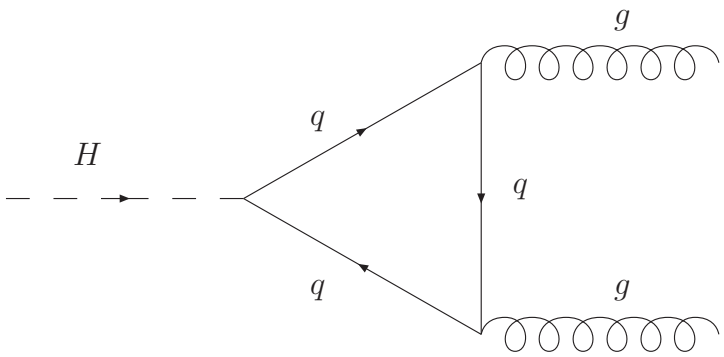

Figure 4.1: The Higgs can decay to a pair of gluons via a quark loop.

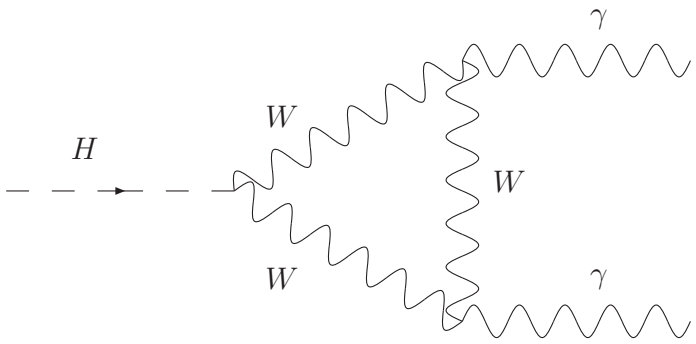

Figure 4.2: The Higgs can decay to a pair of photons via a loop of any charged particle which couples to the Higgs. For example, a loop of $W^{\pm}$ gauge bosons.

Higgs production via gluon fusion is the dominant method of Higgs production at hadron colliders (e.g. the LHC), the cross section for this process being about an order of magnitude higher than the next largest contribution from weak boson fusion in the SM (see, for example, [44]). This makes it of paramount importance to calculate corrections to this coupling in alternative models.

The coupling of the Higgs to photons is also important since this governs the production of the Higgs at photon colliders, which are a satellite mode of e^+e^- or e^-e^- colliders with photon beams created by the Compton backscattering of laser light off the electron beams.

The loop induced couplings of the Higgs to gluons and photons are also important for Higgs decays. The decay to photons is particularly interesting because, although it is a rare decay ($\approx 0.22\%$ [45]), it has a clearer signal than many other Higgs decays (such as $b\bar{b}$, for example).

These loop induced processes are sensitive to new coloured or charged particles which couple to the Higgs since they can contribute by running in the loops. Interestingly, new heavy particles whose coupling to the Higgs are proportional to their masses do not decouple. The Higgs coupling compensates for the inverse power of the mass coming from the loop integral. Although the new particles present in Little Higgs models do not couple to the Higgs in proportion to their masses, their couplings to the Higgs are still large enough to warrant a calculation of their contributions to these processes.

For the SM, the leading order result for the cross section for the process $H \to gg$ has been known for a while [46],[47],[48],[49]. The NLO QCD corrections to loops involving top and bottom quarks have been calculated in full in [50] and can increase the cross section by up to 100%. In the limit of a very large top mass, the NNLO QCD corrections have been calculated in [51] and [52]. These amount to a further increase of $\approx 20 - 30\%$). Also in this limit, the NNNLO corrections are given in [53] and [54] where they are found to be of order $5 - 10\%$.

Due to the possibility of final state gluon radiation, corrections to the inverse process $gg \to H$ must be considered separately. The NLO QCD corrections to the top and bottom loops have been calculated in [50], enhancing the partial decay width by around 70%. In the heavy top limit, the NNLO corrections are found in [55] and the NNNLO corrections in [56] which increase the hadronic widths by about 20% and a few percent respectively.

The leading order (one loop) contribution to the decay $H \to \gamma\gamma$ may be found in refs [57],[58],[59]. The NLO corrections involving QCD and electroweak corrections have been calculated [60]. The QCD and electroweak corrections are negligable below $2M_W$ because they are of opposite sign and similar magnitude, but above $2M_W$ they have the same sign and lead to a correction of about 4%. The NNLO QCD corrections have been calculated in the limit of a heavy top quark and are of the order of a percent or so [61].

The QCD corrections to the cross section of $\gamma\gamma \to H$ are equivalent to those of the decay cross section $H \to \gamma\gamma$. Unlike the case of the Hgg coupling, the external particles are colour neutral so there are no real radiation effects.

Let the Higgs interaction Lagrangian describing the coupling of a single Higgs to the various fermions, gauge bosons and scalars be expressed in the form

$$\mathcal{L} = \sum_f -\frac{M_f}{v} y_f \bar{f} f H + \sum_V 2\frac{M_V^2}{v} y_V V^\dagger V H + \sum_\Phi -2\frac{M_\Phi^2}{v} y_\Phi \Phi^\dagger \Phi H \tag{4.1}$$

where the index f runs over all fermions, V runs over the gauge bosons, and Φ runs over the scalars. Also, in Little Higgs models, the simple relation between the Higgs vev and the Fermi constant G_F (equation (2.69)) will be modified. Let the relation between these parameters in a Little Higgs model be written in the form

$$\frac{1}{v^2} = \sqrt{2} G_F y_{G_F}^2 \tag{4.2}$$

The formulae for the partial widths for the processes $\Gamma(H \to gg)$ and $\Gamma(H \to \gamma\gamma)$ are then given (to one loop level) by [3]

$$\Gamma(H \to gg) = \frac{\sqrt{2} G_F \alpha_s^2 M_H^3 y_{G_F}^2}{32\pi^3} \left| \sum_i -\frac{1}{2} y_i F_{1/2}(\tau_i) \right|^2 \tag{4.3}$$

$$\Gamma(H \to \gamma\gamma) = \frac{\sqrt{2} G_F \alpha^2 M_H^3 y_{G_F}^2}{256\pi^3} \left| \sum_j y_j N_{cj} Q_j^2 F_j(\tau_i) \right|^2 \tag{4.4}$$

where the index i runs over all coloured fermions, the index j runs over all charged particles, and N_{cj} and Q_j are the colour factor and electric charge of particle j. Here, the functions F_j depend on the spin of the particle. They are given by

$$\begin{aligned} F_1 &= 2 + 3\tau + 3\tau(2-\tau) f(\tau) \\ F_{1/2} &= -2\tau[1 + (1-\tau) f(\tau)] \\ F_0 &= \tau[1 - \tau f(\tau)] \end{aligned} \tag{4.5}$$

where

$$f(\tau) = \begin{cases} [\sin^{-1}(1/\sqrt{\tau})]^2 & \text{for } \tau \geq 1 \\ -\frac{1}{4}[\log(\eta_+/\eta_-) - i\pi]^2 & \text{for } \tau < 1 \end{cases} . \tag{4.6}$$

Here τ_j and $\eta_\pm$ are given by

$$\tau_j = \frac{4M_j^2}{M_H^2} \tag{4.7}$$

$$\eta_\pm = 1 \pm \sqrt{1-\tau}. \tag{4.8}$$

For $\tau_j \gg 1$, the function $f(\tau_j)$ is well approximated by

$$f(\tau_j) \approx (\frac{1}{\sqrt{\tau_j}} + \frac{1}{6}\frac{1}{\sqrt{\tau_j}^3})^2. \tag{4.9}$$

In this limit, the functions F_j approach the asymptotic values $F_1 \to 7$, $F_{1/2} \to -4/3$, $F_0 \to -1/3$.

The functions F_j are plotted, along with their asymptotic values, in figures 4.3-4.5. As can be seen, the asymptotic limit is already an excellent approximation if $\tau_j > 16$, corresponding to $M_j > 2M_H$, which is the case for the new particles in the Littlest Higgs and the Schmaltz models.

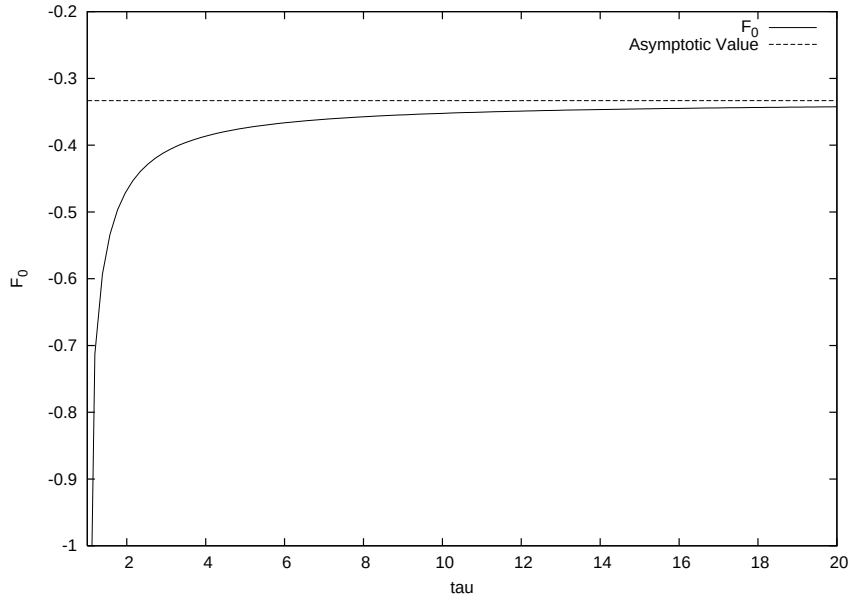

Figure 4.3: The scalar loop function F_0 and its asymptotic value.

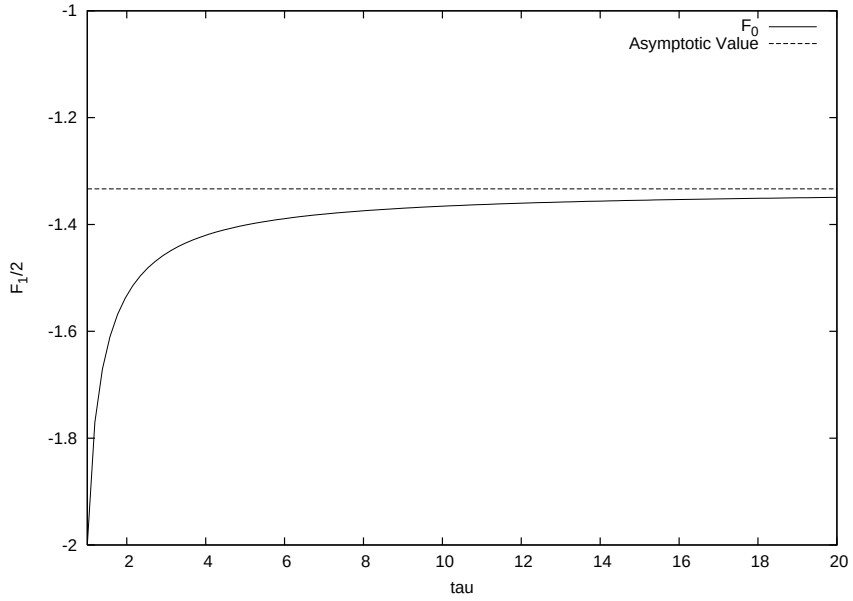

Figure 4.4: The fermion loop function $F_1/2$ and its asymptotic value.

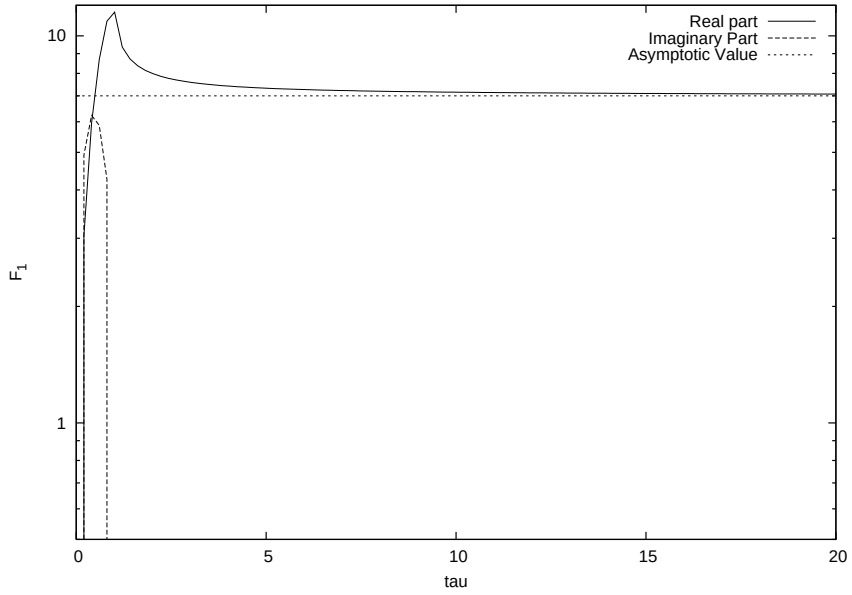

Figure 4.5: The vector loop function F_1 and its asymptotic value. Here a log scale is used on the y-axis and, since $F_1(\tau_W)$ develops an imaginary part for $M_H > 2M_W$, the real and imaginary parts are plotted separately. Note that the asymptotic value is purely real.

4.1 Loop Induced Decays in the Littlest Higgs Model

The loop induced decays of the Higgs to gluons or photons were studied in [34]. However, in light of the errors in their previous paper [33] with respect to the couplings of the top quark to the Higgs, it is important to check these results.

In the Littlest Higgs models there is a new top-like quark T which can contribute to the loop induced decays of the Higgs to either gluons or photons. In addition, the new charged gauge boson W_H and charged scalars Φ^+ and Φ^{++} can also run in the loop contributing to the decay of the Higgs to photons.

Following reference [34], the Littlest Higgs contributions to the loop induced decays of the Higgs are written in terms of the parameters

$$c = \frac{g_1}{\sqrt{g_1^2 + g_2^2}} \tag{4.10}$$

$$c_t = \frac{\lambda_1}{\sqrt{\lambda_1^2 + \lambda_2^2}} \tag{4.11}$$

$$x = \frac{4fv'}{v^2}. \tag{4.12}$$

Each of these parameters may vary between 0 and 1. The constraint $x < 1$ arises from requiring $M_\Phi > 0$. Also, define $s^2 = 1 - c^2$, $s_t^2 = 1 - c_t^2$.

Writing the Lagrangian in the form of equation (4.1), one has

$$\begin{aligned}\mathcal{L} &= -\frac{M_t}{v} y_t \bar{t}tH - \frac{M_T}{v} y_T \bar{T}TH + 2\frac{M_{W_L}^2}{v} y_{W_L} W_L^+ W_L^- H + 2\frac{M_{W_H}^2}{v} y_{W_H} W_H^+ W_H^- H \\ &\quad -2\frac{M_\Phi^2}{v} y_{\Phi^+} \Phi^+ \Phi^- H - 2\frac{M_\Phi^2}{v} y_{\Phi^{+}{}_{+}} \Phi^{++} \Phi^{--} H. \end{aligned} \tag{4.13}$$

The masses of these particles are given by equations (2.38), (2.44), (2.45) and (2.49),

$$M_{W_L}^2 = \frac{g^2 v^2}{4}[1 - \frac{v^2}{f^2}(\frac{1}{6} + \frac{1}{4}(c^2 - s^2)^2 - \frac{x^2}{4})] \tag{4.14}$$

$$M_{W_H}^2 = \frac{f^2 g^2}{4 s^2 c^2} - M_{W_L}^2 \tag{4.15}$$

$$M_t = \frac{\lambda_1 \lambda_2 v}{\sqrt{\lambda_1^2 + \lambda_2^2}}[1 + \frac{v^2}{f^2}(\frac{x}{4} - \frac{1}{3} + c_t^2(1 - c_t^2))] \tag{4.16}$$

$$M_T = \frac{m_t}{s_t c_t}\frac{f}{v} \tag{4.17}$$

$$M_\Phi^2 = \frac{2M_H^2}{1 - x^2}\frac{f^2}{v^2} \tag{4.18}$$

and the couplings y_j are given by equations (2.54), (2.58) and (2.64),

$$\begin{aligned} y_{W_L} &= 1 + \frac{v^2}{f^2}[-\frac{1}{6} - \frac{1}{4}(c^2 - s^2)^2] \\ y_{W_H} &= -s^2 c^2 \frac{v^2}{f^2} \\ y_t &= 1 + \frac{v^2}{f^2}[-\frac{2}{3} + \frac{x}{2} - \frac{x^2}{4} + c_t^2 s_t^2] \\ y_T &= -c_t^2 s_t^2 \frac{v^2}{f^2} \\ y_{\Phi^+} &= \frac{v^2}{f^2}[-\frac{1}{3} + \frac{x^2}{4}] \\ y_{\Phi^{++}} &= \mathcal{O}(\frac{v^4}{f^4}, \frac{v^2}{16\pi^2 f^2}). \end{aligned} \tag{4.19}$$

All SM quarks other than the top are neglected here since their contributions are suppressed by their small Yukawa couplings.

Also, recall the correction to the SM relation between G_F and the vev of the Higgs from equation (2.76),

$$\frac{1}{\sqrt{2}v^2} = G_F y_{G_F}^2 \tag{4.20}$$

where

$$y_{G_F}^2 = 1 + \frac{v^2}{f^2}(\frac{x^2}{4} - \frac{5}{12}). \tag{4.21}$$

4.1.1 Higgs Decay To Gluons

Using equation (4.3), the partial width $\Gamma(H \to gg)$ in the Littlest Higgs model is

$$\Gamma(H \to gg) = \frac{\sqrt{2}G_F\alpha_s^2 M_H^3}{32\pi^3}\left|-\frac{1}{2}F_{1/2}(\tau_t)y_t y_{G_F} - \frac{1}{2}F_{1/2}(\tau_T)y_T y_{G_F}\right|^2. \tag{4.22}$$

Substituting in the expressions for y_t, y_T and y_{G_F} from (4.19) and (4.20) this leads to

$$\begin{aligned}\Gamma(H \to gg) &= \frac{\sqrt{2}G_F\alpha_s^2 M_H^3}{32\pi^3}|-\frac{1}{2}F_{1/2}(\tau_t) - \frac{1}{2}\frac{v^2}{f^2}[(-\frac{7}{8}+\frac{x}{2}-\frac{x^2}{8})F_{1/2}(\tau_t) \\ &\quad +c_t^2 s_t^2(F_{1/2}(\tau_t)-F_{1/2}(\tau_T))]|^2.\end{aligned} \tag{4.23}$$

This is in agreement with equation (11) of (the latest version of) reference [34]. This is perhaps surprising as they take their couplings from their previous paper [33] in which they are incorrect.

The effects of the Littlest Higgs corrections to this process are best illustrated by taking the ratio of the Littlest Higgs result to the SM result.

$$\frac{\Gamma(H \to gg)_{LH}}{\Gamma(H \to gg)_{SM}} = \left|1 + \frac{1}{\sqrt{2}G_F f^2}[-\frac{7}{8}+\frac{x}{2}-\frac{x^2}{8}+c_t^2 s_t^2(1-\frac{F_{1/2}(\tau_T)}{F_{1/2}(\tau_t)})]\right|^2. \tag{4.24}$$

Substituting in the numerical value of G_F [2] and the asymptotic value of $F_{1/2}(\tau_T) = -4/3$, and performing the square to order v^2/f^2 gives

$$\begin{aligned}\frac{\Gamma(H \to gg)_{LH}}{\Gamma(H \to gg)_{SM}} &= 1 + (-0.106 + 0.061x - 0.015x^2 \\ &\quad +0.121c_t^2 s_t^2(1+\frac{4}{3F_{1/2}(\tau_t)}))(\frac{1\text{ TeV}}{f})^2.\end{aligned} \tag{4.25}$$

This equation depends on x, c_t and, implicitly in the function $F_{1/2}(\tau_t)$, the Higgs and top masses.

Most of the deviation from the SM case comes from the terms in y_t and y_{G_F} which are independent of both x and c_t. The process is suppressed relative to the SM case, due to the reduced coupling of the top quark to the Higgs and the correction to the Fermi constant.

The deviation falls off rapidly with increasing f as can be seen from figure 4.6, created by plotting equation (4.25). Even for f as low as 1 TeV the deviation is at most 12%.

The variation with x is plotted in figure 4.7. The effect is largest when $x = 0$ and smallest when $x = 1$. The effect of the terms proportional to c_t is very small as can be seen from figure 4.8 and, since the only dependence on the Higgs mass is in this term, varying the Higgs mass also has little effect as shown in figure 4.9.

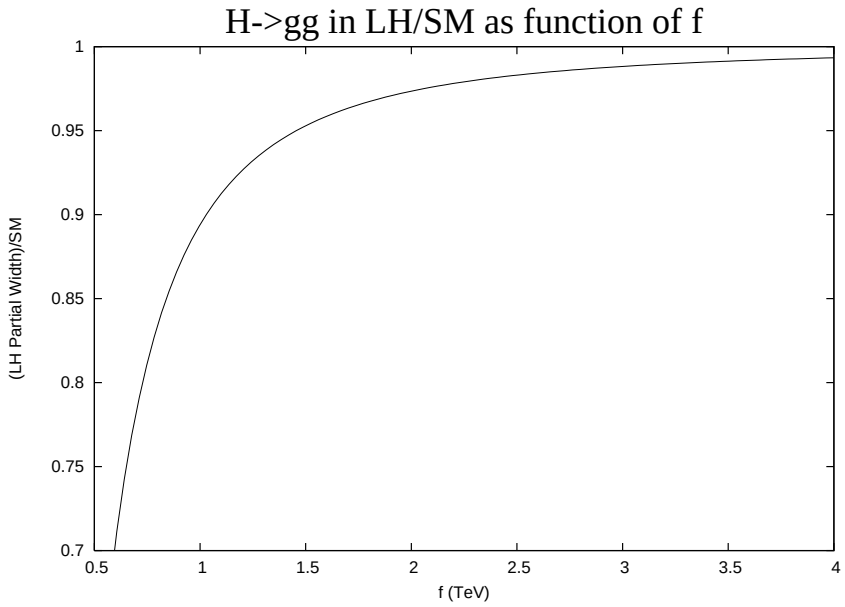

Figure 4.6: Ratio of Little Higgs partial width to SM partial width Vs the value of the scalar condensate f for $c_t = x = 0$.

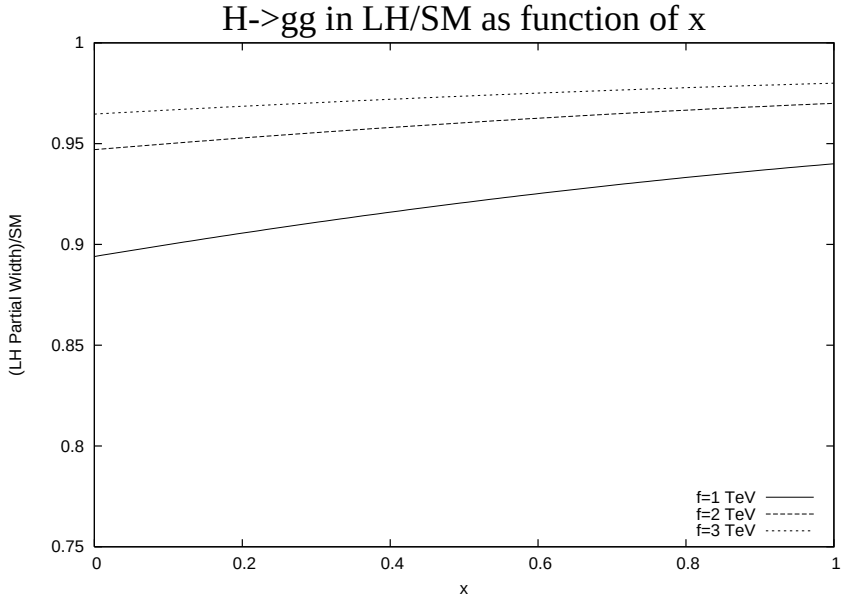

Figure 4.7: Ratio of Little Higgs partial width to SM partial width Vs x (which parameterises the triplet vev) for various f with $c_t = 0$.

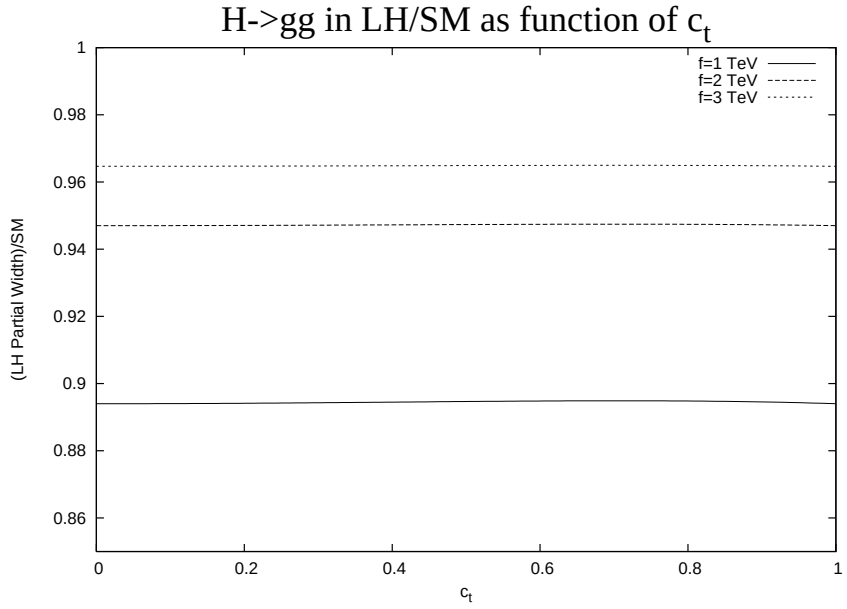

Figure 4.8: Ratio of Little Higgs partial width to SM partial width Vs the parameter c_t for various f with $x = 0$ and $M_H = 120$ GeV.

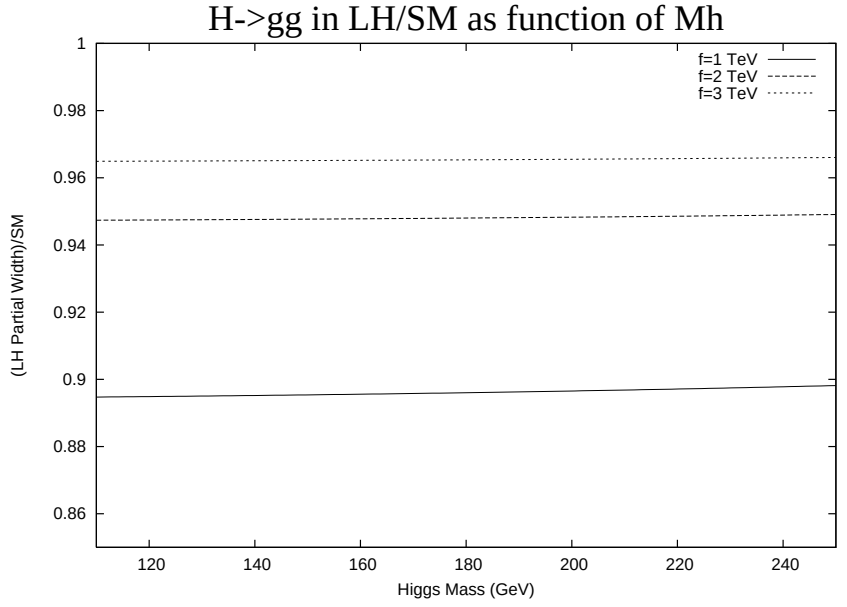

Figure 4.9: Ratio of Little Higgs partial width to SM partial width Vs the Higgs mass for $c_t = x = 0$.

4.1.2 Higgs Decay To Photons

The decay of the Higgs to photons is more complicated than the gluons case because there are more new charged particles which can run in the loop. In addition to the SM top quark and $W_L^\pm$ gauge boson there are the heavy T quark, the heavy gauge boson $W_H^\pm$ and the scalar Φ^+. The doubly charged scalar Φ^{++} might be expected to have a large effect due to its enhancement by a factor of $Q^2 = 4$, but its coupling to the Higgs boson is highly suppressed (equation (4.19)) and it may safely be neglected.

The partial width is obtained from equation (4.3). This gives

$$\begin{aligned}\Gamma(H \to \gamma\gamma) &= \frac{\sqrt{2}G_F\alpha^2 M_H^3}{256\pi^3}|y_{G_F}[\frac{4}{3}y_t F_{1/2}(\tau_t) + y_{W_L}F_1(\tau_{W_L}) \\ &\quad +\frac{4}{3}y_T F_{1/2}(\tau_T) + y_{W_H}F_1(\tau_{W_H}) + y_{\Phi^+}F_0(\tau_{\Phi^+})]|^2. \qquad (4.26)\end{aligned}$$

Plugging in the expressions for y_{G_F} (equation (4.20)) and the other y_j (equations (4.19)) gives

$$\begin{aligned}\Gamma(H \to \gamma\gamma) &= \frac{\sqrt{2}G_F\alpha^2 M_H^3}{256\pi^3}|\frac{4}{3}F_{1/2}(\tau_t) + F_1(\tau_{W_L}) + \frac{v^2}{f^2}[\frac{4}{3}(-\frac{7}{8}+\frac{x}{2}-\frac{x^2}{8})F_{1/2}(\tau_t) \\ &\quad +\frac{4}{3}c_t^2 s_t^2(F_{1/2}(\tau_t) - F_{1/2}(\tau_T)) + (-\frac{5}{8}+\frac{x^2}{8})F_1(\tau_{W_L}) \\ &\quad +c^2 s^2(F_1(\tau_{W_L}) - F_1(\tau_{W_H})) + (-\frac{1}{3}+\frac{x^2}{4})F_0(\tau_\Phi)]|^2 \qquad (4.27)\end{aligned}$$

in agreement with equation (13) of reference [34]. As in the case of the decay to gluons, the results are best illustrated by taking the ratio with respect to the SM value. This gives

$$\begin{aligned}\frac{\Gamma(H \to \gamma\gamma)_{LH}}{\Gamma(H \to \gamma\gamma)_{SM}} &= |1 + \frac{1}{\sqrt{2}G_F f^2}[\frac{4}{3}(-\frac{7}{8}+\frac{x}{2}-\frac{x^2}{8})F_{1/2}(\tau_t) \\ &\quad +\frac{4}{3}c_t^2 s_t^2(F_{1/2}(\tau_t) - F_{1/2}(\tau_T)) + (-\frac{5}{8}+\frac{x^2}{8})F_1(\tau_{W_L}) \\ &\quad +c^2 s^2(F_1(\tau_{W_L}) - F_1(\tau_{W_H})) \\ &\quad +(-\frac{1}{3}+\frac{x^2}{4})F_0(\tau_\Phi)]/[\frac{4}{3}F_{1/2}(\tau_t) + F_1(\tau_{W_L})]|^2. \qquad (4.28)\end{aligned}$$

The process is slightly suppressed relative to the SM. The most important parameter in determining the magnitude of the suppression is f. For f as low as 1 TeV the suppression is only about 7%, and it falls off proportionally with $1/f^2$ as is illustrated in figure 4.10.

The largest contribution to this process comes from the $W_L^\pm$ gauge bosons. Consequently, the correction to the $W_L^+W_L^-H$ coupling is responsible for most of the deviation from the SM. Varying the parameters x and c change the size of the deviation from the SM by less than 1% each, as can be seen from figures 4.11 and 4.12. Varying c_t and M_H has very little effect as is shown in figures 4.13 and 4.14.

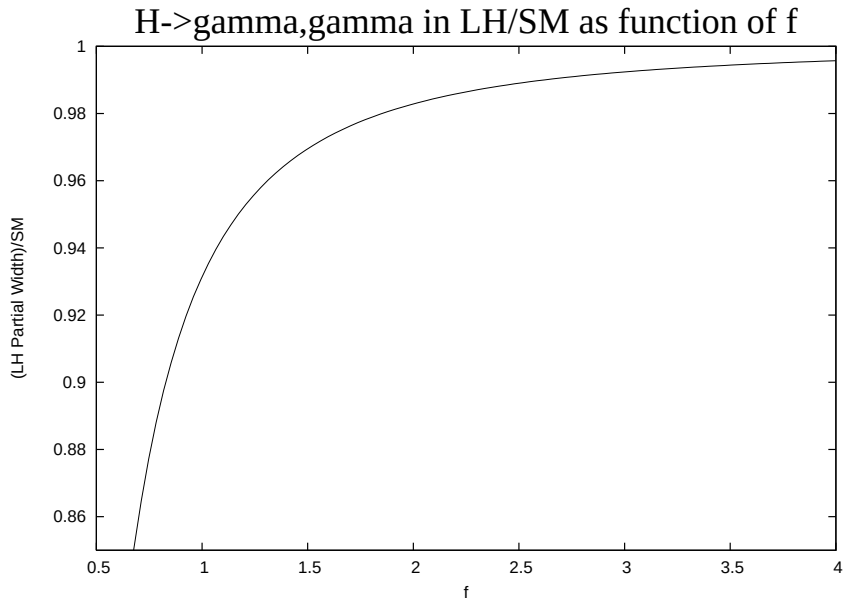

Figure 4.10: Ratio of Little Higgs partial width to SM partial width Vs the scalar vev f for $c = 0$, $x = 0.39$, $c_t = 1/\sqrt{2}$ and $M_H = 120$ GeV.

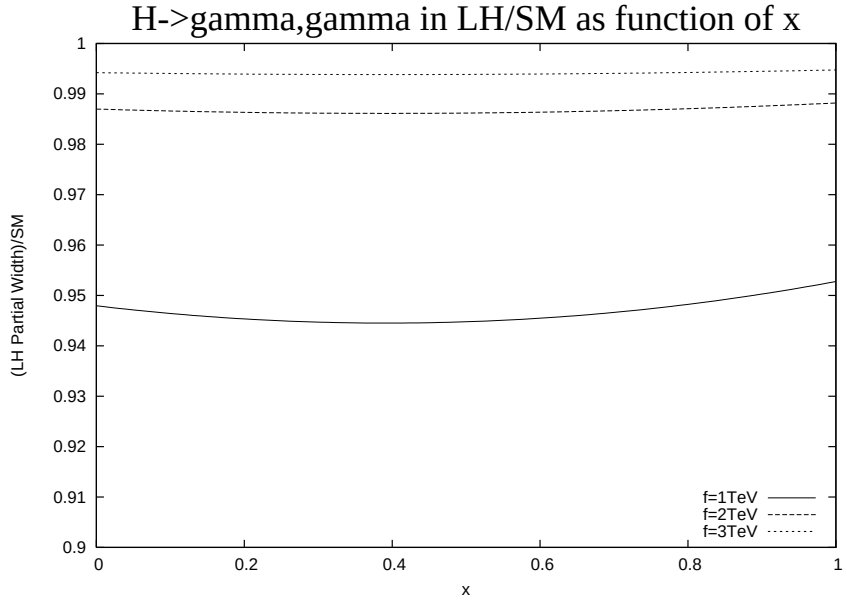

Figure 4.11: Ratio of Little Higgs partial width to SM partial width Vs x, which is proportional to the triplet vev v', for $c = 0$, $c_t = 1/\sqrt{2}$ and $M_H = 120$ GeV.

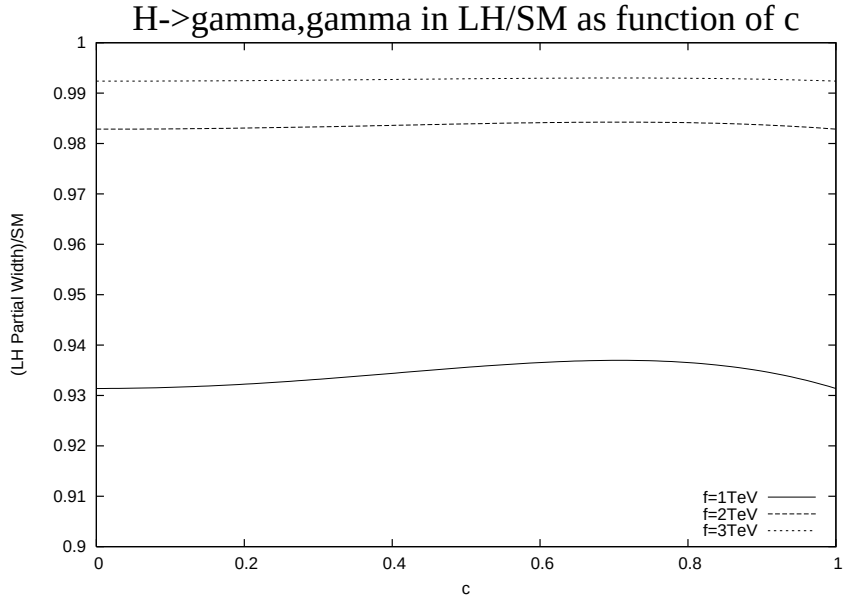

Figure 4.12: Ratio of Little Higgs partial width to SM partial width Vs c, which parameterises the mixing between the SM $W^{\pm}$ and the heavy gauge bosons, for $x = 0.39$, $c_t = 1/\sqrt{2}$ and $M_H = 120$ GeV.

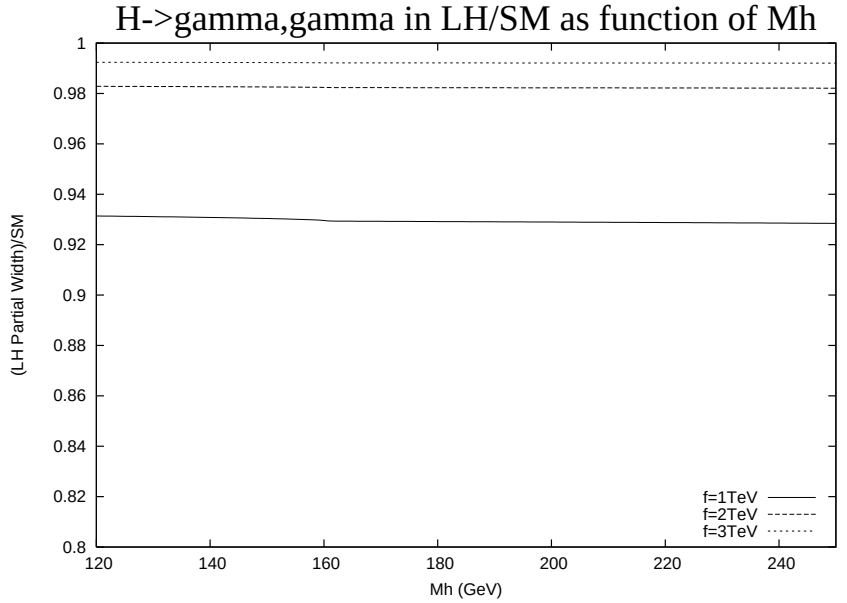

Figure 4.13: Ratio of Little Higgs partial width to SM partial width Vs the Higgs mass for $c = 0$, $x = 0.39$ and $c_t = 1/\sqrt{2}$.

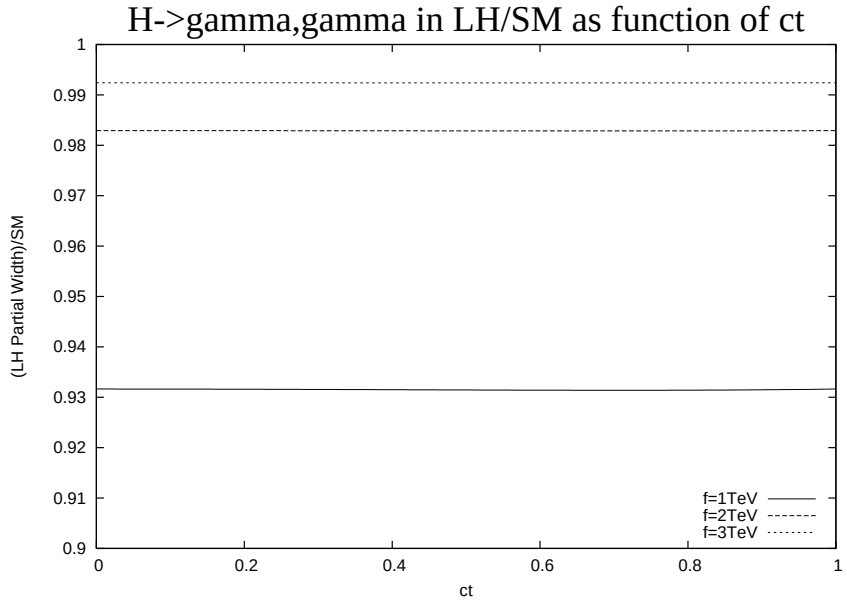

Figure 4.14: Ratio of Little Higgs partial width to SM partial width Vs c_t for $c = 0$, $x = 0.39$ and $M_H = 120$ GeV.

The results presented here are not in exact agreement with those in paper [34]. A close inspection of some of the plots (e.g. figure 4.11 compared with their figure 4) shows some very slight discrepancies. However, the main conclusions are the same. The deviation from the SM result is about 7% for $f = 1$ TeV and scales like $1/f^2$.

4.2 Loop Induced Decays in the Schmaltz Model

In the Schmaltz model the new heavy quark of the third generation contributes to the loop induced decays of the Higgs to gluons or photons. Although there are other heavy quarks living in the first and second generations these couple to the Higgs no more strongly than the other quarks of the first two generations so their contributions to these loop induced decays are negligable.

The other new particle which is relevant to these processes is the heavy gauge boson, $X^{\pm}$, which can contribute to the decay of the Higgs to photons.

The Schmaltz model contains a number of new parameters which enter the couplings of the Higgs. Those relevant to the current process are written in terms of the independent parameters

$$\begin{aligned} \beta &= \tan^{-1}\frac{f_2}{f_1} \\ f &= \sqrt{f_1^2 + f_2^2} \\ k &= \frac{\lambda_2}{\lambda_1} \end{aligned} \tag{4.29}$$

Also, the shorthand notation $t_\beta = \tan\beta$, $s_\beta = \sin\beta$ and $c_\beta = \cos\beta$ will be utilised.

The Lagrangian describing the Higgs couplings of the particles relevant to the loop induced decays of the Higgs can be expressed in the form of equation (4.1) using equations (3.52), (3.53), (3.55) and (3.56),

$$\mathcal{L} = -\frac{M_t}{v} y_t \bar{t}tH - \frac{M_T}{v} y_T \bar{T}TH + 2\frac{M_{W^\pm}^2}{v} y_{W^\pm} W^+W^-H + 2\frac{M_{X^\pm}^2}{v} y_{X^\pm} X^+X^-H \quad (4.30)$$

where the masses of these particles are given (see equations (3.39), (3.48) and (3.49)) by

$$\begin{aligned} M_{W^\pm}^2 &= \frac{g^2v^2}{4}[1 + \frac{v^2}{2f^2}(1 - \frac{1}{3}\frac{1}{s_\beta^2 c_\beta^2})] \\ M_{X^\pm,4}^2 &= \frac{g^2f^2}{2} - M_{W^\pm}^2 \\ M_t &= \lambda_t \frac{v}{\sqrt{2}}[1 + \frac{1}{4}\left(\frac{k^2(1+t_\beta^2)}{(1+k^2t_\beta^2)^2} - \frac{1}{3}\frac{1}{s_\beta^2 c_\beta^2}\right)\frac{v^2}{f^2}] \\ M_T &= m_T(1 - \frac{1}{4}\frac{k^2(1+t_\beta^2)}{(1+k^2t_\beta^2)^2}\frac{v^2}{f^2}) \end{aligned} \quad (4.31)$$

where, recall, $m_T = \sqrt{\lambda_1^2 f_1^2 + \lambda_2^2 f_2^2}$, $\lambda_t = \lambda_1\lambda_2 f/m_T$ and the y_j factors are,

$$\begin{aligned} y_{W^\pm} &= 1 + \frac{1}{2}(1 - \frac{1}{3}\frac{1}{c_\beta^2 s_\beta^2})\frac{v^2}{f^2} \\ y_{X^\pm} &= -\frac{1}{2}\frac{v^2}{f^2} \\ y_t &= 1 + (\frac{k^2}{2}\frac{(1+t_\beta^2)^2}{(1+k^2t_\beta^2)^2} - \frac{1}{6}\frac{1}{c_\beta^2 s_\beta^2})\frac{v^2}{f^2} \\ y_T &= -\frac{k^2}{2}\frac{(1+t_\beta^2)^2}{(1+k^2t_\beta^2)^2}\frac{v^2}{f^2}. \end{aligned} \quad (4.32)$$

Also, recall the correction to the SM relationship between the Higgs vev v and the Fermi constant G_F from equations (3.66) and (3.67)

$$\frac{1}{\sqrt{2}v^2} = G_F y_{G_F}^2 \quad (4.33)$$

where

$$y_{G_F}^2 = 1 + \frac{1}{2}(1 - \frac{1}{3}\frac{1}{c_\beta^2 s_\beta^2} + \frac{1}{t_\beta^2})\frac{v^2}{f^2}. \quad (4.34)$$

4.2.1 Higgs Decay To Gluons

Using equation (4.3), the partial width $\Gamma(H \to gg)$ in the Schmaltz model is given by the expression

$$\Gamma(H \to gg) = \frac{\sqrt{2}G_F\alpha_s^2 M_H^3}{32\pi^3}\left|-\frac{1}{2}F_{1/2}(\tau_t)y_t y_{G_F} - \frac{1}{2}F_{1/2}(\tau_T)y_T y_{G_F}\right|^2. \quad (4.35)$$

Substituting in the expressions for y_t, y_T and y_{G_F} from (4.32) and (4.34) this leads to

$$\begin{aligned}\Gamma(H \to gg) &= \frac{\sqrt{2}G_F\alpha_s^2 M_H^3}{32\pi^3}|-\frac{1}{2}F_{1/2}(\tau_t)-\frac{1}{2}\frac{v^2}{f^2}[-\frac{1}{4}(1+t_\beta^2)F_{1/2}(\tau_t) \\ &\quad +\frac{k^2}{2}\frac{(1+t_\beta^2)^2}{(1+k^2t_\beta^2)^2}(F_{1/2}(\tau_t)-F_{1/2}(\tau_T))]|^2. \end{aligned} \tag{4.36}$$

As in the Littlest Higgs model, the effects of the new terms in the Schmaltz model are best illustrated by taking the ratio of the Schmaltz model partial width to that of the SM.

$$\frac{\Gamma(H \to gg)_{\rm Sch}}{\Gamma(H \to gg)_{\rm SM}} = |1+\frac{v^2}{f^2}[-\frac{1}{4}(1+t_\beta^2)+\frac{k^2}{2}\frac{(1+t_\beta^2)^2}{(1+k^2t_\beta^2)^2}(1-\frac{F_{1/2}(\tau_T)}{F_{1/2}(\tau_t)})]|^2 \tag{4.37}$$

Performing the square, substituting in the numerical value for G_F and taking the asymptotic value for $F_{1/2}(\tau_T)$ leads to the expression

$$\frac{\Gamma(H \to gg)_{\rm Sch}}{\Gamma(H \to gg)_{\rm SM}} = 1+0.606[-0.5-0.5t_\beta^2+k^2\frac{(1+t_\beta^2)^2}{(1+k^2t_\beta^2)^2}(1-\frac{4}{3F_{1/2}(\tau_t)})]\left(\frac{1\ \text{TeV}}{f^2}\right). \tag{4.38}$$

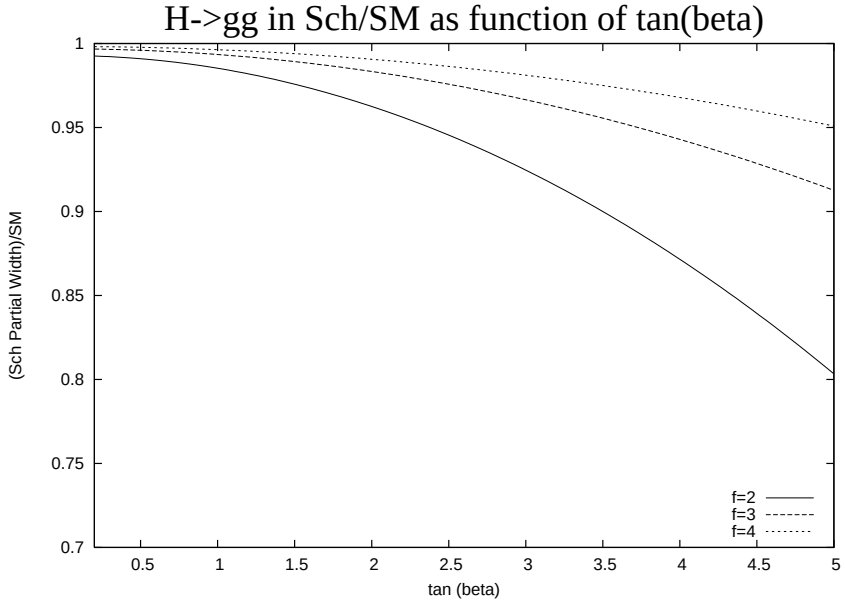

Figure 4.15: Ratio of Schmaltz partial width to SM partial width Vs $\tan\beta$ (The ratio of the scalar triplet vevs) for $k = 1$ and $M_H = 120$ GeV.

The most interesting feature of the Higgs decay to gluons is the variation with t_β, as illustrated in figure 4.15 which is a plot of equation (4.37). The suppression of the Schmaltz model branching ratio becomes large for $t_\beta \gg 1$, which corresponds to taking $f_2 \gg f_1$, with the large deviation coming from the factor y_t.

Since the top sector coupling is symmetric under relabelling t_1^c, λ_1 etc to t_2^c, λ_2 etc, it may at first be surprising that the deviation is large for $f_2 \gg f_1$ but not for $f_1 \gg f_2$.

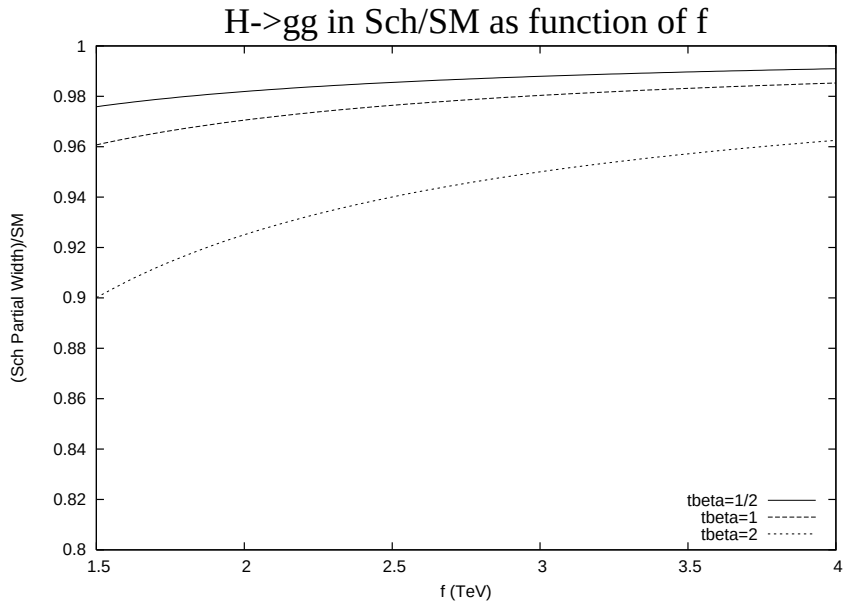

Figure 4.16: Ratio of Schmaltz model partial width to SM partial width Vs f for $k = 1$ and $M_H = 120$ GeV.

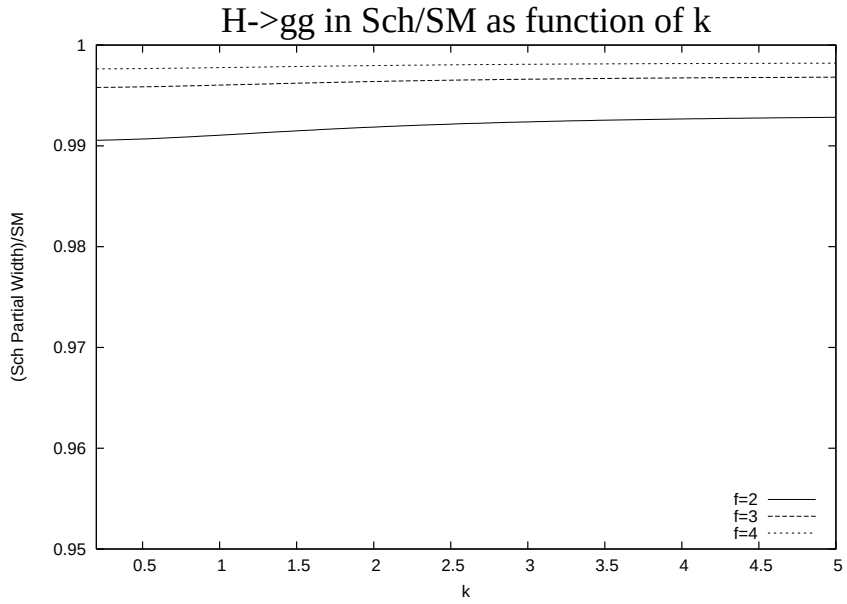

Figure 4.17: Ratio of Schmaltz partial width to SM partial width Vs k for $\tan\beta = 2$ and $M_H = 120$ GeV.

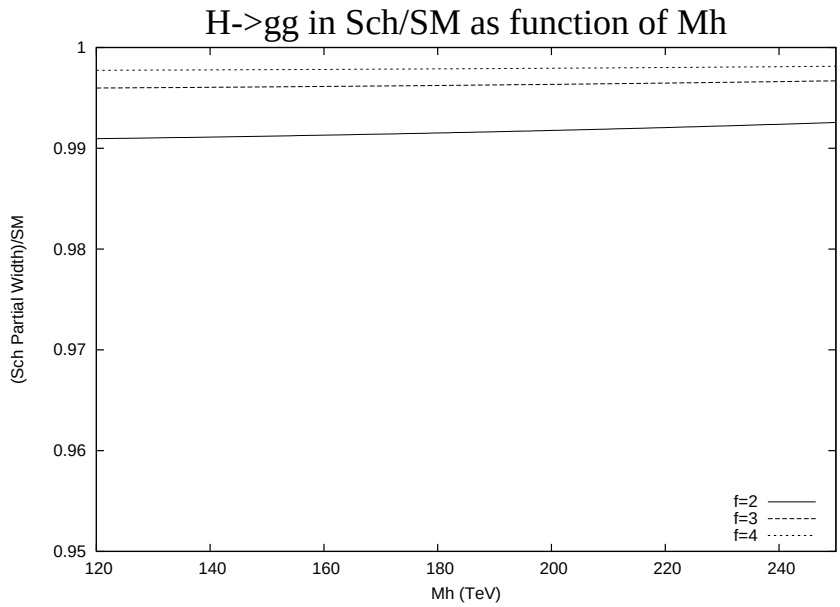

Figure 4.18: Ratio of Schmaltz partial width to SM partial width Vs M_H for $k = 1$ and $\tan\beta = 2$.

The reason for this is that an asymmetry was introduced by defining Φ_2 to be the scalar triplet which couples to the heavy neutral singlet N^c. Because of this, the factor y_{G_F} is not invariant under interchanging f_1 and f_2, and one of the terms in y_{G_F} precisely cancels the term from y_t which would have led to large deviations for $t_\beta \ll 1$ if it had remained present.

The deviation from the SM falls of as f^2 at seen in figure 4.16. For moderate values of t_β the deviation is less than about 10% for $f \gtrsim 1.5$ TeV.

Almost all of the deviation from the SM comes from the first 2 terms in the square brackets in equation (4.38). The terms involving the parameters k and M_H (M_H is implicit in the function $F_{1/2}(\tau_t)$) do not make a large contribution. Figures 4.17 and 4.18 show that the deviation is virtually unchanged when these parameters are varied.

4.2.2 Higgs Decays To Photons

The partial width for the loop induced decay of the Higgs to a pair of photons in the Schmaltz model can be found by using the general formula (4.3) and allowing the t, T, $W^\pm$ and $X^\pm$ particles to run in the loop. This gives

$$\begin{aligned}\Gamma(H \to \gamma\gamma) &= \frac{\sqrt{2}G_F\alpha^2 M_H^3 y_{G_F}^2}{256\pi^3}|y_{G_F}[y_t\frac{4}{3}F_{1/2}(\tau_t) + y_{W^\pm}F_1(\tau_{W^\pm}) \\ &\quad + y_T\frac{4}{3}F_{1/2}(\tau_T) + y_{X^\pm}F_1(\tau_{X^\pm})|^2. \end{aligned} \tag{4.39}$$

Substituting the y_j factors of equations (4.32) and (4.34) into this formula leads to the expression

$$\begin{aligned}\Gamma(H\to\gamma\gamma) &= \frac{\sqrt{2}G_F\alpha^2 M_H^3 y_{G_F}^2}{256\pi^3}|[\frac{4}{3}F_{1/2}(\tau_t)+F_1(\tau_{W^\pm}) \\ &+\frac{v^2}{f^2}[-\frac{1}{4}(1+t^2)(\frac{4}{3}F_{1/2}(\tau_t)+F_1(\tau_{W^\pm}))+\frac{2k^2}{3}\frac{(1+t^2)^2}{(1+k^2t^2)^2} \\ &\times(F_{1/2}(\tau_t)-F_{1/2}(\tau_T.))+\frac{1}{2}(F_1(\tau_{W^\pm})-F_1(\tau_{X^\pm}))]|^2 \qquad (4.40)\end{aligned}$$

Taking the ratio of this and the SM result (given by the first 2 terms inside the square brackets) yields the result

$$\begin{aligned}\frac{\Gamma(H\to\gamma\gamma)_{\rm Sch}}{\Gamma(H\to\gamma\gamma)_{\rm SM}} &= |1+\frac{v^2}{f^2}[-\frac{1}{4}(1+t^2)+\frac{1}{2}\frac{F_1(\tau_{W^\pm})-F_1(\tau X^\pm)}{\frac{4}{3}F_{1/2}(\tau_t)+F_1(\tau_{W^\pm})} \\ &+\frac{2k^2}{3}\frac{(1+t^2)^2}{(1+k^2t^2)^2}\frac{F_{1/2}(\tau_t)-F_{1/2}(\tau_T)}{\frac{4}{3}F_{1/2}(\tau_t)+F_1(\tau_{W^\pm})}]|^2. \qquad (4.41)\end{aligned}$$

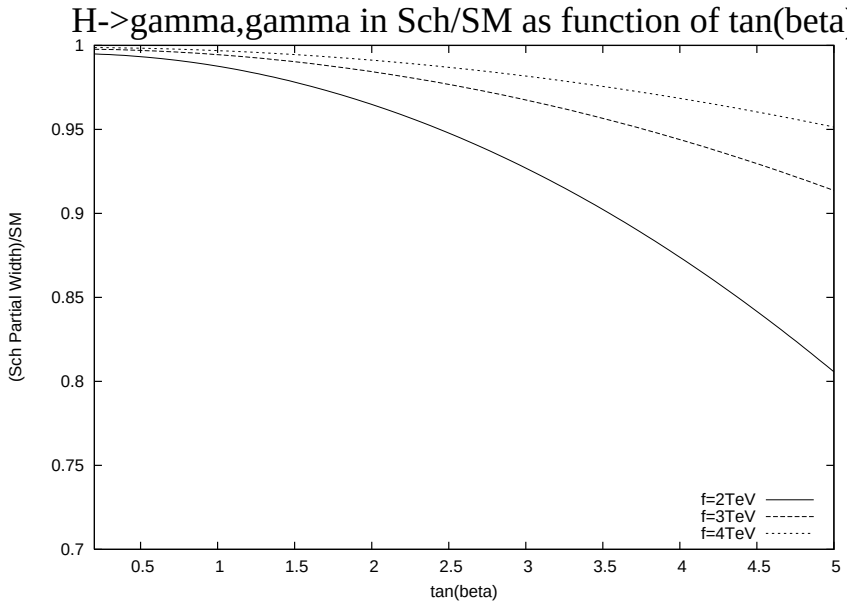

Figure 4.19: Ratio of Schmaltz partial width to SM partial width Vs $\tan\beta$ for $k=1$ and $M_H = 120$ GeV.

As in the case of the decay to gluons, the most interesting feature is how the process is suppressed relative to the SM at large $\tan\beta$, where $f_2 \gg f_1$, as shown in figure 4.19. The suppression falls off proportionally with $1/f^2$ as shown in figure 4.20 and, for moderate values of $\tan\beta$, is less than 10% for all values of f allowed by the EWPCs.

4.3 Prospects For Observation

At a hadron collider such as the LHC, the Higgs may be produced via gluon fusion which allows the coupling of the Higgs to gluon pairs to be probed. A comparison of

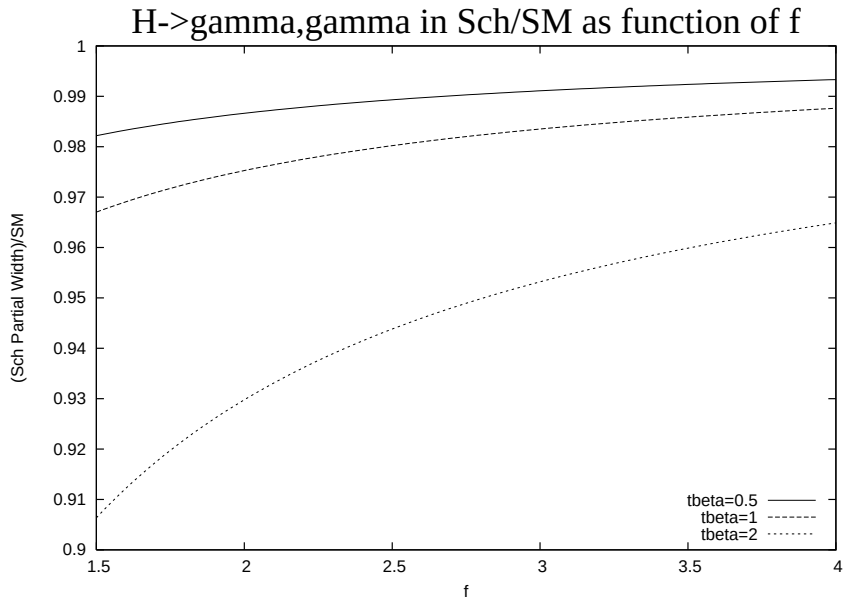

Figure 4.20: Ratio of Schmaltz model partial width to SM partial width Vs f for $k = 1$ and $M_H = 120$ GeV.

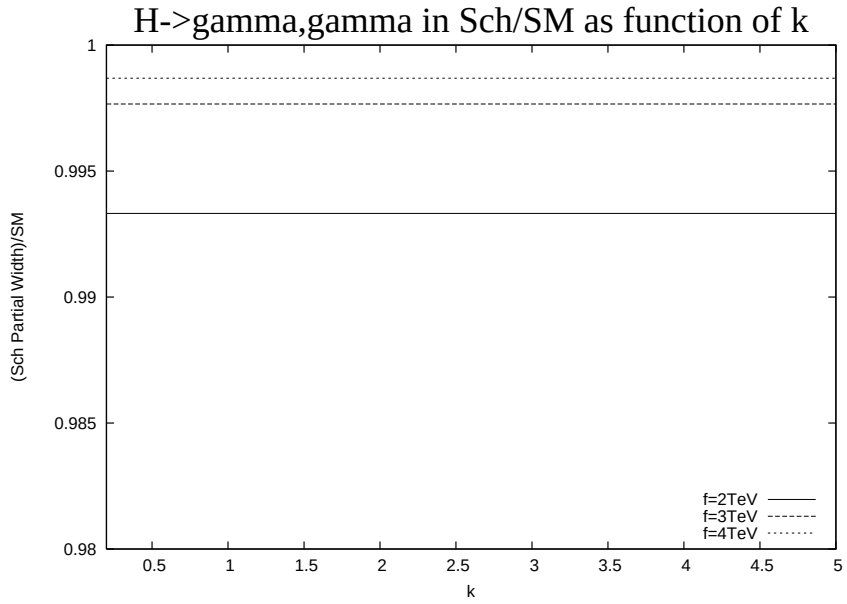

Figure 4.21: Ratio of Schmaltz partial width to SM partial width Vs k for $\tan\beta = 2$ and $M_H = 120$ GeV.

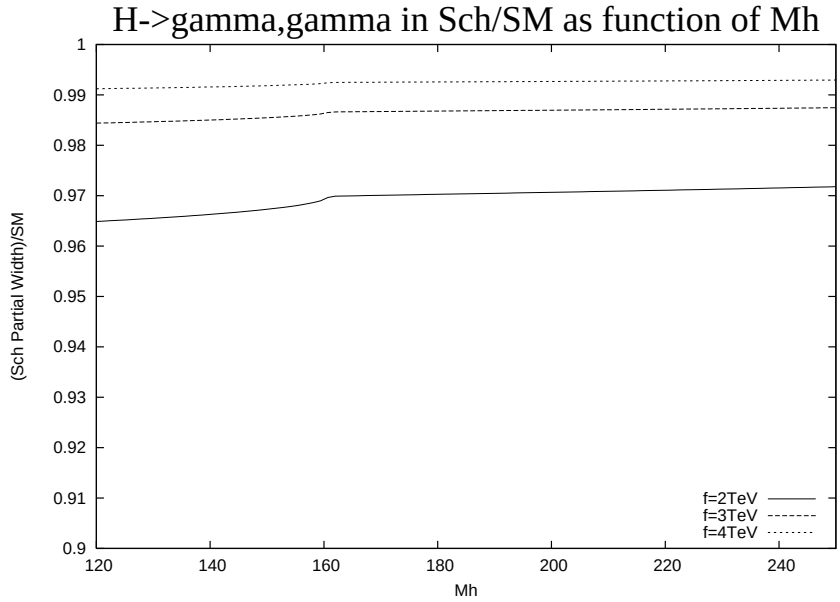

Figure 4.22: Ratio of Schmaltz partial width to SM partial width Vs M_H for $k = 1$ and $\tan\beta = 2$.

the rates for Higgs production via gluon fusion and Higgs production via weak boson fusion with common final states yields the ratio $\Gamma(H \to gg)/\Gamma(H \to WW)$. This can be measured to an accuracy of about $20 - 30\%$ for a Higgs with mass between 100 and 180 GeV [65].

The Higgs coupling to gluons cannot be probed through Higgs decays at the LHC due to overwhelming dijet backgrounds [66].

Similarly, the ratio $\Gamma(H \to \gamma\gamma)/\Gamma(H \to WW)$ can be measured by counting decays with common production methods. Combined with measurements of the partial width $\Gamma(H \to WW)$, these ratios allow the partial widths $\Gamma(H \to gg)$ and $\Gamma(H \to \gamma\gamma)$ to be measured at the LHC with accuracy of about 30% for a Higgs mass below 140 GeV [67],[68].

Taking into account the errors in determining the ratio $\Gamma(H \to \gamma\gamma)/\Gamma(H \to WW)$ and the partial width $\Gamma(H \to WW)$, deviations relative to the SM are only observable in these processes at the LHC if they are of order 50% or larger [67] which is not the case in the Little Higgs models studied here.

At a 500 GeV linear e^+e^- collider Higgs decays may be used to extract the couplings of the Higgs to gluon or photon pairs in a model independent way. Branching fractions can be determined by tagging the process $e^+e^- \to Z^* \to ZH$ (where Z^* denotes an off-shell Z boson) using the Z recoil mass, then counting final states. The Higgs coupling to Ws can then be determined via the process $e^+e^- \to W^*W^* \to H\nu\bar{\nu}$ which allows us to solve for the individual partial widths.

In this fashion, with 500 fb^{-1} of data, the branching ratio $\Gamma(H \to \gamma\gamma)$ can be measured to within about $15 - 25\%$ for a Higgs mass below 140 GeV, the limiting factor being the rarity of this decay [70],[71]. The branching ratio $\Gamma(H \to gg)$ can be measured to as well as $6 - 12.5\%$ if the Higgs is lighter than 140 GeV [73],[72]. For heavier Higgses

measurements of these branching ratios at an e^+e^- collider is not feasible [73]

Although deviations from the SM in the littlest Higgs and Schmaltz models approach the precision with which they can be measured at an e^+e^- collider, the unknown corrections from higher order QCD effects are large so the discrepancy cannot be verified without higher order calculations.

The best prospect for observation of the width $\Gamma(H \to \gamma\gamma)$ comes from $\gamma\gamma$ colliders. Here, a Higgs is produced from photon collisions which can then decay to $b\bar{b}$ pairs. Combining this with measurements of $H \to b\bar{b}$ decays from a linear collider can provide a measurement of the Higgs to photons branching ratio at the order of $2-3\%$ [71],[45], making the suppression with respect to the SM potentially observable in some regions of parameter space. Higgs production at a $\gamma\gamma$ collider was studied in detail for the Littlest Higgs model in [74].

Chapter 5

Two Higgs Production Via Gluon Fusion

5.1 Higgs Pair Production

Pairs of Higgs bosons can be produced from gluon fusion via quark loops. In the SM, there are two topologies which contribute to this process at the one-loop level; the triangle topology, figure 5.1, and the box topology, figure 5.2.

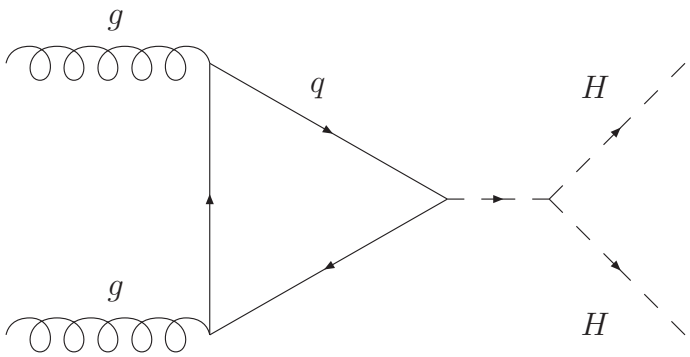

Figure 5.1: Higgs pair production via gluon fusion, triangle topology.

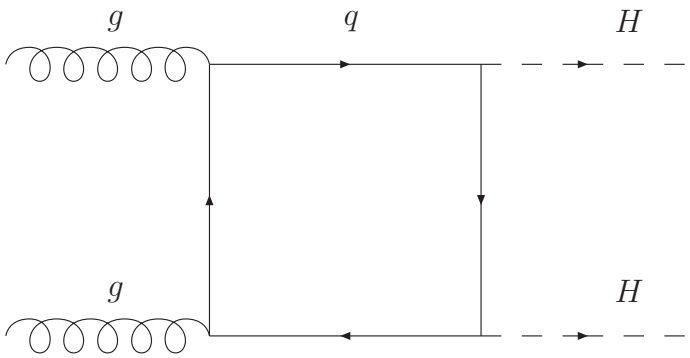

Figure 5.2: Higgs pair production via gluon fusion, box topology.

Variations on these diagrams can be created by permuting the vertices, but all are of either box or triangle type.

For a quark q, the box diagrams are proportional to λ_{qqH}^2 where λ_{qqH} is the Yukawa coupling of the quark q to the Higgs boson. The triangle diagrams are proportional to $\lambda_{qqH}\lambda_3$ where λ_3 is the Higgs trilinear coupling. In the SM only the top quark has a large coupling to the Higgs boson. The other SM quarks can be neglected since their contribution to the amplitude will be suppressed by a factor of $\approx m_q/m_t$.

Gluon fusion is the dominant mechanism for production of Higgs boson pairs at the LHC. It is important to calculate the cross section for this process either as a way to check the SM prediction for the Higgs trilinear coupling, or as a signal for new physics beyond the SM [75].

The leading order (one loop) SM contribution to the process $gg \to HH$ was first computed in [76]. The NLO QCD corrections have been calculated in the heavy top limit where they were found to increase the cross section by about 100% [77], although there is doubt about whether this limit is applicable in multi-Higgs production [75].

5.2 The Program: General Outline

The calculation of the cross section for Higgs pair production from gluon fusion would be extremely arduous to perform by hand. Even in the SM and neglecting all quarks other than the top there are 8 graphs already at the one-loop level. It is much more efficient, and a more reliable result is obtained, if the calculation is automated with a computer. A program for doing this has been created by the authors of [75], who have calculated the cross section for this process at the LHC at the one-loop level in the SM and in the 2 Higgs doublet model. This program was adapted by myself, Stefan Karg and Thomas Binoth to calculate the cross section in the Littlest Higgs and the Schmaltz models. A brief outline of the method employed follows below.

The program Qgraf [78] - if given a process, a list of particles and vertices present in the theory and a number of loops - gives an algebraic representation of all the graphs which contribute to the given process at the given number of loops. Qgraf is used to identify the distinct Feynman diagrams contributing to the process $gg \to HH$ at the one-loop level.

The Qgraf output is then automatically converted into a format suitable for using in the algebra program Form [79]. Form was used to perform the gamma matrix algebra and also to implement tensor integral reduction algorithms. These algorithms take integrals which transform non-trivially under Lorentz transformations and express them in terms of objects built from metric tensors and external momenta (to carry the Lorentz structure) and form factors consisting of linear combinations of integrals which are Lorentz scalars. These tensor reduction algorithms, supplied by Thomas Binoth, make the integrals simpler to perform and will be discussed in more detail below.

The amplitude can be written in the form

$$\Gamma(gg \to HH) = \varepsilon_{1,\mu}\varepsilon_{2,\nu}\mathcal{M}^{\mu\nu} \tag{5.1}$$

where $\varepsilon_{1,\mu}$ and $\varepsilon_{2,\nu}$ are the polarization vectors of the external gluons. Let the external particles be labelled g_1, g_2, h_1 and h_2 with momenta p_1, p_2, p_3 and p_4 respectively. The

only objects which can carry the Lorentz indices of the scattering tensor $\mathcal{M}^{\mu\nu}$ are the metric tensor $g^{\mu\nu}$ and the external momenta. Using this information, and also using momentum conservation to eliminate p_4, the scattering tensor can be written in the form

$$\mathcal{M}^{\mu\nu} = Ag^{\mu\nu} + \sum_{i,j=1}^{3} B_{ij} p_i^\mu p_j^\nu. \tag{5.2}$$

Here, the coefficients A and B_{ij} are linear combinations of scalar loop integrals which fall out of the tensor reduction algorithms. For example, we might write

$$A = \sum_k A^k I_k \tag{5.3}$$

where $\{I_k\}$ is a set of scalar integrals. The coefficients of each of these functions were then exported to Maple for simplification.

Spinor helicity methods [80][81] were employed to simplify the calculation further. Here, the gluon polarization vectors are represented in terms of helicity eigenstates of massless spinors and gamma matrices. These can be chosen in such a way that the contraction of the polarization vectors with the tensor $p_i^\mu p_j^\nu$ vanishes whenever i or j is equal to 1 or 2, drastically reducing the complexity of the amplitude. More details about the helicity method, showing how these contributions vanish, will be given below.

The scalar integrals were evaluated using LoopTools-2.2 [82].

The LHC collides protons, not gluons, so in order to compute the cross section for double-Higgs production at the LHC the cross section for production via gluon fusion must be convoluted with the parton distribution functions (PDFs) using the formula

$$\sigma_{pp\to HH} = \int_0^1 dx_1 dx_2 f_{g1/p}(x_1, \mu_F^2) f_{g2/p}(x_2, \mu_F^2) \sigma_{gg\to HH} \tag{5.4}$$

Here μ_F is the factorisation (and renormalisation) scale. The answer computed to all orders in perturbation theory would be independent of μ_F but at any particular order in perturbation theory some factorisation scale dependence is present. The factorisation scale dependence will be discussed later. The x_i are the ratios of the energy of the gluons g_i to the energy of the protons. The functions $f_{gi/p}(x_i, \mu_F^2)$ are the parton distribution functions which are empirically extracted from deep inelastic scattering experiments, fixed target experiments and jets at Tevatron. The MRST2002nlo PDF set [83] as implemented in LHAPDF [84] was used to provide the gluon density as well as the strong coupling.

The integrations over dx_i, along with the other relevant phase space integrations, were performed numerically using the Monte Carlo (MC) integration package Bases [85].

The program expresses the result in terms of the total cross section $\sigma(PP \to HH)$. The following parameters [2] were used for the SM case,

$$\begin{aligned} E_{\rm com} &= 14 \text{ TeV} \\ \alpha_s(M_Z) &= 0.120 \\ \alpha(0) &= 1/137.036 \\ m_t &= 174.2 \text{ GeV} \\ G_F &= 11.66 \times 10^{-5} \text{ GeV}^{-2} \end{aligned} \tag{5.5}$$

The centre of mass energy $E_{\rm com}$ was taken to be 14 TeV because this is the centre of mass energy of the LHC. The parameter G_F is used to find the Higgs vev via equation (4.20).

5.3 Tensor Integral Reduction Algorithm

One loop Feynman diagrams, of the form of figure 5.3, lead to tensor integrals (i.e., integrals which transform as tensors under Lorentz transformations) of the form

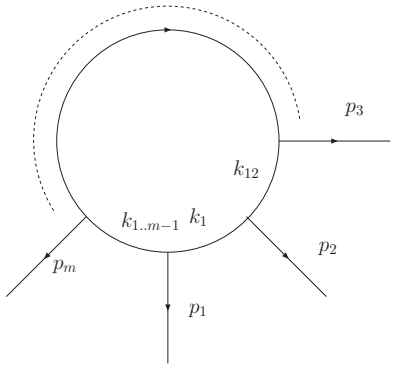

Figure 5.3: A generic loop diagram with m external legs

$$\mathcal{I}_m^{\mu_1..\mu_i} = \int \frac{d^n k}{(2\pi)^n} \frac{k^{\mu_1}..k^{\mu_i}}{(k^2 - m_1^2 + i\epsilon)(k_1^2 - m_2^2 + i\epsilon)..(k_{12..m-1}^2 - m_m^2 + i\epsilon)}. \tag{5.6}$$

Here, $k_{12..j} = k + p_{1..j}$ where $p_{1..j}$ is $p_1 + .. + p_j$ and p_i is the 4-momentum of the particle attached to the i^{th} external leg and k is the loop momentum. The components of k in the numerator may, for example, arise from fermion propagators or gauge boson tri-linear vertices.

The simplest loop integrals are those with no Lorentz indices in the numerator. Since these transform as scalars under Lorentz transformations they are referred to as scalar integrals. It is possible to reduce the calculation of non-scalar tensor integrals to the calculation of linear combinations of scalar integrals. The most well know way of doing this is Passarino-Veltman reduction [86]. The best way to illustrate Passarino-Veltman reduction is by example. The example chosen here is the integral (from [87])

$$\mathcal{I}^{\mu}(p_1, p_2) = \int \frac{d^n k}{(2\pi)^n} \frac{k^{\mu}}{(k^2 + i\epsilon)(k_1^2 + i\epsilon)(k_{12}^2 + i\epsilon)} \tag{5.7}$$

which arises in the case of a loop diagram with 3 external legs and a massless particle running in the loop. $\mathcal{I}$ has been written as a function of p_1 and p_2 only since p_3 can be eliminated by momentum conservation.

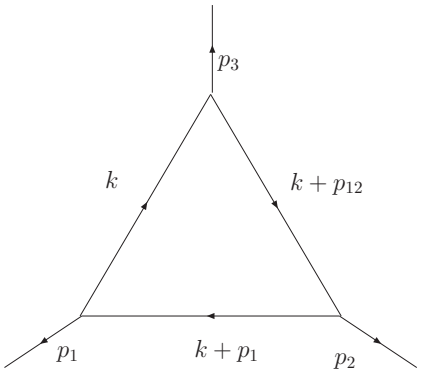

Figure 5.4: A triangle loop diagram

In this case the only objects which can carry the Lorentz index are the external momenta p_1 and p_2. The integral may thus be written

$$\mathcal{I}^\mu(p_1,p_2) = B_1(p_1,p_2)p_1^\mu + B_2(p_1,p_2)p_2^\mu. \tag{5.8}$$

Both sides of this equation may be contracted with the external momenta p_1 and p_2 to obtain the matrix equation

$$\begin{pmatrix} p_1.\mathcal{I} \\ p_2.\mathcal{I} \end{pmatrix} = \begin{pmatrix} p_1^2 & p_1.p_2 \\ p_1.p_2 & p_2^2 \end{pmatrix} \begin{pmatrix} B_1 \\ B_2 \end{pmatrix} \tag{5.9}$$

In order to find the form factors B_1 and B_2 this matrix equation must be inverted. This gives

$$\begin{pmatrix} B_1 \\ B_2 \end{pmatrix} = \frac{1}{\Delta} \begin{pmatrix} p_2^2 & -p_1.p_2 \\ -p_1.p_2 & p_1^2 \end{pmatrix} \begin{pmatrix} p_1.\mathcal{I} \\ p_2.\mathcal{I} \end{pmatrix} \tag{5.10}$$

where Δ is called the *Gram determinant* and is given by

$$\Delta = \begin{vmatrix} p_1^2 & p_1.p_2 \\ p_1.p_2 & p_2^2 \end{vmatrix} = p_1^2p_2^2 - (p_1.p_2)^2. \tag{5.11}$$

The dot product $p_1.k$ may be rewritten by the use of the following relation

$$k_1^2 = k^2 + 2k.p_1 + p_1^2 \tag{5.12}$$

$$\Rightarrow \quad p_1.k = \frac{1}{2}(k_1^2 - k^2 - p_1^2) \tag{5.13}$$

and, similarly, $p_2.k$ may be written in the form

$$p_2.k = \frac{1}{2}(k_{12}^2 - k_1^2 - p_{12}^2 + p_1^2). \tag{5.14}$$

These relations are useful because they express the dot products of loop and external momenta as a linear combination of terms which appear in the denominator of the integral $\mathcal{I}$ and terms involving only the external momenta (i.e., no loop momenta).

They may be used to rewrite the scalar integrals on the right hand side of equation 5.10, viz

$$\begin{aligned} p_1.\mathcal{I} &= \int \frac{d^n k}{(2\pi)^n} \frac{p_1.k}{k^2 k_1^2 k_{12}^2} \\ &= \frac{1}{2} \int \frac{d^n k}{(2\pi)^n} \frac{k_1^2 - k^2 - p_1^2}{k^2 k_1^2 k_{12}^2} \\ &= \frac{1}{2} \int \frac{d^n k}{(2\pi)^n} \frac{1}{k^2 k_{12}^2} - \frac{1}{2} \int \frac{d^n k}{(2\pi)^n} \frac{1}{k_1^2 k_{12}^2} - \frac{1}{2} p_1^2 \int \frac{d^n k}{(2\pi)^n} \frac{1}{k^2 k_1^2 k_{12}^2} \end{aligned} \tag{5.15}$$

and, in a similar fashion

$$p_2.\mathcal{I} = \frac{1}{2} \int \frac{d^n k}{(2\pi)^n} \frac{1}{k^2 k_1^2} - \frac{1}{2} \int \frac{d^n k}{(2\pi)^n} \frac{1}{k^2 k_{12}^2} - \frac{1}{2}(p_{12}^2 - p_1^2) \int \frac{d^n k}{(2\pi)^n} \frac{1}{k^2 k_1^2 k_{12}^2}. \tag{5.16}$$

Evaluating the scalar integrals occuring in (5.15) and (5.16) is much simpler than evaluating the original tensor integral of equation (5.7). These may be performed by the standard method of Feynman parameters.

After calculation of the integrals $p_1.\mathcal{I}$ and $p_2.\mathcal{I}$, the coefficients $B_1(p_1, p_2)$ and $B_2(p_1, p_2)$ may be obtained via equation (5.10) which, in turn, yield an expression for $\mathcal{I}^\mu$ upon substitution into equation (5.8). To summarize, the Passarino-Veltman [86] method for the reduction of tensor integrals with m external legs proceeds in the following steps.

- Use Lorentz invariance to equate the tensor integral with terms proportional to products of metric tensors and external momenta multiplied by form factors, using momentum conservation to eliminate one of the external momenta. (e.g. equation (5.8))
- Take dot products of this equation with the $m - 1$ remaining external momenta to create a set of linear equations. (c.f. equation (5.9))
- Invert the system of linear equations obtained to express the form factors in terms of a linear combination of dot products of the tensor integal with external momenta. (c.f. equation (5.10))
- Rewrite the dot products of the external momenta and the loop momenta in terms of factors which appear in the denominator of the tensor integral (as in equations (5.12),(5.14))
- Substitute these relations into the dot products of the tensor integral with the external momenta to obtain a linear combination of comparatively simple scalar integrals. (c.f. equations (5.15),(5.16))
- Evaluate the scalar integrals to obtain the form factors.
- Combine the form factors with the relevant products of metric tensors and external momenta to obtain the result for the tensor integral.

Some comments on the Passarino-Veltman method can be made.

- There will always occur an inverse Gram determinant (c.f. equation (5.10)) which becomes singular in certain regions of phase space. These singularities are an artifice of this calculational scheme and should cancel out. However, it is often difficult to spot how these cancellations occur and this can lead to numerical instabilities when evaluating the amplitude.

- For higher order tensors the tensor reduction algorithm must be iterated several times. The number of iterations is equal to the rank of the tensor. This leads to multiple Gram determinants in the denominator and in general requires a shift of the loop momentum at each iteration.

The Passarino-Veltman method is used here to evaluate the one loop cross section for the process $gg \to HH$. The form factors are decomposed in terms of a basis of Feynman parameter integrals which is defined in reference [88].

5.4 Spinor Helicity Methods

5.4.1 Introduction And Notation

When computing cross sections (here meaning the squared amplitude $|\mathcal{M}|^2$ before any phase space integration) the standard goal is to reduce the expression to terms involving four-vector dot products. This is achieved by first squaring the amplitude and then using spin sum relations such as

$$\sum_s u^s(p)\bar{u}^s(p) = \not{p} \pm m \tag{5.17}$$

for spinors of fermions of momentum p and mass m, where the sign is $+(-)$ for a fermion (anti-fermion), and

$$\sum_\lambda \varepsilon_\lambda^\mu \varepsilon_\lambda^{*\nu} \to -g^{\mu\nu} \tag{5.18}$$

where λ is helicity, for the polarization vectors of (massless) gauge bosons. Note the above substitution is not an equality, but is valid in the context of a squared amplitude $|\mathcal{M}|^2$ in the Feynman gauge with similar substitutions applicable in other gauges.

Applying these spin-sum relations result in traces over Dirac matrices which can easily be evaluated to yield an expression in terms of four-vector dot products.

Although conceptually simple enough, this scheme runs up against issues of computing capacity when the size of the expressions becomes large. The amplitude must be squared before these techniques can be applied so both the number of traces and their length quickly increases at higher orders in perturbation theory [80]. It is easy to see that any scheme which results in simplifications at the level of $\mathcal{M}$ rather than $|\mathcal{M}|^2$ will eventually become superior to this approach.

In the spinor helicity approach [80],[81] spinor products such as $\bar{u}(k)u(p)$ are used rather than vector products $k.p$. These spinor products are not much more complicated than vector products and, as shall be demonstrated, lead to simplifications at the level of the amplitude $\mathcal{M}$ making them more suitable for use in larger expressions.

In preparation for the discussion of spinor helicity methods it is useful to revise a few important spinor identities. In the case of a massless fermion with momentum p and helicity λ (so $\lambda = \pm 1$) there is the relation

$$u_\lambda(p)\bar{u}_\lambda(p) = \omega_\lambda \not{p} \tag{5.19}$$

where

$$\omega_\lambda = \frac{1}{2}(1 + \lambda\gamma^5). \tag{5.20}$$

Another useful identity relates spinor products of massless fermions to four-vector dot products,

$$\begin{aligned} |\bar{u}_-(p)u_+(k)|^2 &= \bar{u}_-(p)u_+(k)\bar{u}_+(k)u_-(p) \\ &= \mathrm{Tr}[\omega_- \not{p} \omega_+ \not{k}] \\ &= \mathrm{Tr}[\omega_-^2 \not{p} \not{k}] \\ &= p_\alpha k_\beta \mathrm{Tr}[\omega_- \gamma^\alpha \gamma^\beta] \\ &= 4p_\alpha k_\beta \times \frac{1}{2} g^{\alpha\beta} \\ &= 2p.k \end{aligned} \tag{5.21}$$

or, a little more generally,

$$|\bar{u}_\lambda(p)u_{-\lambda}(k)|^2 = 2p.k. \tag{5.22}$$

5.4.2 Spinor Representation Of Polarization Vectors

The polarization vectors for massless gauge bosons with momentum p and of definite helicity, $\varepsilon_\pm$, are required to have the properties [80]

$$\begin{aligned} \varepsilon_\lambda.p &= 0 \\ \varepsilon_\lambda.\varepsilon_\lambda &= 0 \\ \varepsilon^\mu_{-\lambda} &= (\varepsilon^\mu_\lambda)^* \\ \varepsilon_\lambda.\varepsilon_{-\lambda} &= -1 \end{aligned} \tag{5.23}$$

Any object with these properties is valid as a representation of the polarization vectors. In particular, the polarization vectors may be chosen to take the form [80],[81].

$$\varepsilon^\mu_+(p,q) = \frac{\bar{u}_-(q)\gamma^\mu u_-(p)}{\sqrt{2}\bar{u}_-(q)u_+(p)} \tag{5.24}$$

$$\varepsilon^\mu_-(p,q) = \frac{\bar{u}_-(p)\gamma^\mu u_-(q)}{\sqrt{2}\bar{u}_+(q)u_-(p)} \tag{5.25}$$

where q is any vector such that $q^2 = 0$ and q is not collinear with p. In general changing q results in changing the polarization vector by a gauge transformation and a complex

phase. This freedom to choose the vector q is what makes it possible to achieve a simplified form for the amplitude.

Going back to equation (5.1), the tensor $\mathcal{M}^{\mu\nu}$ must be contracted with external gluon polarization vectors of helicity $(++)$, $(+-)$, $(-+)$ and $(--)$. Due to parity invariance, only two of these helicity amplitudes need be known.

$$\begin{aligned} \mathcal{M}^{--} &= \mathcal{M}^{++} \\ \mathcal{M}^{-+} &= \mathcal{M}^{+-} \end{aligned} \tag{5.26}$$

The combination of external gluon polarization vectors which contract with $\mathcal{M}^{++}$ is

$$\varepsilon^{\mu}_{1+}\varepsilon^{\nu}_{2+} = \frac{\bar{u}_-(q_1)\gamma^{\mu}u_-(p_1)\bar{u}_-(q_2)\gamma^{\nu}u_-(p_2)}{2\bar{u}_-(q_1)u_+(p_1)\bar{u}_-(q_2)u_+(p_2)} \tag{5.27}$$

Here q_1 and q_2 are arbitrary other than that they must satisfy the constraints $q_1^2 = q_2^2 = 0$ and $q_1(q_2)$ not collinear with $p_1(p_2)$. It shall be shown that simplifications in the calculation may be achieved by setting $q_1 = p_2$ and $q_2 = p_1$, so that

$$\varepsilon^{\mu}_{1+}\varepsilon^{\nu}_{2+} = \frac{\bar{u}_-(p_2)\gamma^{\mu}u_-(p_1)\bar{u}_-(p_1)\gamma^{\nu}u_-(p_2)}{2\bar{u}_-(p_2)u_+(p_1)\bar{u}_-(p_1)u_+(p_2)} \tag{5.28}$$

The numerator of this expression may be written

$$\begin{aligned} \bar{u}_-(p_2)\gamma^{\mu}u_-(p_1)\bar{u}_-(p_1)\gamma^{\nu}u_-(p_2) &= \mathrm{Tr}[\omega_- \not{p}_1 \gamma^{\nu} \omega_- \not{p}_2 \gamma^{\mu}] \\ &= \mathrm{Tr}[\omega_- \not{p}_1 \gamma^{\nu} \not{p}_2 \gamma^{\mu}] \end{aligned}$$

where equation (5.19) has been utilized. Also, the denominator may be rewritten,

$$\begin{aligned} 2\bar{u}_-(p_2)u_+(p_1)\bar{u}_-(p_1)u_+(p_2) &= \frac{2\bar{u}_-(p_2)u_+(p_1)\bar{u}_-(p_1)u_+(p_2)\bar{u}_+(p_2)u_-(p_1)}{\bar{u}_+(p_2)u_-(p_1)} \\ &= \frac{2\bar{u}_-(p_2)u_+(p_1)\mathrm{Tr}[\omega_- \not{p}_1 \omega_+ \not{p}_2]}{\bar{u}_+(p_2)u_-(p_1)} \\ &= \frac{4\bar{u}_-(p_2)u_+(p_1)p_1.p_2}{\bar{u}_+(p_2)u_-(p_1)} \end{aligned}$$

Then, defining $s_{12} = (p_1 + p_2)^2 = 2p_1.p_2$ (since $p_1^2 = p_2^2 = 0$ for the external gluons) and using the identity $\bar{u}_-(p_2)u_+(p_1) = -\bar{u}_-(p_1)u_+(p_2)$, the denominator is found to be

$$\frac{-2s_{12}\bar{u}_-(p_1)u_+(p_2)}{u_+(p_2)u_-(p_1)} \tag{5.29}$$

Finally, putting the numerator and denominator together leads to the expression

$$\varepsilon^{\mu}_{1+}\varepsilon^{\nu}_{2+} = -\frac{\bar{u}_+(p_2)u_-(p_1)}{2s_{12}\bar{u}_-(p_1)u_+(p_2)}\mathrm{Tr}[\omega_- \not{p}_1 \gamma^{\nu} \not{p}_2 \gamma^{\mu}] \tag{5.30}$$

The other combination of polarization vectors which is needed is $\varepsilon^{\mu}_{1-}\varepsilon^{\nu}_{2+}$, which contracts with $\mathcal{M}^{+-}$.

$$\varepsilon^{\mu}_{1+}\varepsilon^{\nu}_{2-} = \frac{\bar{u}_-(q_1)\gamma^{\mu}u_-(p_1)\bar{u}_-(p_2)\gamma^{\nu}u_-(q_2)}{2\bar{u}_-(q_1)u_+(p_1)\bar{u}_+(q_2)u_-(p_2)} \tag{5.31}$$

Again putting $q_1 = p_2$ and $q_2 = p_1$, the polarization vectors may be written in the form,

$$\varepsilon^{\mu}_{1+}\varepsilon^{\nu}_{2-} = \frac{\bar{u}_-(p_2)\gamma^\mu u_-(p_1)\bar{u}_-(p_2)\gamma^\nu u_-(p_1)}{\bar{u}_-(p_2)u_+(p_1)\bar{u}_+(p_1)u_-(p_2)} \tag{5.32}$$

The value of this spinor representation of the polarization vectors is seen when they are contracted with the scattering tensor $\mathcal{M}^{\mu\nu}$ as given in equation (5.2). Many of the external momenta contract with the epsilon tensors to give zero. For example,

$$\begin{aligned}
\varepsilon^{\mu}_{1+}\varepsilon^{\nu}_{2+}p^{\mu}_i p^{\nu}_1 &\approx p^{\mu}_i p^{\nu}_1 \mathrm{Tr}[\omega_- \not{p}_1 \gamma^\nu \not{p}_2 \gamma^\mu] \\
&= \mathrm{Tr}[\omega_- \not{p}_1 \not{p}_1 \not{p}_2 \not{p}_i] \\
&= \mathrm{Tr}[\omega_- p_1^2 \not{p}_2 \not{p}_i] \\
&= 0
\end{aligned} \tag{5.33}$$

After the dust settles all the terms involving B_{ij} vanish when i or j is equal to 1 or 2 for all helicities as well as the term proportional to A in the opposite helicity, i.e. $(+-)$ or $(-+)$, case and only the following terms are left.

$$\mathcal{M}^{++} = \frac{\bar{u}_+(p_2)u_-(p_1)}{\bar{u}_-(p_1)u_+(p_2)}(A - \frac{\mathrm{Tr}[\omega_- \not{p}_1 \not{p}_3 \not{p}_2 \not{p}_3]}{2s_{12}} B_{33}) \tag{5.34}$$

$$\mathcal{M}^{+-} = \frac{\bar{u}_-(p_2)\not{p}_3 u_-(p_1)}{\bar{u}_-(p_1)\not{p}_3 u_-(p_2)} \frac{\mathrm{Tr}[\omega_- \not{p}_1 \not{p}_3 \not{p}_2 \not{p}_3]}{2s_{12}} B_{33} \tag{5.35}$$

This results in a much shorter expression for the amplitude because it contains only 2 form factors leading to speedy evaluation.

5.5 The Standard Model Case

A calculation of the cross section for the process $gg \to HH$ in the SM, using the same computational methods employed in this thesis to calculate the process in little Higgs models, was presented in the paper [75]. The motivation for studying this process in the SM is to measure the parameter λ_3 and to check the SM relation $\lambda_3 = 3M_H^2/v$. Modifications to this relation could, for example, arise from higher dimensional operators of the type [75]

$$\sum_{k=1}^{\infty} \frac{g_k}{\Lambda^{2k}}(h^\dagger h - \frac{v^2}{2})^{2+k} \tag{5.36}$$

where g_k is a coupling constant and Λ is some mass scale.

The SM result for the total cross section $\sigma(gg \to HH)$ at the LHC is shown in figure 5.5. This shows that for a Higgs mass ranging between 110 GeV and 250 GeV the total LHC cross section falls from about 23 fb to about 2.5 fb. These results are those from the leading order (1-loop) processes. Next to leading order corrections are expected to be large leading to k-factors as large as 2 [77][89].

Of particular interest is the dependence on the factorisation and renormalisation scale (which are set to be equal and are denoted by μ) plotted in figure 5.6. For figure 5.5,

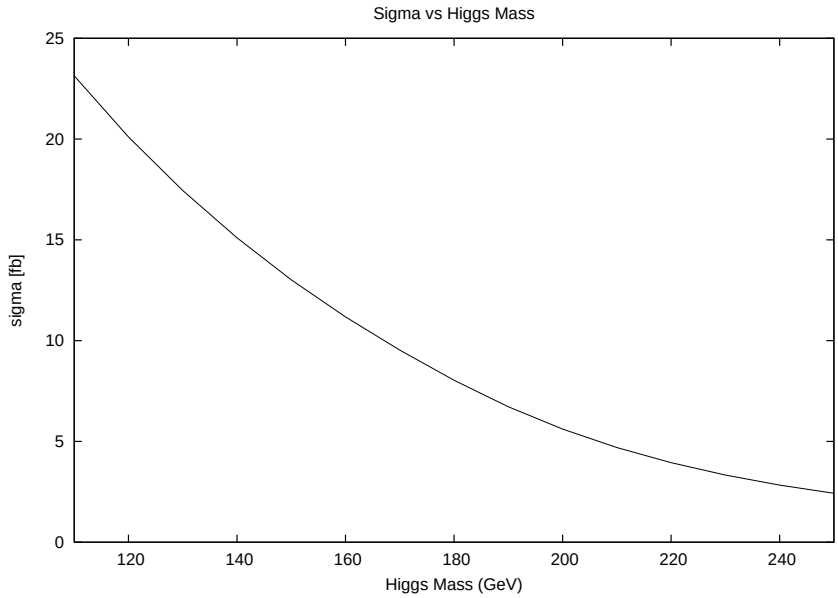

Figure 5.5: Higgs mass dependence of LHC cross section (i.e. at $E_{com} = 14$ TeV) for the process $gg \to HH$ in the SM using $\mu = 2M_H$

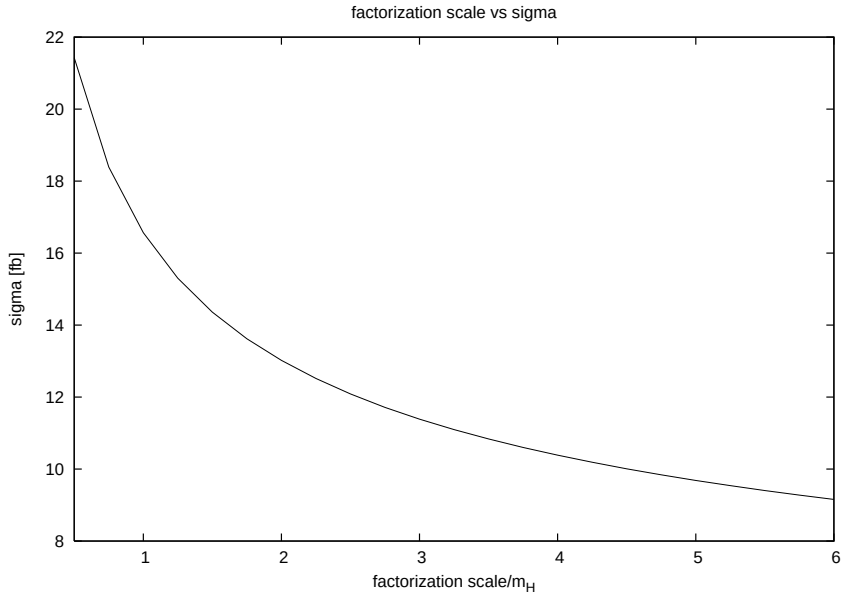

Figure 5.6: Factorisation and Renormalisation scale dependence of the LHC cross section for the process $gg \to HH$ in the SM using $M_H = 150$ GeV

and for all other figures in this chapter except for figure 5.6, the value $\mu_0 = 2M_H$ was used. Varying μ between $\mu_0/3$ and $3\mu_0$ leads to a variation in the cross section of order 50%. This uncertainty is due to the large next to leading order (NLO) corrections to QCD processes and dominates any uncertainties from the parameters and PDFs.

5.6 The Littlest Higgs Model Case

The same computational methods as used in the SM case (see [75]) are here employed to calculate the total LHC cross section for the process $gg \to HH$ in the Littlest Higgs model. The new particles and interactions of the Littlest Higgs model introduce many new channels for this process.

The box and triangle diagrams as were present in the SM case are also present in the Littlest Higgs case, only now the heavy T quark can also run in the loop as shown in figures 5.7, 5.8. In addition, there are new types of box diagram where t and T quarks both run in the loop in the same diagram as shown in figure 5.9. This diagram appears because of the tTH coupling of the Littlest Higgs model.

There are also new triangle diagrams. Those in figure 5.10 arise because of the dimension 5 $ttHH$ and $TTHH$ couplings, while those in figure 5.11 are similar to those in figure 5.8 except that there is an intermediate Φ particle instead of a H.

As in the SM case variations on these diagrams exist with different permutations of the Higgs and gluon vertices.

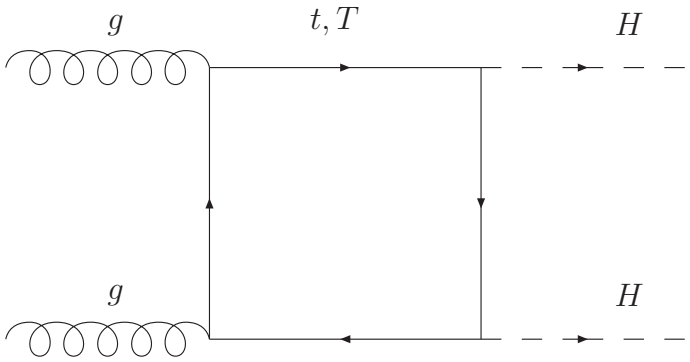

Figure 5.7: Box topology

The top-Higgs couplings are given in table 2.1 with the masses of the quarks given by equations (2.49). The scalar masses and trilinear couplings are given by equations (2.37) and (2.38) and table 2.5.3. All these couplings were included up to order v^2/f^2.

A number of features of this calculation make it more tricky than the SM case. There are, of course, a larger number of Feynman diagrams to evaluate. There are 36 in total after all the possible permutations of the vertices are taken into account (swap incoming gluons, swap outgoing Higgses, different combinations of t and T quarks in the loop). Compare this with the SM where there are only 8. However, the calculation is highly automated so that the higher number of diagrams is not in itself a problem.

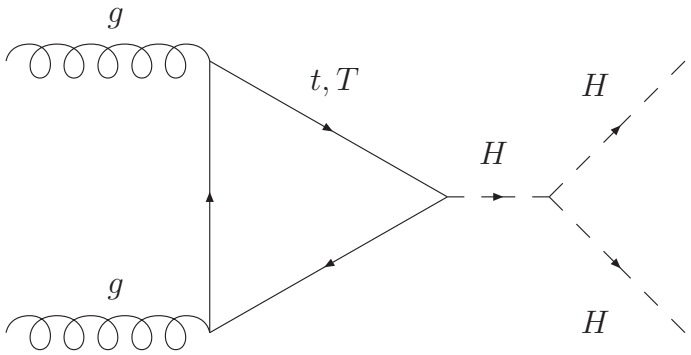

Figure 5.8: Triangle topology

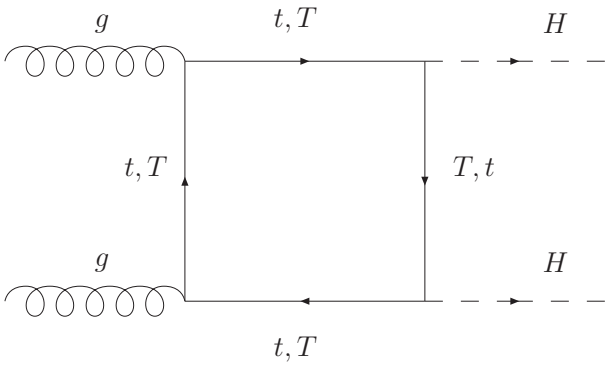

Figure 5.9: Box topology with tTH couplings

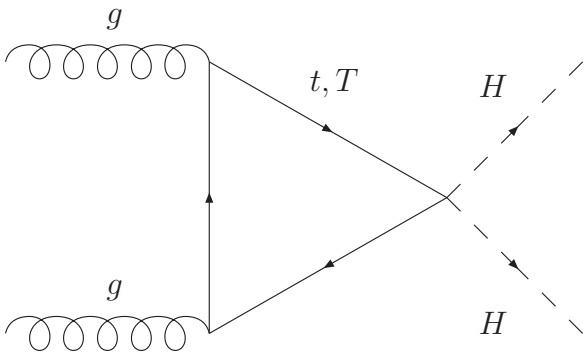

Figure 5.10: Triangle topology with dimension 5 vertex

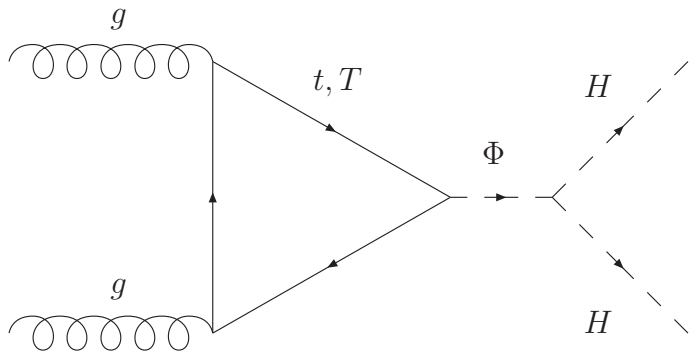

Figure 5.11: Triangle topology with intermediate Φ scalar

One complication of the Littlest Higgs model is that there are box diagrams with more than one type of quark in the loop. In the SM case all box diagrams have only t quarks in the loop which makes the tensor reduction simpler to perform. In the Littlest Higgs model this is no longer the case. This makes this stage of the calculation slower in the Littlest Higgs model.

Perhaps the most important new feature of the Littlest Higgs model is that there are couplings which contain the matrix γ^5. This causes a problem because the calculation is performed in dimensional regularisation and γ^5 cannot be defined in general for $d \neq 4$. This problem was solved using the methods presented in the paper [90].

Originally, the plan was to perform an independent calculation of the $PP \to HH$ cross section which had previously been presented in the papers [91],[92], then there would be an original calculation of the Schmaltz model case. These papers present calculations of the total LHC cross sections for $PP \to HH$ in the Littlest Higgs model and the Littlest Higgs model with T-parity. According to these authors the T-parity case is the same as the non T-parity case except that there is no contribution from the Φ particle. However this is not the case. The T-parity case contains more heavy fermions and cannot be obtained in any simple limit of the non T-parity case.

The authors of the above papers also neglect mixing effects in both the Higgs and the top sectors which gave them only very small deviations from the SM. However, the mixing effects are at least as important as the direct corrections from the propagation of new virtual particles and cannot be neglected.

A more thorough calculation which takes mixing effects into account is presented in [35]. However, these authors take their couplings from the paper [33] which, as was shown in chapter 2, has an incorrect expression for the mixing in the top sector, meaning that the couplings of the t and T quarks with the Higgs are not correct. The results presented here are therefore the first treatment of this process which correctly takes into account all contributions from new particles and mixing at order v^2/f^2.

The cross section depends on the Littlest Higgs model parameters $\{\lambda_1, \lambda_2, f, v, v'\}$. However, these parameters are constrained in that they must recreate the experimentally determined top mass according to the formula (2.49) and also the Fermi constant G_F as in equation (2.76). The cross section may be reexpressed in terms of the set of parameters $\{m_t, G_F, k, f, x\}$ where

$$\begin{aligned} k &= \lambda_2/\lambda_1 \\ x &= \frac{4fv'}{v^2} \end{aligned} \tag{5.37}$$

Graphs which plot the dependence of the total LHC cross section on the free parameters M_H, f, k, x are shown below. All graphs show LHC cross sections with the factorisation and renormalisation scales taken at $2M_H$.

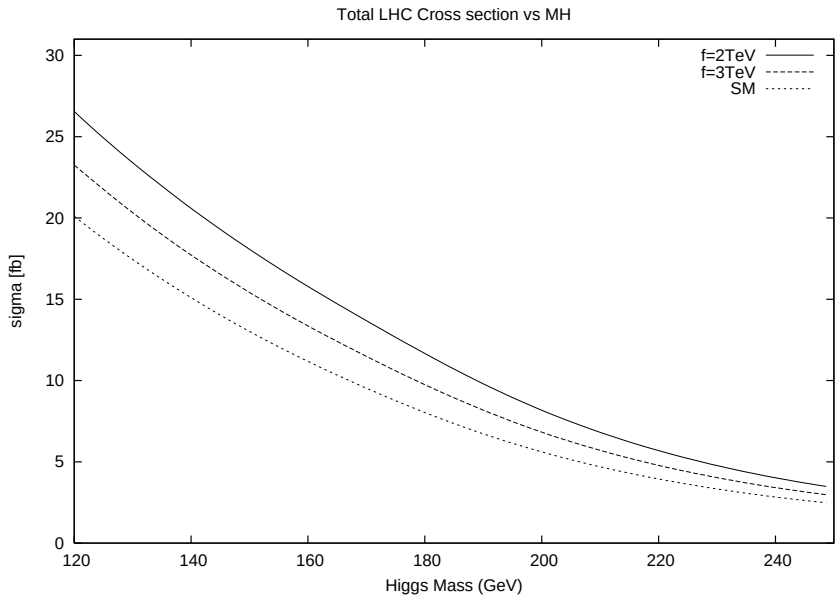

Figure 5.12: Higgs mass dependence of LHC cross section for the process $PP \to HH$ in the Littlest Higgs Model. For $x = 0.85$, $k = 2.5$ and $f = 2$ TeV, $M_T = 4.10$ TeV and M_Φ runs from 2.61 to 5.44 TeV as M_H runs from 120 to 250 GeV. Changing f to 3 TeV leads to $M_T = 6.15$ TeV and M_Φ running from 3.92 to 8.17 TeV.

The cross section falls off with increasing Higgs mass in both the SM and the Littlest Higgs model as shown in figure 5.12. Plotting the ratio of these cross section as in figure 5.13 shows that the cross section is enhanced in the littlest Higgs model and that this enhancement is largest for a relatively heavy Higgs of about 190 GeV.

Plots 5.14 and 5.15 show the dependence on the parameter f. These plots show that the enhancement can be substantial if f is very low at about 1 TeV, as is allowed in some variations of the Littlest Higgs models, but falls off rapidly as f increases.

The dependence of the cross section on the parameter k is shown in figures 5.16 and 5.17. These plots show that the enhancement of the cross section is most pronounced in the region $k \gtrsim 2$.

Finally the dependence on the parameter x is shown in figures 5.18 and 5.19. These show that the cross section can be substantially enhanced as x approaches 1. This behaviour is also seen in [35] where it is noted that it is due to a term in the Higgs trilinear coupling which is proportional to $1/(1-x)$. They also note that in the limit $x \to 1$ the Higgs potential behaves badly. For $x \gtrsim 0.95$ the Higgs potential parameters

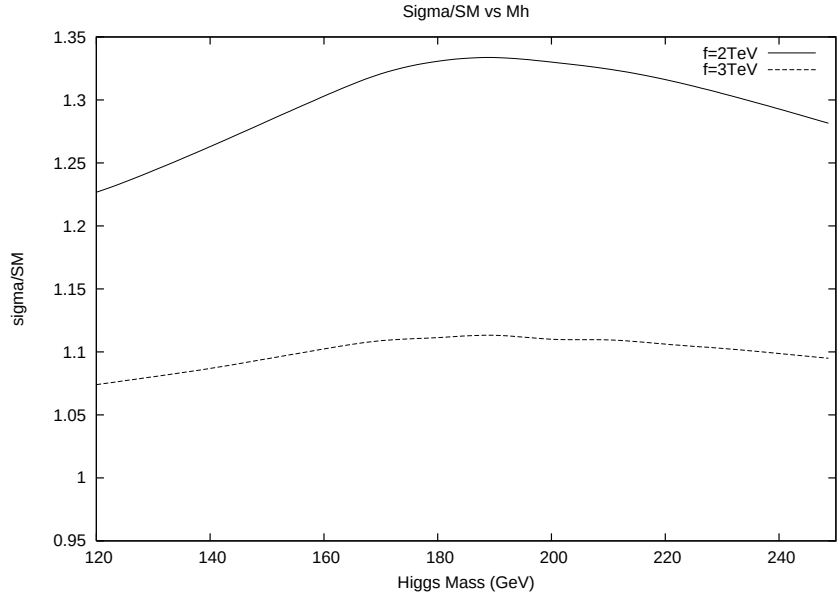

Figure 5.13: Higgs mass dependence of LHC cross section for the process $PP \to HH$ in the Littlest Higgs model vs the SM. For $x = 0.85$, $k = 2.5$ and $f = 2$ TeV, $M_T = 4.10$ TeV and M_Φ runs from 2.61 to 5.44 TeV as M_H runs from 120 to 250 GeV. Changing f to 3 TeV leads to $M_T = 6.15$ TeV and M_Φ running from 3.92 to 8.17 TeV.

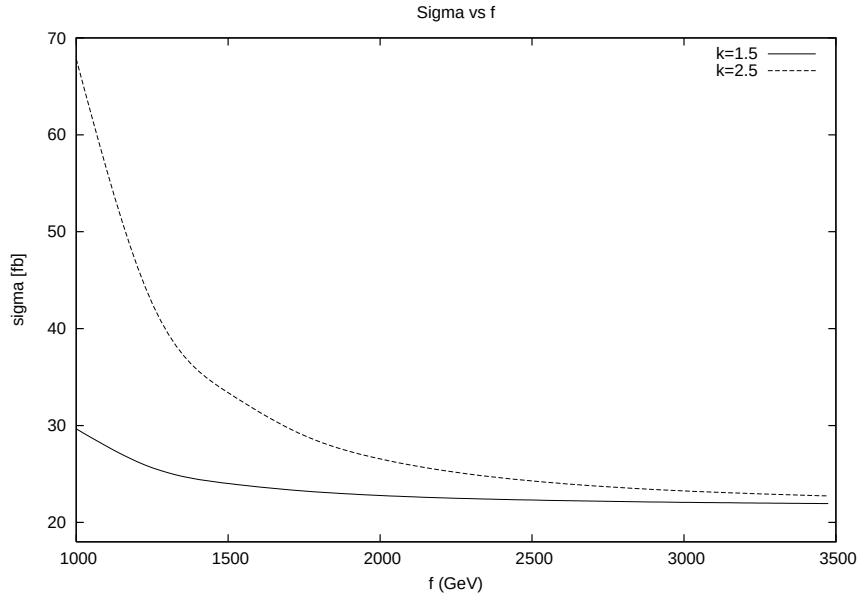

Figure 5.14: Dependence of the LHC cross section on the parameter f for the process $PP \to HH$ in the Littlest Higgs model. For $x = 0.85$, $M_H = 120$ GeV and k=1.5, M_T runs from 1.51 to 5.36 TeV and M_Φ runs from 1.30 to 4.58 TeV as M_H runs from 120 to 250 GeV. When k is changed to 2.5, M_T runs from 2.04 to 7.18 TeV whilst the range for M_Φ is unchanged.

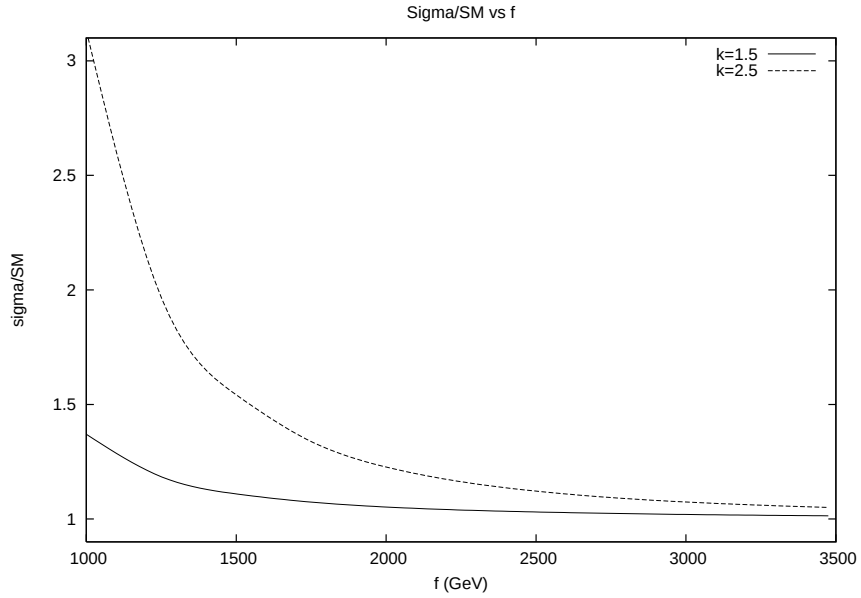

Figure 5.15: Dependence of LHC cross section on f for the process $PP \to HH$ in the Littlest Higgs model vs the SM. For $x = 0.85$, $M_H = 120$ GeV and k=1.5, M_T runs from 1.51 to 5.36 TeV and M_Φ runs from 1.30 to 4.58 TeV as M_H runs from 120 to 250 GeV. When k is changed to 2.5, M_T runs from 2.04 to 7.18 TeV whilst the range for M_Φ is unchanged.

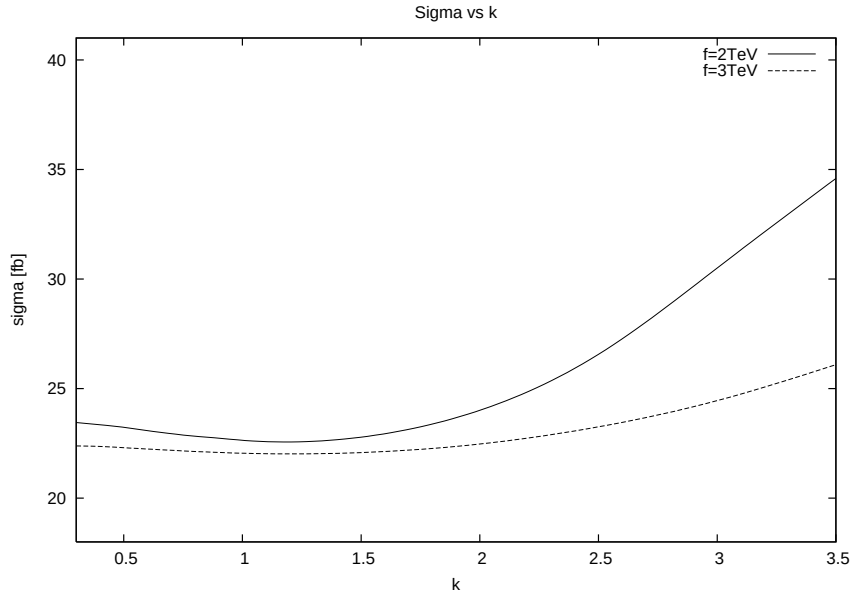

Figure 5.16: Dependence of the LHC cross section on the parameter $k = \lambda_2/\lambda_1$ for the process $PP \to HH$ in the Littlest Higgs model with $M_H = 120$ GeV and $x = 0.85$. For $f = 2$ TeV, $M_\Phi = 2.612$ TeV and M_T runs from 5.14 to 5.35 TeV when k runs over the range 0.3 to 3.5, whilst for $f = 3$ TeV, $M_\Phi = 3.92$ TeV and M_T runs from 7.71 to 8.03 TeV.

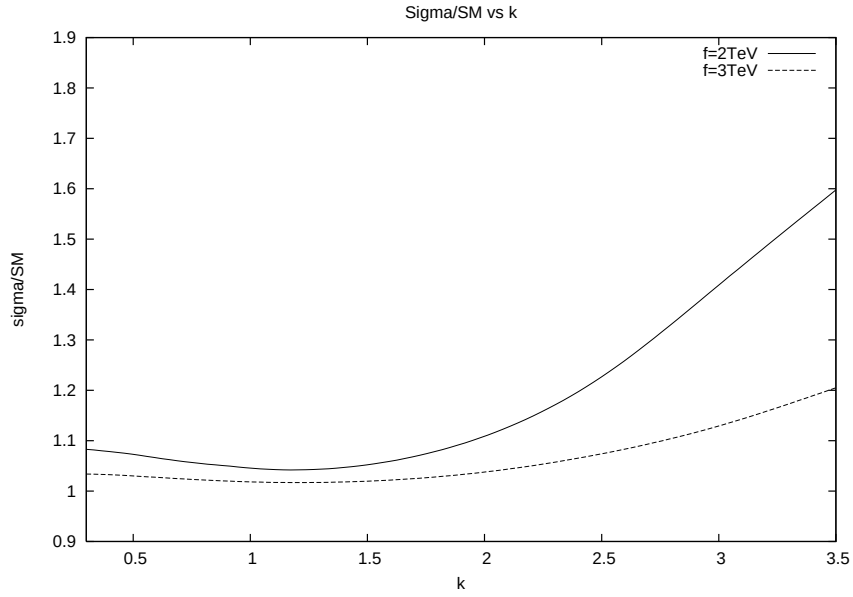

Figure 5.17: Dependence of LHC cross section on $k = \lambda_2/\lambda_1$ for the process $PP \to HH$ in the Littlest Higgs model vs the SM with $M_H = 120$ GeV and $x = 0.85$. For $f = 2$ TeV, $M_\Phi = 2.61$ TeV and M_T runs from 5.14 to 5.35 TeV when k runs over the range 0.3 to 3.5, whilst for $f = 3$ TeV, $M_\Phi = 3.92$ TeV and M_T runs from 7.71 to 8.03 TeV.

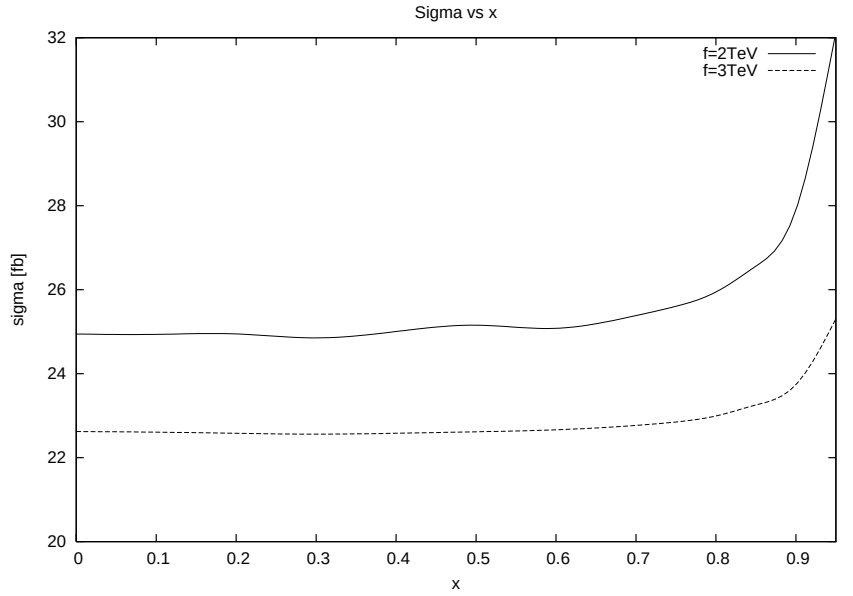

Figure 5.18: Dependence of the LHC cross section on the parameter 'x' for the process $PP \to HH$ in the LH model with $M_H = 120$ GeV and $k = 2.5$. For $f = 2$ TeV, M_T is 4.10 TeV for x between 0 and 0.95, and M_Φ runs between 1.37 and 4.41 TeV. For $f = 3$ TeV M_T is increased to 6.15 TeV and M_Φ runs between 2.07 and 6.62 TeV.

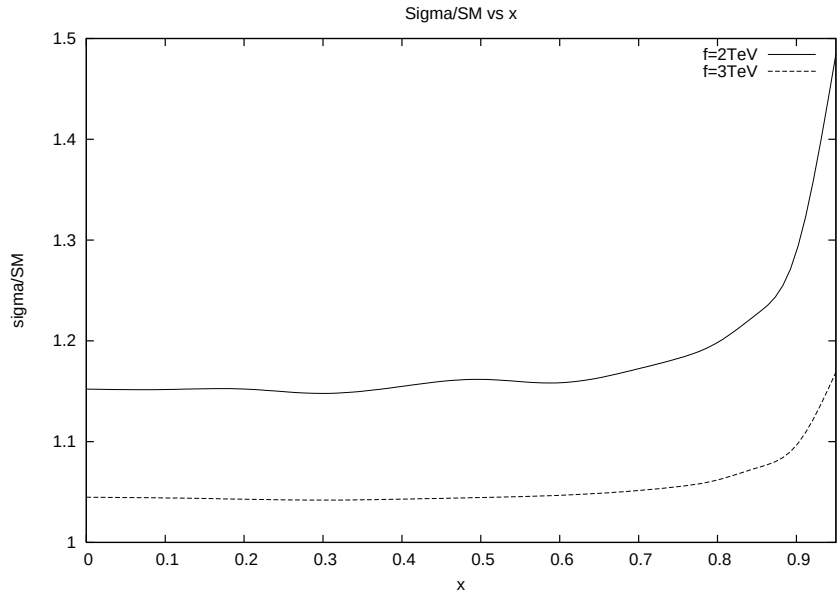

Figure 5.19: Dependence of LHC cross section on 'x' for the process $PP \to HH$ in the LH model vs the SM with $M_H = 120$ GeV and $k = 2.5$. For $f = 2$ TeV, M_T is 4.10 TeV for x between 0 and 0.95, and M_Φ runs between 1.37 and 4.41 TeV. For $f = 3$ TeV M_T is increased to 6.15 TeV and M_Φ runs between 2.07 and 6.62 TeV.

$|\lambda_{\phi^2}|$, $|\lambda_{h\phi h}|$, $|\lambda_{h^4}|$ and $|\lambda_{h\phi\phi h}|$ are all beyond order 1 so such high values of x should not be considered physical.

5.7 The Schmaltz Model Case

The Feynman diagrams contributing to the process $gg \to HH$ in the Schmaltz model have the same structure as those in the Littlest Higgs model. There is a heavy T quark in the Schmaltz model as in the Littlest Higgs case and the same couplings appear. The only difference being that there is no particle which plays the role of the Φ particle in diagrams like figure 5.11. There is a neutral scalar, the η particle, which might be expected to contribute to this process, but it has no tri-linear coupling to two Higgs particles. There are also two more heavy quarks (up-type in model I, down-type in model II), but their coupling to the Higgs is highly suppressed making their contribution negligible.

The relevant couplings of the Higgs to t and T quarks are summarised in table 3.2. The only other coupling which is needed to perform this calculation is the Higgs tri-linear coupling. Since the Higgs potential is the same as in the SM a Higgs-trilinear coupling contributes $-3iM_H^2/v$ to a Feynman diagram, as in the SM.

There are no complications in the Schmaltz model case beyond those encountered in the Littlest Higgs model. There are 6 parameters which appear in the Feynman rules. These are,

$$\{\lambda_1, \lambda_2, f_1, f_2, v, M_H\} \tag{5.38}$$

These parameters are not all independent. They are constrained by equation 3.48 since the top mass is known from experiment. The following parameters may be used instead,

$$\{m_t, k, f, \beta, v, M_H\} \tag{5.39}$$

where m_t is as defined in equation 3.48 and

$$\begin{aligned} k &= \frac{\lambda_2}{\lambda_1} \\ f^2 &= f_1^2 + f_2^2 \\ \beta &= \tan^{-1}\frac{f_2}{f_1} \end{aligned} \tag{5.40}$$

In the following figures all cross sections are LHC cross sections and the factorization and renormalization scales were set at $2M_H$.

In figure 5.20 the Higgs mass dependence of the total LHC cross section is plotted for values of M_H between 110 GeV and 250 GeV. The values $\tan\beta = 3$ and $k = 1$ and 2 values of f were used, $f = 2, 3$ TeV. The results show that the cross section falls off as M_H increases, as one would expect, and is slightly enhanced relative to the SM. In figure 5.21 the ratio of the Schmaltz model cross section to the SM are plotted for the same parameter choices. This shows that the enhancement is larger for lower Higgs masses but falls off to the SM value for larger Higgs masses.

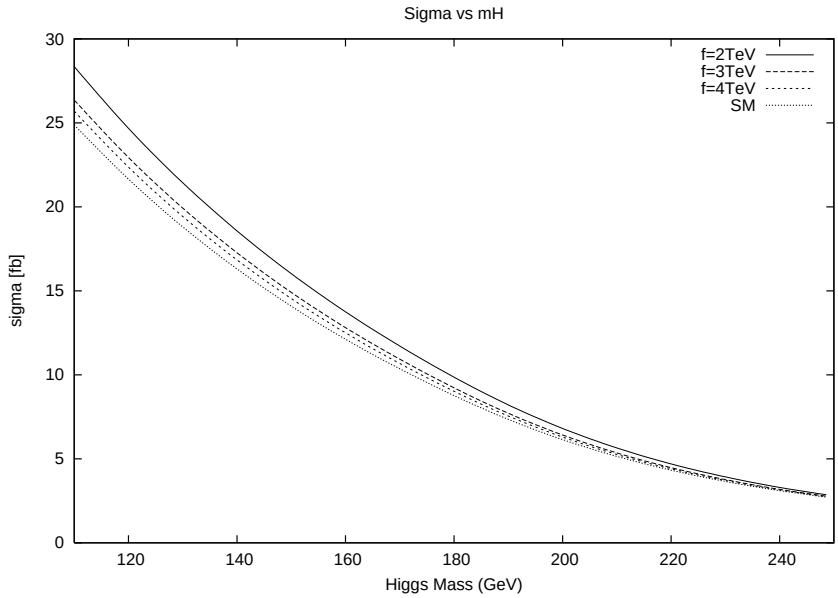

Figure 5.20: Higgs mass dependence of LHC cross section for the process $PP \to HH$ in the Schmaltz Model with $\tan\beta = 3$, $k = 1$. For $f = 2, 3, 4$ TeV, $M_T = 1.99, 2.00, 3.00$ TeV.

The dependence of the cross section on the parameter f is shown in figure 5.22 for $M_H = 120$ GeV and $k = 1$, with various values of $\tan\beta$. This plot shows that the result tends towards the SM value for large f, as expected since the SM Feynman rules

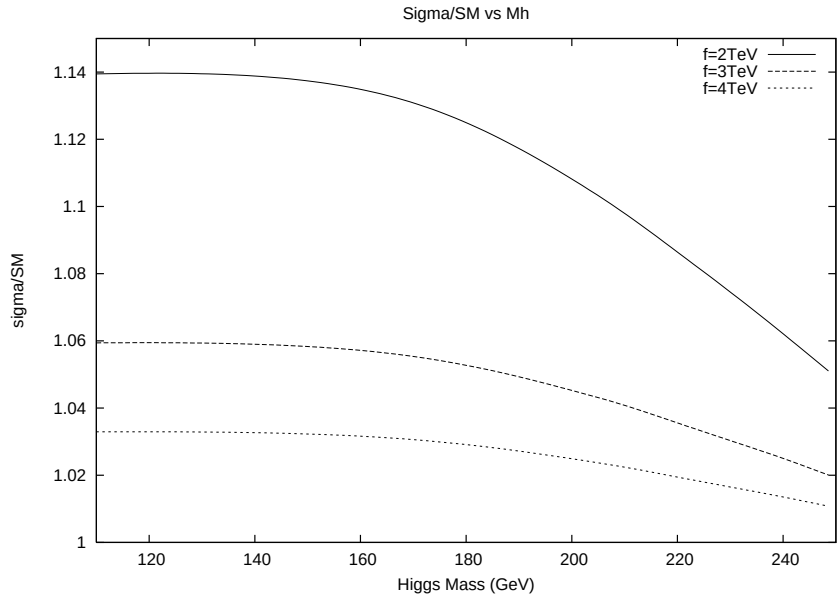

Figure 5.21: Higgs mass dependence of LHC cross section for the process $PP \to HH$ in the Schmaltz model vs the SM with $\tan\beta = 3$, $k = 1$. For $f = 2, 3, 4$ TeV, $M_T = 1.99, 2.00, 3.00$ TeV.

are recovered in the limit $f \to \infty$. Figure 5.23 shows the ratio to the SM result, this shows that the enhancement is typically less than 15% for values of f greater than about 3 TeV.

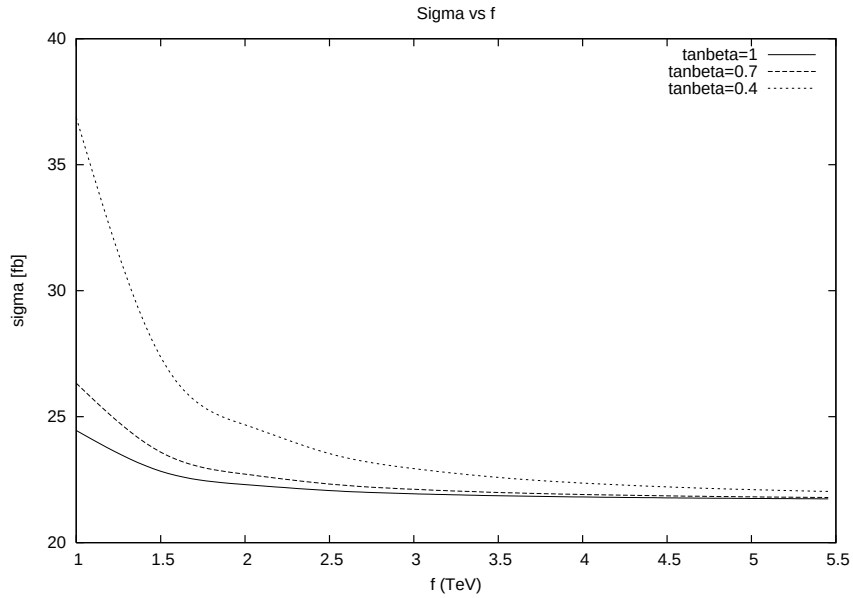

Figure 5.22: Dependence of the LHC cross section on the parameter f for the process $PP \to HH$ in the Schmaltz model with $M_H = 120$ GeV and $k = 1$. Over this range of f, M_T runs over approximately 1 to 5.5 TeV.

Figure 5.24 shows the variation of the cross section with the parameter $\tan\beta$ in the

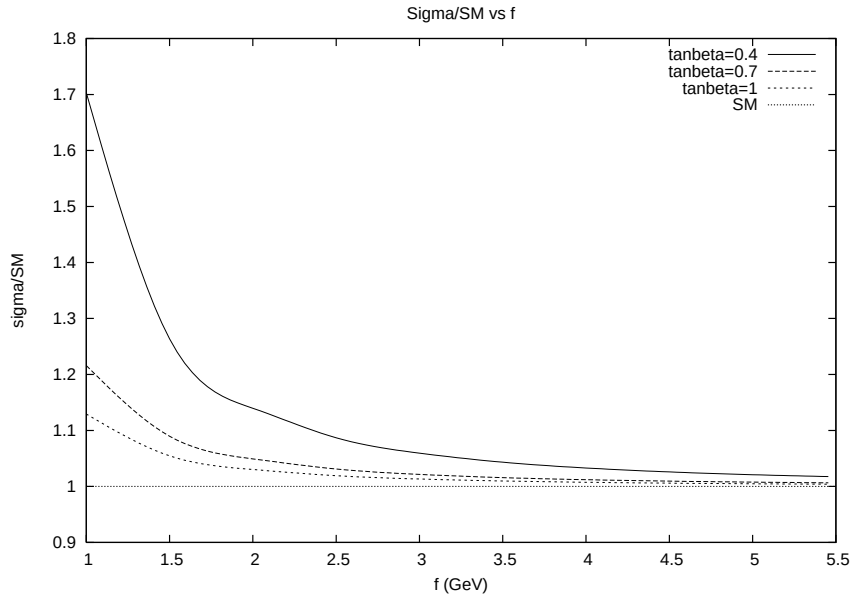

Figure 5.23: Dependence of LHC cross section on f for the process $PP \to HH$ in the Schmaltz model vs the SM with $M_H = 120$ GeV and $k = 1$. Over this range of f, M_T runs over approximately 1 to 5.5 TeV.

range 1/5 to 5 with the other parameters taking the values $k = 1$ and $M_H = 120$ GeV. The cross section varies substantially as a function of $\tan\beta$. There is a large enhancement when $\tan\beta$ is significantly different from 1, particularly for $\tan\beta \lesssim 0.5$. Figure 5.25 shows the enhancement relative to the SM. This shows that even for f as large as 3 TeV the enhancement relative to the SM can be larger than 25% when $\tan\beta$ is significantly less than 1.

The dependence on k is shown in figure 5.26 showing that the cross section increases as k increases. Here $M_H = 120$ GeV and $\tan\beta = 3$. The enhancement over the SM cross section is shown in figure 5.27 which shows that decreasing k can also lead to significant enhancement relative to the SM.

5.8 Prospects For Observation

Higgs pair production is difficult to measure at the LHC. A light Higgs decays predominantly to $b\bar{b}$ pairs and Higgs pairs decaying to 2 $b\bar{b}$ pairs are overwhelmed by QCD backgrounds, which are more than two orders of magnitude larger than the signal [93].

The case where one Higgs decays to a $b\bar{b}$ pair and the other to a $\tau\bar{\tau}$ pair was also examined in [94]. It was found that although the signal to background ratio is better than in $b\bar{b}b\bar{b}$, multiple additional small branching ratios in the observable part of the decay mode make this signal useless too. Even for a luminosity upgraded LHC (SLHC) achieving a 3000 fb^{-1}, the measurement of the cross section is too weak to be useful [94].

Higgs pair production can, however, be identified by utilizing rare decays. The case where the Higgs decays to $b\bar{b}\gamma\gamma$ and one of the bs is tagged is the most promising [94].

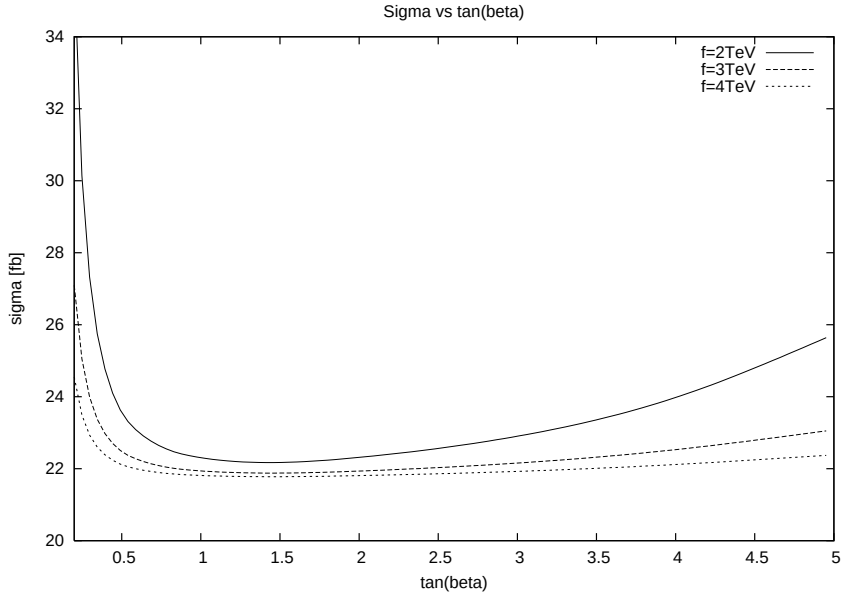

Figure 5.24: Dependence of the LHC cross section on the parameter $\tan\beta$ for the process $PP \to HH$ in the Schmaltz model with $M_H = 120$ GeV and $k = 1$. The mass of the heavy T quark is $\approx f$ over this range.

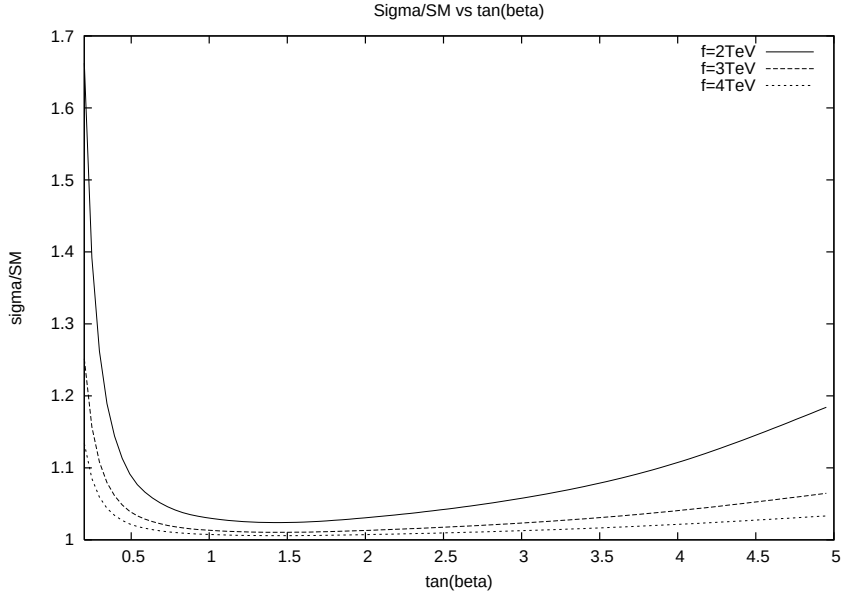

Figure 5.25: Dependence of LHC cross section on $\tan\beta$ for the process $PP \to HH$ in the Schmaltz model vs the SM with $M_H = 120$ GeV and $k = 1$. The mass of the heavy T quark is $\approx f$ over this range.

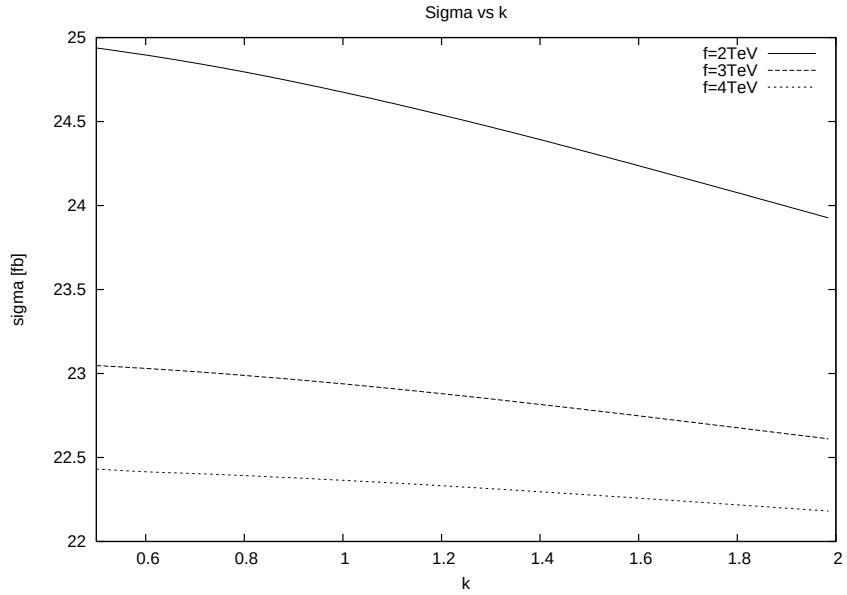

Figure 5.26: Dependence of the LHC cross section on the parameter 'k' for the process $gg \to HH$ in the Schmaltz model with $\tan\beta = 0.3$ and $M_H = 120$ GeV. For this range of k and $f = 2$ TeV M_T runs between 1.28 and 3.71 TeV. For $f = 3$ TeV this range changes to 1.94 to 5.56 TeV and for $f = 4$ TeV it becomes 2.59 to 7.41 TeV.

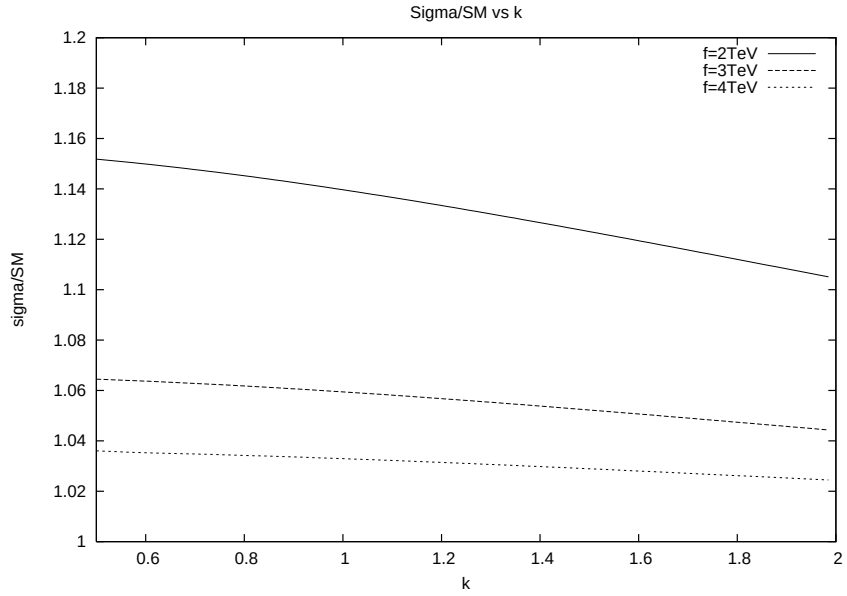

Figure 5.27: Dependence of LHC cross section on 'k' for the process $PP \to HH$ in the Schmaltz model vs the SM with $\tan\beta = 0.3$ and $M_H = 120$ GeV. For this range of k and $f = 2$ TeV M_T runs between 1.28 and 3.71 TeV. For $f = 3$ TeV this range changes to 1.94 to 5.56 TeV and for $f = 4$ TeV it becomes 2.59 to 7.41 TeV.

The background for this process is from QCD as well as single Higgs production followed by $H \to b\bar{b}$ or $H \to \gamma\gamma$ as well as from fake signals such as c quarks misidentified as b quarks or a light jet misidentified as a photon.

Even in this case, with a reasonable set of cuts the SM predicts only about 6 signal and 14 background events with 600 fb^{-1} of data [93], [95]. Given the factorisation scale uncertainties in our calculation and the typical size of little Higgs model corrections this means the enhancement due to little Higgs model effects is too small to be observable at the LHC. At the SLHC it is necessary to tag both b quarks to reduce the background from multiple interactions. In this case it is possible to improve to 21 signal with 25 background events. This is however still too small to allow the measurement of deviations from the SM due to Little Higgs corrections.

Although the cross section for Higgs pair production is smaller at larger Higgs masses the signal is much cleaner. For a larger Higgs mass the Higgs predominantly decays to weak boson pairs. States involving six or more jets are overwhelmed by QCD background. The most useful case is $HH \to W^+W^-W^+W^- \to l^\pm\nu jj l'^\pm\nu jj$ where j is a jet and the two $l^\pm$ are charged leptons with the same sign. This eliminates the background from Drell-Yan ($q\bar{q} \to \gamma^* \to l^+l^-$ where γ^* is an off-shell photon) and $t\bar{t}$ [96].

In this case, for 600 fb^{-1} of data, the SM expectation is for about 110 events with signal to background ratio of about 1:5 [95]. In this case even an enhancement of 50% over the SM cross section leads only to a 2σ deviation. This, in addition to the large factorization scale uncertainty, means that the little Higgs enhancement of the cross section is not observable at the LHC.

For the SLHC with 6000 fb^{-1} and after all cuts there are 350 signal events to 4180 background events for a Higgs of mass 170 GeV, whilst for a Higgs of mass 200 GeV this changes to 220 signal events vs 3280 background [97]. This is still too small to observe deviations from the SM cross section but will help provide a very useful measurement of the Higgs tri-linear coupling.

Chapter 6

The 2HDM and the Multiple Point Principle

6.1 The Scalar Potential

In this work the approximation of the renormalisation group improved effective potential [98] is used. This has the form of the tree level potential but with running coefficients where the renormalisation point is taken to be the field strength. In this case the scalar potential of the 2HDM, equation (1.19) may be written

$$\begin{aligned} V_{\rm eff}(H_1,H_2) &= m_1^2(\Phi)H_1^\dagger H_1 + m_2^2(\Phi)H_2^\dagger H_2 - [m_3^2(\Phi)H_1^\dagger H_2 + \text{h.c.}] + \\ &\frac{1}{2}\lambda_1(\Phi)(H_1^\dagger H_1)^2 + \frac{1}{2}\lambda_2(\Phi)(H_2^\dagger H_2)^2 + \lambda_3(\Phi)(H_1^\dagger H_1)(H_2^\dagger H_2) \\ &+\lambda_4(\Phi)|H_1^\dagger H_2|^2 + [\frac{1}{2}\lambda_5(\Phi)(H_1^\dagger H_2)^2 + \lambda_6(\Phi)(H_1^\dagger H_1)(H_1^\dagger H_2) \\ &+\lambda_7(\Phi)(H_2^\dagger H_2)(H_2^\dagger H_1) + \text{h.c.}]. \end{aligned} \tag{6.1}$$

The parameters are assumed only to depend on the sum of the squared norms of the Higgs doublets,

$$\Phi^2 = \Phi_1^2 + \Phi_2^2 \tag{6.2}$$

where

$$\Phi_n^2 = H_n^\dagger H_n = \frac{1}{2}[(H_n^0)^2 + (A_n^0)^2] + |\chi_n^+|^2. \tag{6.3}$$

Minimising this potential leads the Higgs doublets to develop vevs. In order for these vevs to break the electroweak $SU_W(2) \otimes U_Y(1)$ down to the electroweak $U_{\rm em}(1)$ it is necessary that only the neutral components of the Higgs doublets aquire a vev. Define these vevs to be

$$\langle H_n \rangle = \frac{v_n}{\sqrt{2}}. \tag{6.4}$$

The overall squared sum of these vevs, $v^2 = v_1^2 + v_2^2$, where $v = 246$ GeV, is known through the masses of the weak gauge bosons. The ratio of the vevs remains arbitrary and is parameterised through the definition $\tan\beta = |v_2|/|v_1|$.

In accordance with the MPP, assume that this potential has another minimum degenerate with our current vacuum with the scalar fields aquiring vevs much larger than the electroweak scale. Due to gauge invariance, these vevs may be written without loss of generality in the form

$$\langle H_1 \rangle = \Phi_1 \begin{pmatrix} 0 \\ 1 \end{pmatrix}, \qquad \langle H_2 \rangle = \Phi_2 \begin{pmatrix} \sin\theta \\ \cos\theta\, e^{i\omega} \end{pmatrix}. \tag{6.5}$$

Define Λ, called the MPP scale, through the relation $\Lambda^2 = \Phi_1^2 + \Phi_2^2$. It is assumed that $\Lambda \gg v$ so it is a good approximation to take $V(H_1, H_2) = 0$ at the MPP scale because all the couplings in the potential must be very close to zero to suppress terms of order Λ^2 or Λ^4. Also, if Φ_1 and Φ_2 are of order Λ, it follows that the terms quartic in the Higgs fields are much larger than the terms quadratic in the Higgs fields so the mass terms may be neglected.

The MPP requires a large set of degenerate vacua so search for the conditions required for degeneracy with respect to the parameter ω.

Substituting the vacuum configuration (6.5) into the potential (6.1) shows that the part of the potential which depends on the parameter ω is

$$V_\omega = \frac{1}{2}\lambda_5(\Phi)\Phi_1^2\Phi_2^2\cos^2\theta\, e^{2i\omega} + [\lambda_6(\Phi)\Phi_1^3\Phi_2 + \lambda_7(\Phi)\Phi_1\Phi_2^3]\cos\theta\, e^{i\omega} + \text{h.c.}. \tag{6.6}$$

Note that in order for there to be degeneracy with respect to ω it is necessary that $\cos\theta$ and both Φ_1 and Φ_2 are non-zero. For the potential to be independent of ω at the scale Λ implies that $\lambda_5(\Lambda) = 0$ and $\lambda_6(\Lambda)\Phi_1^2 + \lambda_7(\Lambda)\Phi_2^2 = 0$.

Information can also be extracted from the requirement that the vacuum configuration 6.5 minimizes the potential at the scale Λ. Derivatives of the potential with respect to Φ_1 and Φ_2 should be zero at the minimum and for this to be the case for all ω it is required that these derivatives are independent of ω. This leads to the requirement

$$\begin{aligned} \frac{\partial V_\omega}{\partial \Phi_1} &= [\lambda_5(\Lambda)\Phi_1\Phi_2^2 + \beta_{\lambda_5}(\Phi)\frac{\Phi_1^3\Phi_2^2}{2\Phi^2}]\cos^2\theta\, e^{2i\omega} + \\ &\quad [3\lambda_6(\Phi)\Phi_1^2\Phi_2 + \beta_{\lambda_6}(\Phi)\frac{\Phi_1^4\Phi_2}{\Phi^2} + \lambda_7(\Phi)\Phi_2^3 + \beta_{\lambda_7}(\Phi)\frac{\Phi_1^2\Phi_2^3}{\Phi^2}]\cos\theta\, e^{i\omega} + \text{h.c.}|_{\Phi=\Lambda} \\ &= 0 \end{aligned} \tag{6.7}$$

and

$$\begin{aligned} \frac{\partial V_\omega}{\partial \Phi_2} &= [\lambda_5(\Lambda)\Phi_1^2\Phi_2 + \beta_{\lambda_5}(\Phi)\frac{\Phi_1^2\Phi_2^3}{2\Phi^2}]\cos^2\theta\, e^{2i\omega} + \\ &\quad [\lambda_6(\Phi)\Phi_1^3 + \beta_{\lambda_6}(\Phi)\frac{\Phi_1^3\Phi_2^2}{\Phi^2} + 3\lambda_7(\Phi)\Phi_1\Phi_2^2 + \beta_{\lambda_7}(\Phi)\frac{\Phi_1\Phi_2^4}{\Phi^2}]\cos\theta\, e^{i\omega} + \text{h.c.}|_{\Phi=\Lambda} \\ &= 0. \end{aligned} \tag{6.8}$$

Here the renormalisation group beta functions are defined by $\beta_{\lambda_i}(\Phi) = \dfrac{d\,\lambda_i(\Phi)}{d\,\ln\Phi}$. For both the derivatives to vanish it is required that the coefficients of $e^{i\omega}$ and $e^{2i\omega}$ are zero for both equations.

The vanishing of the coefficients of $e^{2i\omega}$ combined with the previously derived condition $\lambda_5(\Lambda) = 0$ require that $\beta_{\lambda_5}|_{\Phi=\Lambda} = 0$. The vanishing of the coefficients of $e^{i\omega}$ along with the previously derived condition for $\lambda_6(\Lambda)$ and $\lambda_7(\Lambda)$ give three linear equations relating the four unknowns $\lambda_6(\Lambda)$, $\lambda_7(\Lambda)$, $\beta_{\lambda_6}|_{\Phi=\Lambda}$ and $\beta_{\lambda_7}|_{\Phi=\Lambda}$.

Solving this system of linear equations gives the MPP conditions $\lambda_6(\Lambda) = \lambda_7(\Lambda) = 0$ and $(\beta_{\lambda_6}\Phi_1^2 + \beta_{\lambda_7}\Phi_2^2)|_{\Phi=\Lambda} = 0$. Of course, the partial derivatives of the potential with respect to the parameters θ and ω must also be independent of ω, but it is easy to see that this yields no new information about the parameters.

To summarise the progress so far, for the potential to exhibit degeneracy with respect to ω at the MPP scale minimum the restrictions on the Higgs self couplings are

$$\lambda_5(\Lambda) = \lambda_6(\Lambda) = \lambda_7(\Lambda) = 0 \tag{6.9}$$

$$\beta_{\lambda_5}|_{\Phi=\Lambda} = (\beta_{\lambda_6}\Phi_1^2 + \beta_{\lambda_7}\Phi_2^2)|_\Lambda = 0. \tag{6.10}$$

This means that near the MPP scale the potential (6.1) takes the form

$$\begin{aligned} V_{\text{eff}}(H_1, H_2) \;\approx\; & \frac{1}{2}(\sqrt{\lambda_1(\Phi)}\Phi_1^2 - \sqrt{\lambda_2(\Phi)}\Phi_2^2)^2 + \\ & (\sqrt{\lambda_1(\Phi)\lambda_2(\Phi)} + \lambda_3(\Phi) + \lambda_4(\Phi)\cos^2\theta)\Phi_1^2\Phi_2^2. \end{aligned} \tag{6.11}$$

For $\lambda_4(\Lambda) > 0$ this potential is minimized for $\cos\theta = 0$. Since degeneracy with respect to ω can only be realised if $\cos\theta \neq 0$ this leads to the requirement that $\lambda_4 < 0$. In this case the potential is minimized for $\cos\theta = \pm 1$. Then near the MPP scale minimum the potential has the form

$$V_{\text{eff}}(H_1, H_2) \approx \frac{1}{2}(\sqrt{\lambda_1(\Phi)}\Phi_1^2 - \sqrt{\lambda_2(\Phi)}\Phi_2^2)^2 + \tilde{\lambda}(\Phi)\Phi_1^2\Phi_2^2. \tag{6.12}$$

where $\tilde{\lambda}(\Phi) = \sqrt{\lambda_1(\Phi)\lambda_2(\Phi)} + \lambda_3(\Phi) + \lambda_4(\Phi)$.

For the vacuum to be a stable minimum clearly $\tilde{\lambda}$ cannot be negative. However, if $\tilde{\lambda} > 0$ the potential has a greater than zero energy density and cannot be degenerate with our current vacuum. The only option then is that

$$\tilde{\lambda} = 0. \tag{6.13}$$

Furthermore, the minimum of the potential is reached for values of Φ_1 and Φ_2 such that the condition

$$\sqrt{\lambda_1(\Lambda)}\Phi_1^2 - \sqrt{\lambda_2(\Lambda)}\Phi_2^2 = 0 \tag{6.14}$$

is fulfilled. This requirement, along with the requirement that $\Phi_1^2 + \Phi_2^2 = \Lambda^2$, determine that

$$\Phi_1 = \Lambda\cos\gamma, \quad \Phi_2 = \Lambda\sin\gamma, \quad \tan\gamma = (\frac{\lambda_1}{\lambda_2})^{1/4}. \tag{6.15}$$

Since this represents a minimum of the potential the partial derivatives with respect to Φ_1 and Φ_2 must vanish. When combined with the condition $\tilde{\lambda} = 0$ and equation (6.14) this leads to the requirement

$$\beta_{\tilde{\lambda}}|_{\Phi=\Lambda} = [\frac{1}{2}\beta_{\lambda_1}\sqrt{\frac{\lambda_2(\Phi)}{\lambda_1(\Phi)}} + \frac{1}{2}\beta_{\lambda_2}\sqrt{\frac{\lambda_1(\Phi)}{\lambda_2(\Phi)}} + \beta_{\lambda_3} + \beta_{\lambda_4}]|_{\Phi=\Lambda} = 0. \tag{6.16}$$

The potential is also minimized with respect to θ and ω but no information is gained from this because partial derivatives with respect to θ vanish when $\cos\theta = \pm 1$ and the potential is degenerate with respect to ω by construction.

To summarise the results of this section, the MPP conditions derived are

$$\tilde{\lambda}(\Lambda) = \lambda_5(\Lambda) = \lambda_6(\Lambda) = \lambda_7(\Lambda) = 0 \tag{6.17}$$

and

$$\beta_{\tilde{\lambda}}|_{\Lambda} = \beta_{\lambda_5}|_{\Lambda} = (\beta_{\lambda_6}\Phi_1^2 + \beta_{\lambda_7}\Phi_2^2)|_{\Lambda} = 0. \tag{6.18}$$

Also, the condition $\cos\theta = \pm 1$ means that the vacuum expectation values of the Higgs fields at the MPP scale vacuum are given by

$$\langle H_1\rangle = \begin{pmatrix} 0 \\ \Phi_1 \end{pmatrix}, \quad \langle H_2\rangle = \begin{pmatrix} 0 \\ \Phi_2 e^{i\omega} \end{pmatrix} \tag{6.19}$$

where Φ_1 and Φ_2 fulfill equation (6.15).

6.2 Yukawa Couplings

In the most general 2HDM all quarks and leptons can couple to both Higgs doublets. The largest couplings appear in the third generation for the t and b quarks and the τ lepton. Defining Q and L as the left handed third generation quark and lepton doublets, the third generation Yukawa couplings may be written in the form

$$\begin{aligned} \mathcal{L}_{\text{Yuk}} &= h_t(H_2\varepsilon Q)\bar{t}_R + g_b(H_2^\dagger Q)\bar{b}_\tau(H_2^\dagger L)\bar{\tau}_R + g_t(H_1\varepsilon Q)\bar{t}_R \\ &\quad h_b(H_1^\dagger Q)\bar{b}_R + h_\tau(H_1^\dagger L)\bar{\tau}_R + \text{h.c.}. \end{aligned} \tag{6.20}$$

These couplings appear in the renormalisation group equations (RGEs) for the Higgs self couplings, presented in Appendix A. Using the explicit forms of the beta functions along with the MPP conditions (6.17), (6.18), (6.19) leads to two conditions that the Yukawa couplings must satisfy at the MPP scale. Note that the Higgs fields can always be defined so that $g_t(\Lambda) = 0$. The first condition comes from the vanishing of β_{λ_5},

$$3h_b^2(\Lambda)g_b^{*2}(\Lambda) + h_\tau^2(\Lambda)g_\tau^{*2}(\Lambda) = 0. \tag{6.21}$$

The second condition comes from the condition relating $\beta_{\lambda_6}|_\Lambda$ and $\beta_{\lambda_7}|_\Lambda$,

$$\begin{aligned} &3h_b^2(\Lambda)g_b^{*2}(\Lambda)[\sqrt{\lambda_2(\Lambda)}|h_b(\Lambda)|^2 + \sqrt{\lambda_1(\Lambda)}|g_b(\Lambda)^2] \\ &+h_\tau^2(\Lambda)g_\tau^{*2}(\Lambda)[\sqrt{\lambda_2(\Lambda)}|h_\tau(\Lambda)|^2 + \sqrt{\lambda_1(\Lambda)}|g_\tau(\Lambda)^2] \;=\; 0. \end{aligned} \tag{6.22}$$

In order that both of these conditions are satisfied simultaneously, it is required that the b quark and the τ lepton each couple to only one of the Higgs fields. There are four possibilities which are labelled Models (I)-(IV).

$$\begin{array}{ll} \text{Model I} & h_b(\Lambda) = h_\tau(\Lambda) = 0 \\ \text{Model II} & g_b(\Lambda) = g_\tau(\Lambda) = 0 \\ \text{Model III} & h_b(\Lambda) = g_\tau(\Lambda) = 0 \\ \text{Model IV} & g_b(\Lambda) = h_\tau(\Lambda) = 0. \end{array}$$

These are exactly the conditions required for the absence of FCNCs at tree level. Each fermion field couples to only one of the Higgs doublets and the third generation Yukawa couplings possess a $U(1)$ symmetry (Peccei-Quinn symmetry). Precisely which $U(1)$ symmetry depends on which of the four models is correct but whichever one it is the symmetry excludes FCNCs at tree level.

The MPP conditions also require that $\lambda_5(\Lambda) = \lambda_6(\Lambda) = \lambda_7(\Lambda) = 0$. If in addition the mass term which mixes the two Higgs doublets, m_3^2, is zero then the full Lagrangian is invariant under a $U(1)$ global symmetry. This global symmetry is spontaneously broken when the Higgs fields aquire vevs leading to a massless axion [99],[100]. In this case the QCD θ term [101] [102] [103] is eliminated from the theory.

The MPP conditions do not, however, require that $m_3^2 = 0$ so there is no reason to expect this to be the case. For $m_3^2 \neq 0$ the $U(1)$ symmetry is explicitly (softly) broken in which case the QCD θ term cannot be eliminated by an axion.

This does not destroy the suppression of FCNCs. The renormalisation group equations for the Yukawa couplings and the Higgs self couplings are given in Appendix A. Given the derived MPP conditions, these show that if the $U(1)$ symmetry violating couplings are zero (or small) at the scale Λ, they will remain zero (or small) at any scale below Λ. (For example, λ_5, λ_6 and λ_7 remain zero (or small) below the scale Λ.)

The most stringent constraints on FCNCs come from processes involving fermions of the first and second generations. So far, the symmetries which protect the theory from FCNCs have only been derived for the third generation fermions.

The method used to show how the $U(1)$ symmetry violating couplings are suppressed for the third generation fermions cannot be generalized to all fermions. If other fermion Yukawa couplings are not neglected they appear in the RGEs for the couplings λ_5, λ_6 and λ_7. Then the two constraint equations, (6.21) and (6.22), now contain extra terms involving the other fermions' Yukawa couplings. These equations cannot be used to derive strong constraints on the Yukawa couplings.

To see how to achieve constraints on all fermion Yukawa couplings we must consider the effective potential. The one loop contribution to the effective potential may be written

$$V_1 = \frac{1}{64\pi^2}\text{Str}|M|^4[\ln\frac{|M|^2}{\mu^2} - C]. \tag{6.23}$$

Here "Str" is the "super-trace" operator which counts the number of bosonic (fermionic) degrees of freedom with a $+(-)$ sign. Also, C is a diagonal matrix which depends on the renormalisation scheme and μ is the renormalisation scale.

The MPP scale minimum of the effective potential must be degenerate with respect to ω. This means all order partial derivatives of the effective potential with respect to ω must be zero. This can only be the case for the one loop contribution (6.23) if the mass matrix M is independent of ω.

The most general Yukawa Lagrangian not including neutrino masses of the 2HDM may be written.

$$\begin{aligned}\mathcal{L}_{\text{Yuk}} &= \bar{U}_{Ri}Y_{Uij}(H_2\varepsilon Q_{Lj}) + \bar{D}_{Ri}X_{Dij}(H_2^\dagger Q_{Lj}) + \bar{E}_{Ri}X_{Lij}(H_2^\dagger L_{Lj}) \\ &\quad \bar{U}_{Ri}X_{Uij}(H_1\varepsilon Q_{Lj}) + \bar{D}_{Ri}Y_{Dij}(H_1^\dagger Q_{Lj}) + \bar{E}_{Ri}Y_{Lij}(H_1^\dagger L_{Lj}) \end{aligned} \tag{6.24}$$

Here $\bar{U}_{Ri}$, $\bar{D}_{Ri}$ and $\bar{E}_{Ri}$ are the i^{th} generation right handed up type quark, down type quark and charged lepton respectively. Also, Q_{Lj} and L_{Lj} are the j^{th} generation left handed quark and lepton doublets and the various X and Y matrices contain the Yukawa couplings.

Define the mass matrices of the fermions through the relation

$$\mathcal{L}_{\text{masses}} = \sum_{f=U,D,L} \begin{pmatrix} \bar{f}_R & \bar{f}_L \end{pmatrix} \begin{pmatrix} 0 & M_f \\ M_f & 0 \end{pmatrix} \begin{pmatrix} f_R \\ f_L \end{pmatrix} \tag{6.25}$$

Then substituting the MPP scale Higgs vevs (6.19) into the Lagrangian (6.24) yields the fermion mass matrices

$$\begin{aligned} M_U &= Y_U\Phi_2 e^{i\omega} + X_U\Phi_1 \\ M_D &= X_D\Phi_2 e^{i\omega} + Y_D\Phi_1 \\ M_L &= X_E\Phi_2 e^{i\omega} + Y_L\Phi_1 \end{aligned} \tag{6.26}$$

The eigenvalues of the matrices $M_f M_f^\dagger$ are the absolute values of the fermion masses squared. For the up type quarks the matrix $M_U M_U^\dagger$ is given by

$$M_U M_U^\dagger = Y_U Y_U^\dagger \Phi_1^2 + Y_U X_U^\dagger \Phi_1\Phi_2 e^{i\omega} + X_U Y_U^\dagger \Phi_1\Phi_2 e^{-i\omega} + Y_U Y_U^\dagger \Phi_1^2 \tag{6.27}$$

The eigenvalues of this matrix are independent of ω if

$$Y_U X_U^\dagger = X_U Y_U^\dagger = 0 \tag{6.28}$$

Similar reasoning for the down type quarks and charged leptons lead to the conclusion that the masses are independent of ω only if

$$Y_f X_f^\dagger = X_f Y_f^\dagger = 0 \tag{6.29}$$

Through transformations on the right handed and left handed fermion fields it is always possible to find a basis in which one of the Yukawa matrices for each species, H_f say, is diagonal. Then applying (6.29) implies that the matrices can be written in the form

$$Y_f = \begin{pmatrix} y_{f_1} & 0 & 0 \\ 0 & y_{f_2} & 0 \\ 0 & 0 & y_{f_3} \end{pmatrix}, \quad X_f = \begin{pmatrix} x_{f_1} & 0 & 0 \\ 0 & x_{f_2} & 0 \\ 0 & 0 & x_{f_3} \end{pmatrix} \tag{6.30}$$

where $y_{f_i}.x_{f_i} = 0$ (note there is no summation here, the product vanishes for each value of i). This result shows that either y_{f_i} or $x_{f_i} = 0$. In other words, each fermion couples to only one Higgs doublet. This guarantees that FCNCs are forbidden at tree level as required by the experimental data.

When the Yukawa couplings take this form the Yukawa sector of the 2HDM is invariant under extra symmetry transformations. Writing those right handed fermions which couple to H_1 with a prime (f'_R) and those which couple to H_2 with two primes (f''_R) these symmetries are

$$\begin{aligned} H_1 &\rightarrow e^{i\alpha} H_1 \\ U'_{Ri} &\rightarrow e^{i\alpha} U'_{Ri} \\ D'_{Ri} &\rightarrow e^{-i\alpha} D'_{Ri} \\ e'_{Ri} &\rightarrow e^{-i\alpha} e'_{Ri} \end{aligned} \tag{6.31}$$

and

$$\begin{aligned} H_2 &\rightarrow e^{i\beta} H_2 \\ U''_{Ri} &\rightarrow e^{i\beta} U''_{Ri} \\ D''_{Ri} &\rightarrow e^{-i\beta} D''_{Ri} \\ e''_{Ri} &\rightarrow e^{-i\beta} e''_{Ri} \end{aligned} \tag{6.32}$$

These symmetries forbid the appearence of tree level FCNCs. All the terms which break these symmetries in a general 2HDM are forced to be zero by the MPP with the exception of the Higgs mass term m_3^2. However, m_3^2 does not contribute to FCNCs so this is not a problem. Furthermore, all the terms which appear in the RGEs respect these symmetries so the renormalisation group running does not cause the troublesome terms to appear at scales below the MPP scale making the theory safe from FCNC effects.

Chapter 7

2HDM Phenomenology

7.1 Quasi-Fixed Point in 2HDM

It can be the case that for a large range of parameters at a high energy scale the solutions of the RGEs (see Appendix A) are concentrated around some particular value at low energy scales. If the interval between the MPP scale and the electroweak scale is large there will be a large range of parameters at the MPP scale which tend towards such quasi-fixed point (QFP) values at the electroweak scale.

In this chapter the QFPs of the MPP inspired 2HDM are investigated. Firstly, the Yukawa couplings are examined and are found to lead to a prediction for $\tan\beta$, the ratio of the vevs of the Higgs doublets. Then the Higgs self couplings are examined followed by the implications for Higgs phenomenology in terms of the scalar mass spectrum and couplings to top quarks and gauge bosons.

7.2 Yukawa Couplings

7.2.1 QFP Solutions At Low-Moderate $\tan\beta$

Consider the case where only the top quark has a large Yukawa coupling. This is guaranteed to be the case if the Yukawa couplings satisfy the conditions in Model I. In this case the bottom quark and tau lepton get their masses from the same Higgs doublet as the top and their Yukawa couplings must be strongly suppressed in order to generate the required mass hierarchy. It will also be the case if $\tan\beta$ is small compared with m_t/m_b, since in this case also the b and τ Yukawa couplings must be small in order to generate the observed fermion mass hierarchy.

The RGE for the top Yukawa coupling h_t is given in Appendix A. As noted before, by appropriate redefinition of the Higgs fields the coupling g_t may without loss of generality be taken to be zero. Also, in the case currently considered the bottom and tau Yukawa couplings may be neglected. This leaves the RGE

$$\frac{dh_t}{dt} = \frac{1}{16\pi^2}[h_t\frac{9}{2}|h_t|^2 - h_t(8g_3^2 + \frac{9}{4}g_2^2 + \frac{17}{12}g_1^2)]. \tag{7.1}$$

Some transformations of the variables of this equation serve to simplify it somewhat. Define $Y_t = (h_t/4\pi)^2$ and $\alpha_i = (g_i/4\pi)^2$ (note: don't confuse this with the common definition $\alpha_i = g_i^2/4\pi$. This normalization removes awkward factors of 4π from the

RGEs). Also, change the variable $t = \ln(\mu)$ to $t = \ln(\Lambda^2/\mu^2)$. The equation then takes the form

$$\frac{dY_t}{dt} = -\frac{9}{2}Y_t^2 + Y_t(\sum_i c_i\alpha_i) \tag{7.2}$$

where $\sum_i c_i\alpha_i = 8\alpha_3 + \frac{9}{4}\alpha_2 + \frac{17}{12}\alpha_1$. Then another change of variables, $Y_t = 1/X$, serves to turn the equation into a linear equation,

$$\frac{dX}{dt} + (\sum_i c_i\alpha_i)X = \frac{9}{2}. \tag{7.3}$$

The definition of a (first order) linear differential equation is that it is of the form

$$\frac{dy}{dx} + p(x)y = q(x) \tag{7.4}$$

and the general solution is

$$y = \frac{C + \int u(x)q(x)dx}{u(x)} \tag{7.5}$$

where C is a constant and $u(x)$ is an *integrating factor* defined as

$$u(x) = \exp(\int p(x)dx). \tag{7.6}$$

Define the integrating factor for the top RGE to be $E(t)$. This is given by

$$E(t) = \exp(\int \sum_i c_i\alpha_i(\mu)dt). \tag{7.7}$$

To find the integrating factor, the form of the running gauge couplings must be known. The RGEs for the gauge couplings are

$$\frac{d\alpha_i}{dt} = -b_i\alpha_i^2 \tag{7.8}$$

where $b_1 = 7$, $b_2 = -3$ and $b_3 = -7$. Defining the couplings in terms of $\alpha_i(\Lambda)$, these equations have solutions

$$\alpha_i(\mu) = \frac{\alpha_i(\Lambda)}{1 + b_i\alpha_i(\Lambda)t}. \tag{7.9}$$

Using the above expression for the functions $\alpha_i(\mu)$ to find the integrating factor gives

$$E(t) = \Pi_i \left[\frac{\alpha_i(\mu)}{\alpha_i(\Lambda)}\right]^{-c_i/b_i} = \left[\frac{\alpha_3(\mu)}{\alpha_3(\Lambda)}\right]^{8/7} \left[\frac{\alpha_2(\mu)}{\alpha_2(\Lambda)}\right]^{3/4} \left[\frac{\alpha_1(\mu)}{\alpha_1(\Lambda)}\right]^{-17/84}. \tag{7.10}$$

Using this expression the solution for the function X can be found

$$X(\mu) = \frac{\frac{9}{2}F(t) + C}{E(t)}. \tag{7.11}$$

Here $F(t)$ is defined as

$$F(t) = \int_0^t E(t')dt'. \tag{7.12}$$

Defining the solution in terms of $Y_t(\Lambda)$, the expression for $Y_t(\mu)$ is then found to be

$$Y_t(\mu) = \frac{\frac{2E(t)}{9F(t)}}{1 + \frac{2}{9Y_t(\Lambda)F(t)}}. \tag{7.13}$$

For Λ of order the Planck scale, the function $F(t)$ is found (via numerical integration) to be about 170 when $t = t_0 = \ln(\Lambda^2/M_t^2)$ where M_t is the pole mass of the top quark. In this case the denominator of the above expression for $Y_t(\mu)$ is approximately equal to $1 + 1/5h_t^2(\Lambda)$. This means that when $h_t(\Lambda) \gtrsim 1$ the solution for the RGE becomes approximately independent of $h_t(\Lambda)$. The solutions are gathered in the region of the quasi fixed point (QFP),

$$Y_t^{\mathrm{qfp}}(M_t) = \frac{2E(t_0)}{9F(t_0)}. \tag{7.14}$$

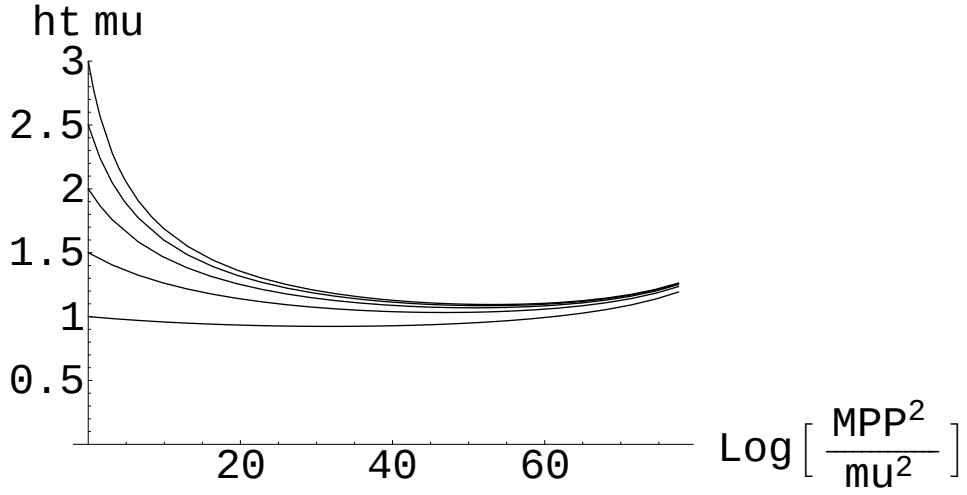

Figure 7.1: Top Yukawa coupling $h_t(\mu)$ vs $\ln(\Lambda^2/\mu^2)$ for Λ at the Planck scale. The renormalisation group running is plotted for various values of the top Yukawa coupling at the Planck scale.

The renormalisation group running for $h_t(\mu)$ is shown in figures 7.1 and 7.2 for the MPP scale at the Planck scale (1.22×10^{19} GeV) and at 10^{13} GeV respectively. These plots show how the top Yukawa couplings are gathered near the QFP at the scale M_t for $h_t(\Lambda) \gtrsim 1$.

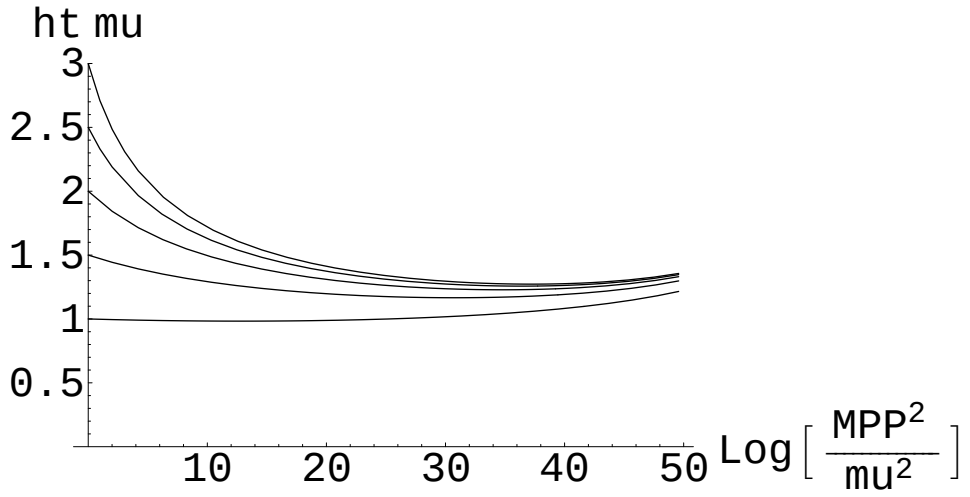

Figure 7.2: $h_t(\mu)$ vs $\ln(\Lambda^2/\mu^2)$ for $\Lambda = 10^{13}$ GeV. The renormalisation group running is plotted for various values of the top Yukawa coupling at the MPP scale.

The top running mass, $m_t(\mu)$, is related to the Yukawa coupling,

$$m_t(\mu) = \frac{h_t(\mu)}{\sqrt{2}} v \sin(\beta). \tag{7.15}$$

The running mass can also be calculated from experimental data. The running mass is related to the pole mass via the two loop relation in the $\overline{MS}$ scheme [104],[105],

$$m_t(M_t) = M_t[1 - 1.333\frac{\alpha_s(M_t)}{\pi} - 9.125(\frac{\alpha_s(M_t)}{\pi})^2]. \tag{7.16}$$

Here $\alpha_s(\mu)$ is the strong running coupling defined in the usual way, $\alpha_s(\mu) = g_s^2(\mu)/4\pi$, not to be confused with $\alpha_3(\mu)$ which is smaller by a factor of 4π.

The world average top mass is $M_t = 171.4 \pm 2.1$ GeV [106]. This gives a running mass $m_t(M_t) = 161.6 \pm 2$ GeV. Using this experimentally determined value of the top running mass and the solution for the running top Yukawa coupling (7.13), the angle β can be determined via equation (7.16) if $h_t(\Lambda)$ is known.

Perhaps more usefully, a lower bound on $\tan\beta$ can be extracted. The QFP value for the top Yukawa coupling given in equation (7.14) represents an upper bound. This translates into a lower bound on β which is calculated via equation (7.15).

Table 7.1: Lower bounds on $\tan\beta$

MPP scale (GeV)	$\tan(\beta)$
1.22×10^{19}	1.07
10^{13}	0.91

Table 7.1 shows the lower bounds on $\tan(\beta)$ for Λ at the Planck scale and for $\Lambda = 10^{13}$ GeV. If $\Lambda > 10^{13}$ GeV and $h_t(\Lambda) \gtrsim 1$, $\tan\beta$ will be close to 1.

7.2.2 QFP Solutions At Large $\tan\beta$

If $\tan\beta$ is large it is no longer the case that only the top quark may have $\mathcal{O}(1)$ Yukawa coupling. In this case the fermion mass hierarchy can be generated by the ratios of the Higgs doublet vevs if the b and/or τ masses are generated by different Higgs doublets from the t quark.

In model IV $h_b(\Lambda)$ and $g_\tau(\Lambda)$ are non-zero. In this case the τ lepton gets its mass from the same Higgs doublet as the t quark so it must be strongly suppressed and may safely be neglected. The b quark, however, gets its mass from the other Higgs doublet and so can be large.

The RGEs describing the evolution of $h_t(\mu)$ and $h_b(\mu)$ take very similar forms (Appendix A). In fact, if g_1 (which doesn't have a large effect on the running) is neglected and if the Yukawa couplings are equal at the scale Λ then the equations are invariant under interchanging $h_t(\mu)$ and $h_b(\mu)$. In this limit, and defining $Y_b(\mu) = (h_b(\mu)/4\pi)^2$, the solutions for the RGEs are

$$Y_t(\mu) = Y_b(\mu) = \frac{\dfrac{E_1(t)}{5F_1(t)}}{1 + \dfrac{1}{5Y_0F_1(t)}} \tag{7.17}$$

where $Y_0 = Y_t(\Lambda) = Y_b(\Lambda)$ and

$$E_1(t) = \left[\frac{\alpha_3(\mu)}{\alpha_3(\Lambda)}\right]^{8/7}\left[\frac{\alpha_2(\mu)}{\alpha_2(\Lambda)}\right]^{3/4}, \quad F_1(t) = \int_0^t E_1(t')dt'. \tag{7.18}$$

For large values of Y_0 the solutions are gathered in the vicinity of the QFP,

$$Y_t^{\rm qfp}(M_t) \approx Y_b^{\rm qfp}(M_t) \approx \frac{E_1(t_0)}{5F_1F_1(t_0)}. \tag{7.19}$$

The b quark running mass is related to its Yukawa coupling at the scale M_t via the equation

$$m_b(M_t) = \frac{h_b(M_t)}{\sqrt{2}} v\cos(\beta). \tag{7.20}$$

For $h_b(M_t) \approx h_t(M_t)$ this means $\tan(\beta) \approx m_t(M_t)/m_b(M_t) \approx 55-60$. Using this value of $\tan(\beta)$ leads to a running top mass in excess of 200 GeV which is unacceptably large. This rules out the QFP solution in model IV.

In model III $g_b(\Lambda)$ and $h_\tau(\Lambda)$ are non-zero. The coupling $h_\tau(\Lambda)$ can be large but $g_b(\Lambda)$ must be highly suppressed (in order to generate the required mass hierarchy between the b and t quarks). Neglecting $g_b(\Lambda)$ the RGEs (Appendix A) for $h_t(\mu)$ and $h_\tau(\mu)$

are independent. The solution for the top Yukawa is given by equation (7.13) and the solution for the τ Yukawa in terms of $Y_\tau(\mu) = (h_\tau(\mu)/4\pi)^2$ is found to be

$$Y_\tau(\mu) = \frac{\dfrac{2E_2(t)}{5F_2(t)}}{1 + \dfrac{2}{5Y_\tau(\Lambda)F_2(t)}} \tag{7.21}$$

where

$$E_2(t) = \left[\frac{\alpha_2(\mu)}{\alpha_2(\Lambda)}\right]^{3/4} \left[\frac{\alpha_1(\mu)}{\alpha_1(\Lambda)}\right]^{-15/28}, \quad F_2(t) = \int_0^t E_2(t')dt'. \tag{7.22}$$

The QFP value for the τ mass is obtained in the limit where $Y_\tau(\Lambda)$ becomes large,

$$Y_\tau^{\rm qfp} = \frac{2E_2(t_0)}{5F_2(t_0)} \tag{7.23}$$

The running mass of the τ lepton is given by

$$m_\tau(M_t) = \frac{h_\tau(M_t)}{\sqrt{2}} v\cos(\beta). \tag{7.24}$$

Using the fixed point solution for $h_\tau(M_t)$ leads to $\tan\beta \approx 100$. Such a large $\tan\beta$ leads to a running top mass in excess of 200 GeV which is unacceptably large. This means the QFP solution is also ruled out in model III.

The most tricky case is for model II where $h_t(\Lambda)$, $h_b(\Lambda)$ and $h_\tau(\Lambda)$ may all be large. In this case more advanced techniques are needed.

In the Yukawa coupling parameter space there is an object called the invariant line. The invariant line is such that if the boundary values of the parameters are on the line (i.e. at $t = 0$) then the parameters will remain on the line when evolved with the RGEs (i.e. for all t). Solutions of the RGEs often are attracted to the invariant line. In particular the QFPs are located on the invariant line [107],[108],[109].

The QFPs regime corresponds to the case when the Yukawa couplings at the MPP scale are large. The gauge couplings are relatively small at the MPP scale so the invariant line can be located in the ultraviolet (UV) limit by looking for fixed points in the limit where the gauge couplings go to zero. In this region the equations take the form

$$\begin{aligned}
\frac{dY_t}{dt} &= -\frac{9}{2}Y_t^2 - \frac{1}{2}Y_tY_b \\
\frac{dY_b}{dt} &= -\frac{9}{2}Y_b^2 - \frac{1}{2}Y_tY_b + Y_\tau Y_b \\
\frac{dY_\tau}{dt} &= -\frac{5}{2}Y_\tau^2 - 3Y_\tau Y_b
\end{aligned} \tag{7.25}$$

where $t = \ln(\Lambda^2/\mu^2)$. Then, differentiating the ratio of Y_b and Y_t gives

$$\frac{d}{dt}\left(\frac{Y_b}{Y_t}\right) = \frac{\dfrac{dY_b}{dt}Y_t - Y_b\dfrac{dY_t}{dt}}{Y_t^2}. \tag{7.26}$$

Substituting in the derivatives from equation (7.25) and simplifying then gives the equation

$$4\frac{Y_b}{Y_t} + \frac{Y_\tau}{Y_t} = 4. \tag{7.27}$$

Similarly, differentiating the ratio of Y_τ and Y_t leads to the equation

$$5\frac{Y_\tau}{Y_t} + 5\frac{Y_b}{Y_t} = 9. \tag{7.28}$$

Soving these simultaneous equations leads to the conditions for the UV fixed point in the gaugeless limit,

$$\begin{aligned} Y_b &= \frac{11}{15}Y_t \\ Y_\tau &= \frac{16}{15}Y_t. \end{aligned} \tag{7.29}$$

Starting with large values of Yukawa couplings which fulfill the above conditions at the MPP scale and numerically evolving the couplings produces the invariant line to which all solutions converge. Evolving this line down to the scale of M_t locates the vicinity of the QFPs at this scale [107],[108],[109]. Using the running τ mass to find $\tan\beta$ in this model allows the running t and b masses to be calculated.

The top running mass is again found to be in excess of 200 GeV which is too high while the bottom running mass is found to be less than 2.5 GeV which is too low. This shows that the QFP solution is not viable in model II either. Consistent realisation of the QFP scenario is only possible in the case when only h_t is large and in this case $\tan\beta$ can be found via comparison with the top running mass and is found to be of order 1 for large values of the MPP scale.

7.3 Higgs Self Couplings

The technique of finding UV fixed points in the gaugeless limit and evolving them down to the scale of M_t may also be used to find QFPs for the Higgs self couplings. It will be useful to define $R_i(\mu)$ by

$$R_i(\mu) = \frac{\lambda_i(\mu)}{h_t^2(\mu)}. \tag{7.30}$$

Recall that in our model only the top quark has a non-negligible Yukawa coupling and the Higgs self couplings which are non-zero at the MPP scale are λ_1, λ_2, λ_3 and λ_4.

The RGEs for the λ_i are given in appendix A. In order to rewrite these equation in terms of the ratios R_i, we differentiate R_i with respect to $t = \ln(\Lambda^2/\mu^2)$,

$$\frac{dR_i}{dt} = \frac{1}{h_t^2}(\frac{d\lambda_i}{dt} - 2R_i h_t \frac{dh_t}{dt}). \tag{7.31}$$

In the gaugeless limit the RGE for h_t is

$$\frac{dh_t}{dt} = -\frac{1}{16\pi^2}\frac{9}{4}h_t^3. \tag{7.32}$$

Substituting this into equation (7.31) gives

$$\frac{d\lambda_i}{dt} = h_t^2 \frac{dR_i}{dt} - \frac{1}{16\pi^2}\frac{9}{2} R_i h_t^4. \tag{7.33}$$

Using this equaiton to rewrite the RGEs in terms of the ratios R_i gives

$$\begin{aligned}
-2\frac{16\pi^2}{h_t^2}\frac{dR_1}{dt} &= 12R_1^2 + 4R_3^2 + 4R_3R_4 + 2R_4^2 - 9R_1 \\
-2\frac{16\pi^2}{h_t^2}\frac{dR_2}{dt} &= 12R_2^2 + 4R_3^2 + 4R_3R_4 + 2R_4^2 + 3R_2 - 12 \\
-2\frac{16\pi^2}{h_t^2}\frac{dR_3}{dt} &= 2(R_1+R_2)(3R_3+R_4) + 4R_3^2 + 2R_4^2 - 3R_3 \\
-2\frac{16\pi^2}{h_t^2}\frac{dR_4}{dt} &= 2R_4(4R_1 + R_2 + 4R_3 + 2R_4) - 3R_4.
\end{aligned} \tag{7.34}$$

In order to locate UV fixed points in the gaugeless limit we look for values of the functions R_i such that

$$\frac{dR_i}{dt} = 0. \tag{7.35}$$

This leads to four algebraic equations involving $R_1, .., R_4$. These equations have six solutions with all the R_i real,

Table 7.2: Values of R_i satisfying equation (7.35)

Solution	R_1	R_2	R_3	R_4
i	0.75	-1.133	0	0
ii	0	-1.133	0	0
iii	0	0.883	0	0
iv	0.742	0.880	-0.166	0.259
v	0.75	0.883	0	0
vi	0.742	0.880	0.099	-0.259

Solutions which are compatible with the MPP must fulfill the MPP conditions for vacuum stability,

$$\lambda_1(\Phi) > 0, \quad \lambda_2(\Phi) > 0 \quad \tilde{\lambda}(\Phi) \geq 0 \tag{7.36}$$

which must be fulfilled for all Φ between the electroweak scale and the MPP scale. This immediately implies that solutions (i), (ii) and (iii) are not valid.

Furthermore, the fixed point should be a *stable* fixed point, which means that small deviations should tend to die off. To examine the behaviour of small deviations write

$$R_i(t) \approx R_i^0 + r_i(t) \tag{7.37}$$

where the R_i^0 solve equation (7.35) and $r_i(t)$ is small. To linearise the RGEs, we perform a Taylor series expansion around $R_i = R_i^0$. The linearized system of equations is

$$\frac{dr_i}{dt} = \sum_{j=1}^{4} \left.\frac{\partial \beta_{R_i}}{\partial R_j}\right|_{R_j=R_j^0} r_j, \qquad \left.\frac{\partial \beta_{R_i}}{\partial R_j}\right|_{R_j=R_j^0} = -2\frac{h_t^2}{16\pi^2} a_{ij} \tag{7.38}$$

where the matrix a_{ij} is given by

$$a_{ij} = \begin{pmatrix} 24R_1^0 - 9 & 0 & 8R_3^0 + 4R_4^0 & 4(R_3^0 + R_4^0) \\ 0 & 24R_2^0 + 3 & 8R_3^0 + 4R_4^0 & 4(R_3^0 + R_4^0) \\ 6R_3^0 + 2R_4^0 & 6R_3^0 + 2R_4^0 & 6R_1^0 + 6R_2^0 + 8R_3^0 - 3 & 2R_1^0 + 2R_2^0 + 4R_4^0 \\ 2R_4^0 & 2R_4^0 & 8R_4^0 & 2R_1^0 + 2R_2^0 + 8R_3^0 + 8R_4^0 - 4 \end{pmatrix}.$$

The fixed point is stable when the eigenvalues of this matrix are positive. This rules out solutions (iv) and (vi) so only solution (v) is valid. Solution (v) may be written as

$$\begin{aligned} R_1 &= \frac{3}{4} \\ R_2 &= \frac{\sqrt{65} - 1}{8} \\ R_3 &= 0 \\ R_4 &= 0. \end{aligned} \tag{7.39}$$

The position of the QFP at the electroweak scale is found by numerically evolving the couplings via the RGEs using the above equations as boundary conditions and a large top Yukawa coupling. This gives

$$\begin{aligned} \lambda_1^{\rm qfp} &= 0.465 \\ \lambda_2^{\rm qfp} &= 0.946 \\ \lambda_3^{\rm qfp} &= -0.015 \\ \lambda_4^{\rm qfp} &= -0.018 \\ \tilde{\lambda}^{\rm qfp} &= 0.631. \end{aligned} \tag{7.40}$$

The MPP conditions (6.17) and (6.18) require

$$\tilde{\lambda}(\Lambda) = \beta_{\tilde{\lambda}} \,|_{\Lambda} = 0. \tag{7.41}$$

These lead to conditions that the Higgs self couplings must satisfy at the MPP scale,

$$\begin{aligned} \lambda_4^2(\Lambda) &= \frac{6h_t^4(\Lambda)\lambda_1(\Lambda)}{(\sqrt{\lambda_1(\Lambda)} + \sqrt{\lambda_2(\Lambda)})^2} - 2\lambda_1(\Lambda)\lambda_2(\Lambda) - \frac{3}{8}(3g_2^4(\Lambda) + 2g_2^2(\Lambda)g_1^2(\Lambda) + g_1^4(\Lambda)) \\ \lambda_3(\Lambda) &= -\sqrt{\lambda_1(\Lambda)\lambda_2(\Lambda)} - \lambda_4(\Lambda). \end{aligned} \tag{7.42}$$

Here $\lambda_4(\Lambda) < 0$. These conditions show that if values are chosen for $\lambda_1(\Lambda)$, $\lambda_2(\Lambda)$ and $h_t(\Lambda)$, these will set the values for $\lambda_3(\Lambda)$ and $\lambda_4(\Lambda)$.

There are restrictions on the allowed range of $\lambda_1(\Lambda)$ and $\lambda_2(\Lambda)$. The quantity $\lambda_4^2(\Lambda)$ must remain greater than zero. For example, when $\lambda_1(\Lambda) = \lambda_2(\Lambda) = \lambda_0$ this leads to the restriction

$$\lambda_0 < \sqrt{\frac{3h_t^4(\Lambda)}{4} - \frac{3}{8}(3g_2^4(\Lambda) + 2g_2^2(\Lambda)g_1^2(\Lambda) + g_1^4(\Lambda))}. \tag{7.43}$$

The other restriction on the allowed range comes from the vacuum stability condition. The function $\tilde{\lambda}(\mu)$ must remain positive for all μ between the electroweak scale and the MPP scale, otherwise there is another minimum of the potential with much lower energy than our current vacuum.

These conditions constrain the values of $\lambda_1(\Lambda)$ and $\lambda_2(\Lambda)$ to be close to the UV fixed point values. For example, let us set $\lambda_1(\Lambda) = \lambda_2(\Lambda) = \lambda_0$. Then, taking $h_t(\Lambda) = 1.5$ and setting the MPP scale to be the Planck scale, numerical studies show that R_0 must lie between 0.79 and 0.86. The lower limit comes from the vacuum stability condition and the upper limit from the condition $\lambda_4^2(\Lambda) > 0$.

Increasing $h_t(\Lambda)$ narrows the range of allowed values for R_0. Taking $h_t(\Lambda) = 2.5$, R_0 is constrained to lie in the range 0.83 to 0.87. On the other hand, the bounds are less tight if the MPP scale is lowered.

The running of the Higgs self couplings is examined in figures 7.3-7.7 below. Here the solid thick line is the QFP solution and the other lines are solutions satisfying the MPP boundary conditions. Since there is a close relation between $h_t(\Lambda)$ and $\lambda_0(\Lambda)$ these are varied simultaneously with each curve representing a solution for a different pair $(h_t(\Lambda), \lambda_0(\Lambda))$. The solid thin line is for (2.65,6), the dot-dash line is for (2.3,4.5), the dashed line is for (1.9,3) and the dotted line is for (1.35,1.5).

These plots show that the convergence to the fixed point is strong for λ_1, λ_2 and λ_3 but is weaker for λ_4 and $\tilde{\lambda}$ (because it depends on λ_4). Also, note that $\lambda_4 < 0$ which is necessary if the minimum of the potential is to preserve electric charge.

7.4 Higgs Masses

The Higgs doublets aquire vevs which trigger EWSB with $\langle H_1 \rangle = v \sin\beta$ and $\langle H_2 \rangle = v \cos\beta$. The Higgs doublets may be written in terms of the field basis (h, H), defined through the relation

$$\begin{pmatrix} h \\ H \end{pmatrix} = \begin{pmatrix} \cos\beta & \sin\beta \\ -\sin\beta & \cos\beta \end{pmatrix} \begin{pmatrix} H_1 \\ H_2 \end{pmatrix}. \tag{7.44}$$

In this basis $\langle h \rangle = v$ and $\langle H \rangle = 0$ so all the symmetry breaking comes from the doublet h. Also, all components of h other than the neutral CP-even component are eaten by the W and Z bosons via the Higgs mechanism, whereas H contains the charged $\chi^{\pm}$, the neutral CP-odd A and another neutral CP-even scalar.

The pseudoscalar (CP-odd) state aquires a tree level mass

$$m_A^2 = \frac{2m_3^2}{\sin 2\beta} \tag{7.45}$$

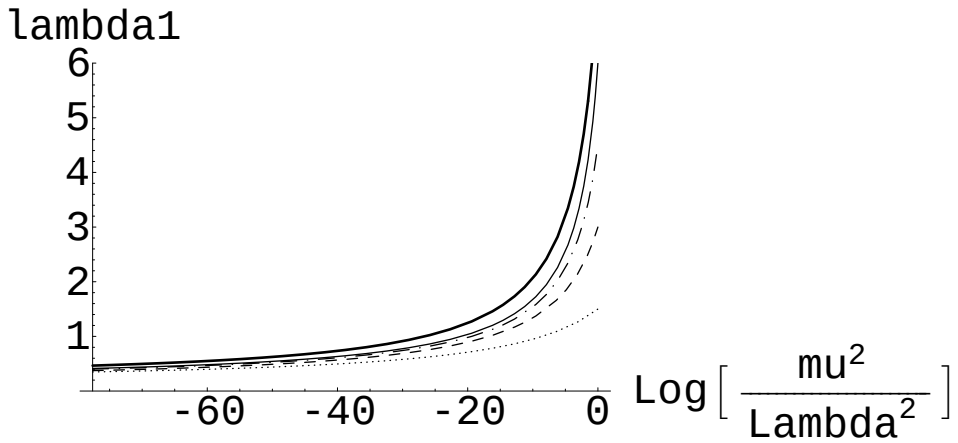

Figure 7.3: $\lambda_1(\mu)$ vs $\ln(\mu^2/\Lambda^2)$ for Λ at the Planck scale. The solid thick line is the QFP solution (the invariant line). The other lines are for various values of $(h_t(\Lambda), \lambda_0(\Lambda))$ where $\lambda_0(\Lambda) = \lambda_1(\Lambda) = \lambda_2(\Lambda)$ and then $\lambda_3(\Lambda)$ and $\lambda_4(\Lambda)$ are chosen so as to satisfy the MPP boundary conditions. The solid thin line is for $(h_t(\Lambda), \lambda_0(\Lambda)) = (2.65, 6)$, the dot-dash line is for (2.3,4.5), the dashed line is for (1.9,3) and the dotted line is for (1.35,1.5).

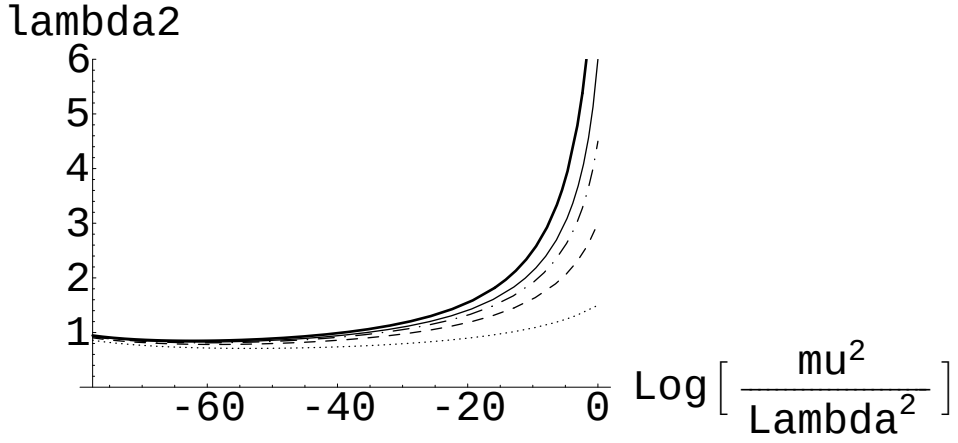

Figure 7.4: $\lambda_2(\mu)$ vs $\ln(\mu^2/\Lambda^2)$ for Λ at the Planck scale. The solid thick line is the QFP solution (the invariant line). The other lines are for various values of $(h_t(\Lambda), \lambda_0(\Lambda))$ where $\lambda_0(\Lambda) = \lambda_1(\Lambda) = \lambda_2(\Lambda)$ and then $\lambda_3(\Lambda)$ and $\lambda_4(\Lambda)$ are chosen so as to satisfy the MPP boundary conditions. The solid thin line is for $(h_t(\Lambda), \lambda_0(\Lambda)) = (2.65, 6)$, the dot-dash line is for (2.3,4.5), the dashed line is for (1.9,3) and the dotted line is for (1.35,1.5).

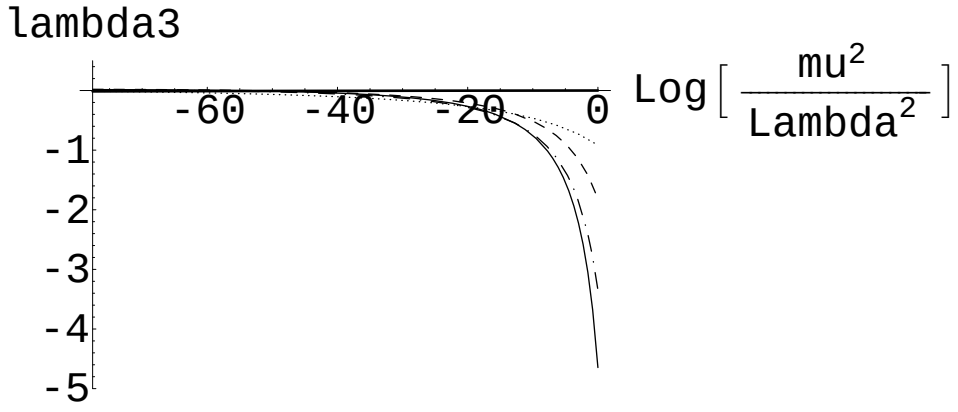

Figure 7.5: $\lambda_3(\mu)$ vs $\ln(\mu^2/\Lambda^2)$ for Λ at the Planck scale. The solid thick line is the QFP solution (the invariant line). The other lines are for various values of $(h_t(\Lambda), \lambda_0(\Lambda))$ where $\lambda_0(\Lambda) = \lambda_1(\Lambda) = \lambda_2(\Lambda)$ and then $\lambda_3(\Lambda)$ and $\lambda_4(\Lambda)$ are chosen so as to satisfy the MPP boundary conditions. The solid thin line is for $(h_t(\Lambda), \lambda_0(\Lambda)) = (2.65, 6)$, the dot-dash line is for (2.3,4.5), the dashed line is for (1.9,3) and the dotted line is for (1.35,1.5).

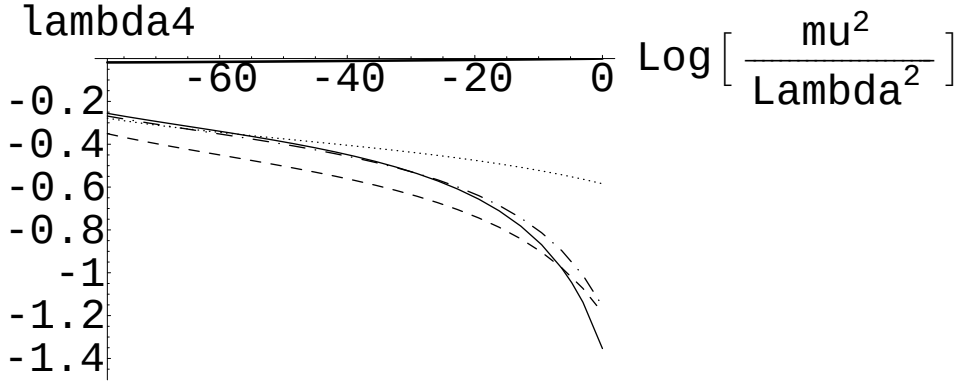

Figure 7.6: $\lambda_4(\mu)$ vs $\ln(\mu^2/\Lambda^2)$ for Λ at the Planck scale. The solid thick line is the QFP solution (the invariant line). The other lines are for various values of $(h_t(\Lambda), \lambda_0(\Lambda))$ where $\lambda_0(\Lambda) = \lambda_1(\Lambda) = \lambda_2(\Lambda)$ and then $\lambda_3(\Lambda)$ and $\lambda_4(\Lambda)$ are chosen so as to satisfy the MPP boundary conditions. The solid thin line is for $(h_t(\Lambda), \lambda_0(\Lambda)) = (2.65, 6)$, the dot-dash line is for (2.3,4.5), the dashed line is for (1.9,3) and the dotted line is for (1.35,1.5).

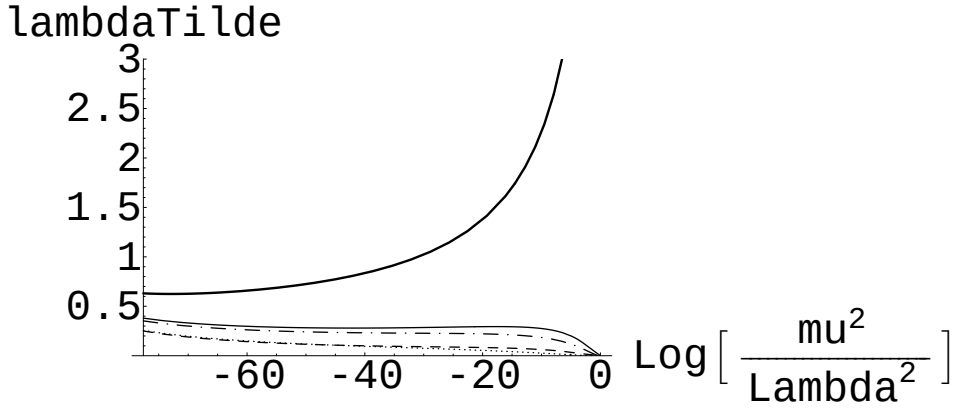

Figure 7.7: $\tilde{\lambda}(\mu)$ vs $\ln(\mu^2/\Lambda^2)$ for Λ at the Planck scale. The solid thick line is the QFP solution (the invariant line). The other lines are for various values of $(h_t(\Lambda), \lambda_0(\Lambda))$ where $\lambda_0(\Lambda) = \lambda_1(\Lambda) = \lambda_2(\Lambda)$ and then $\lambda_3(\Lambda)$ and $\lambda_4(\Lambda)$ are chosen so as to satisfy the MPP boundary conditions. The solid thin line is for $(h_t(\Lambda), \lambda_0(\Lambda)) = (2.65, 6)$, the dot-dash line is for (2.3,4.5), the dashed line is for (1.9,3) and the dotted line is for (1.35,1.5).

and the charged state gains a tree level mass

$$m^2_{\chi^\pm} = m^2_A - \frac{\lambda_4}{2}v^2. \tag{7.46}$$

The mass terms mix the 2 neutral CP-even scalars. The mass matrix has the form

$$M^2 = \begin{pmatrix} M^2_{11} & M^2_{12} \\ M^2_{21} & M^2_{22} \end{pmatrix} \tag{7.47}$$

where, at tree level,

$$\begin{aligned} M^2_{11} &= (\lambda_1 \cos^4\beta + \lambda_2 \sin^4\beta + \frac{\lambda}{2}\sin^2 2\beta)v^2 \\ M^2_{12} = M^2_{21} &= \frac{v^2}{2}(-\lambda_1 \cos^2\beta + \lambda_2 \sin^2\beta + \lambda\cos 2\beta)\sin 2\beta \\ M^2_{22} &= m^2_A + \frac{v^2}{4}(\lambda_1 + \lambda_2 - 2\lambda)\sin^2 2\beta \end{aligned} \tag{7.48}$$

and $\lambda = \lambda_3 + \lambda_4$. Note, dependence on m^2_1 and m^2_2 has been eliminated using the equations for the extrema of the potential.

Define the lighter of these CP-even scalars to be h_1 and the heavier to be h_2. Then, the masses are given by the eigenvalues of the mass matrix,

$$m^2_{h_1,h_2} = \frac{1}{2}(M^2_{11} + M^2_{22} \mp \sqrt{(M^2_{22} - M^2_{11})^2 + 4M^4_{12}}). \tag{7.49}$$

The mass eigenstates h_1 and h_2 are related to the original fields H_1 and H_2 via the transformation

$$\begin{pmatrix} h_2 \\ h_1 \end{pmatrix} = \begin{pmatrix} \cos\alpha & \sin\alpha \\ -\sin\alpha & \cos\alpha \end{pmatrix} \begin{pmatrix} H_1^0 - v_1 \\ H_2^0 - v_2 \end{pmatrix} \tag{7.50}$$

where the mixing angle α is given by

$$\tan\alpha = \frac{(\lambda v^2 - m_A^2)\sin\beta\cos\beta}{m_A^2\sin^2\beta + \lambda_1 v^2\cos^2\beta - m_{h_1}^2}. \tag{7.51}$$

Other than m_3^2 (or equivalently m_A^2) the parameters which determine the Higgs masses can be obtained by evolving the RGEs with appropriate boundary conditions at the MPP scale down to the electroweak scale. This allows the scalar masses to be predicted.

We choose $R_1(\Lambda) = 0.75$, $R_2(\Lambda) = (\sqrt{65} - 1)/8$ (the values taken at the UV fixed point) and take $R_3(\Lambda)$ and $R_4(\Lambda)$ to fulfill the MPP condtions (7.42). Taking the MPP scale to be the Planck scale and $h_t^2(\Lambda) = 10$, the scalar mass spectrum is plotted as a function of m_A in figure 7.8. The thick solid line is the light CP-even Higgs, the thin solid line is the heavy CP-even scalar and the dotted line is the charged scalar. Recall that these scalar masses are computed from the renormalisation group improved effective potential, so they contain the leading logarithms of the one-loop potential.

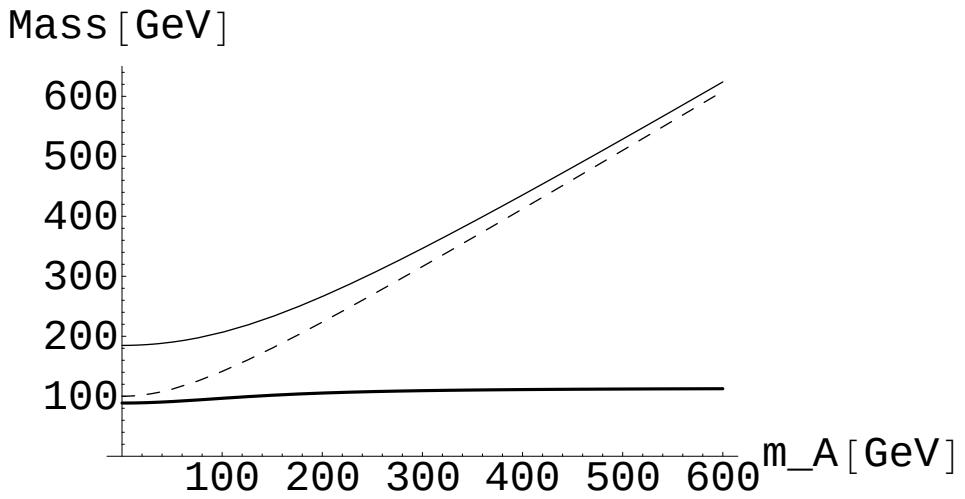

Figure 7.8: The scalar mass spectrum as a function of m_A, the CP odd Higgs mass, for $h_t^2(\Lambda) = 10$. The thick solid line is the light CP even Higgs, the thin solid line is the heavy CP even Higgs and the dashed line is the charged Higgs.

Figure 7.9 shows how the scalar mass spectrum changes for $h_t^2(\Lambda) = 2.25$, with the other parameters the same as for figure 7.8.

The mass of the lightest CP-even Higgs is relatively insensitive to the mass of the pseudo-scalar m_A. For $h_t^2(\Lambda) = 10$ the mass of the lightest Higgs is below 113 GeV

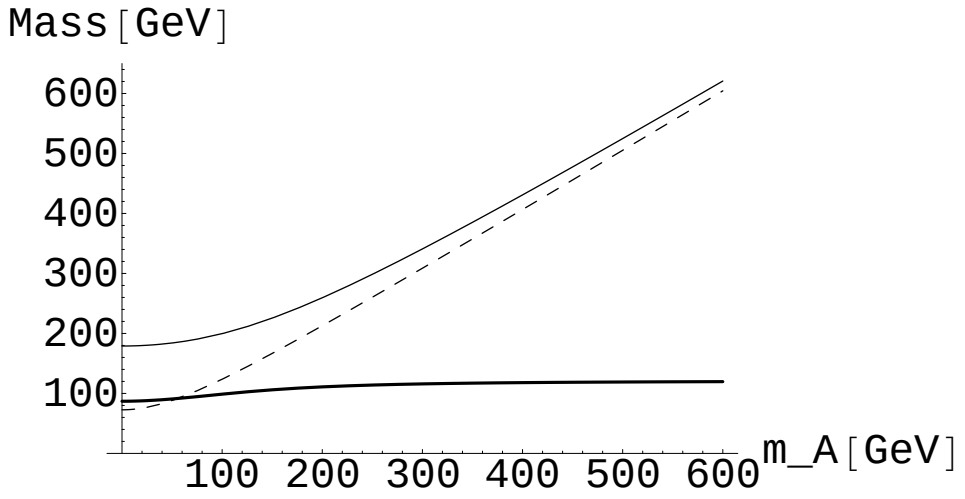

Figure 7.9: The scalar mass spectrum as a function of m_A, the CP odd Higgs mass, for $h_t^2(\Lambda) = 2.25$. The thick solid line is the light CP even Higgs, the thin solid line is the heavy CP even Higgs and the dashed line is the charged Higgs.

even for m_A as large as 600 GeV (figure 7.8), whilst for $h_t^2(\Lambda) = 2.25$ this is raised to 120 GeV (figure 7.9). The masses of the heavy CP-even Higgs and the charged scalar by contrast strongly depend on the parameter m_A, being given by m_A plus terms of order v^2/m_A^2.

7.5 Higgs Couplings

In this section the couplings of the Higgs to weak gauge bosons and the top quark are examined. These couplings are important because they control the generation of Higgs bosons at the LHC.

The coupling of the neutral scalars to Z bosons takes a particularly simple form in the field basis (h, H) [110].

$$\mathcal{L}_{H_i-Z} = \frac{g}{2} M_Z Z_\mu Z^\mu h + \frac{g}{2} Z^\mu [H(\partial_\mu A) - (\partial_\mu H)A] \tag{7.52}$$

However, these are not the mass eigenstates. After transforming to the mass eigenstates, which are given by equation (7.50), both the light h_1 and the heavy h_2 couple to Z pairs and to a Z and an A.

These couplings may be parameterized as $g_{ZZh_i} = R_{ZZh_i}\frac{g}{2}M_Z$ and $g_{ZAh_i} = \frac{g}{2}R_{ZAh_i}$. They may be expressed in terms of the angles α and β [111],

$$R_{ZZh_1} = -R_{ZAh_2} = \sin(\beta - \alpha) \tag{7.53}$$

$$R_{ZZh_2} = R_{ZAh_1} = \cos(\beta - \alpha). \tag{7.54}$$

Similarly, the coupling to W pairs may be defined as $g_{WWh_i} = \frac{g}{2} M_W R_{WWh_i}$ where $R_{WWh_i} = R_{ZZh_i}$.

In the original Higgs field basis the top quark coupled only to H_2. The coupling is given by h_t which is proportional to $1/v \sin\beta$. The coupling to the mass eigenstates is then determined by the mixing angle α. The couplings may be defined to be the SM coupling multiplied by an R-factor,

$$g_{\bar{t}th_i} = -\frac{m_t(M_t)}{v} R_{\bar{t}th_i}. \tag{7.55}$$

Then

$$R_{\bar{t}th_1} = \frac{\cos\alpha}{\sin\beta}, \qquad R_{\bar{t}th_2} = \frac{\sin\alpha}{\sin\beta}. \tag{7.56}$$

The R-factors parameterizing the couplings of the Higgs to the top quark and weak gauge bosons can be calculated from the coupings $\lambda_i(M_t)$ and $h_t(M_t)$. The MPP scale is taken to be at the Planck scale and $h_t^2(\Lambda)$ is taken to be 10, firmly in the QFP regime. The couplings $\lambda_1(\Lambda)$ and $\lambda_2(\Lambda)$ are calculated using the UV fixed point values $R_1 = 0.75$ and $R_2 = 0.833$, whilst $\lambda_3(\Lambda)$ and $\lambda_4(\Lambda)$ are found using the MPP conditions 7.42.

The R-factors found are plotted in figures 7.10 and 7.11. Here the solid lines denote the coupling of the light Higgs h_1 and the dotted line denotes the coupling of the heavy Higgs h_2.

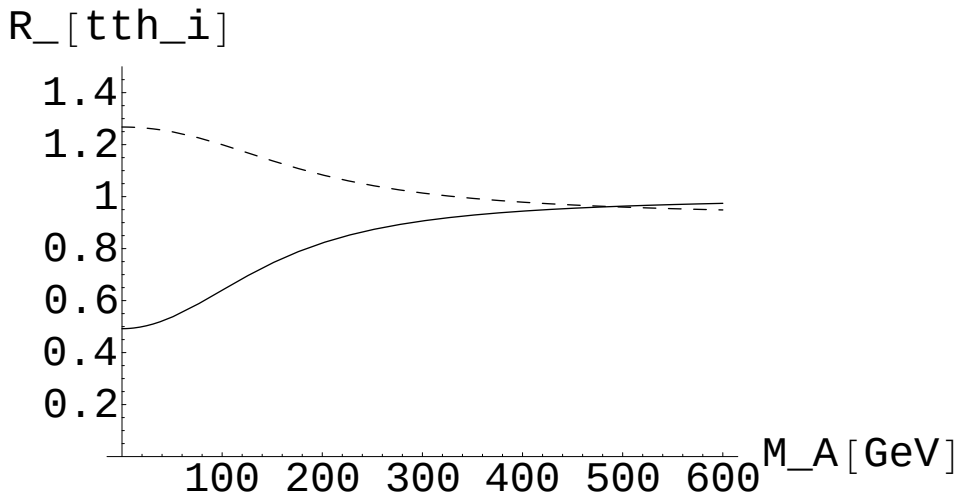

Figure 7.10: The R-factors for the Higgs-gauge boson couplings with Λ at the Planck scale and $h_t^2(\Lambda) = 10$. These denote the modification to the coupling of the Higgses to the W and Z gauge bosons. The solid line is for the light Higgs and the dashed line is for the heavy Higgs.

At such a large MPP scale the couplings of the light Higgs to Z is within about 10% of the SM value for all m_A, and extremely close for $m_A \gtrsim 200$ GeV. The coupling of

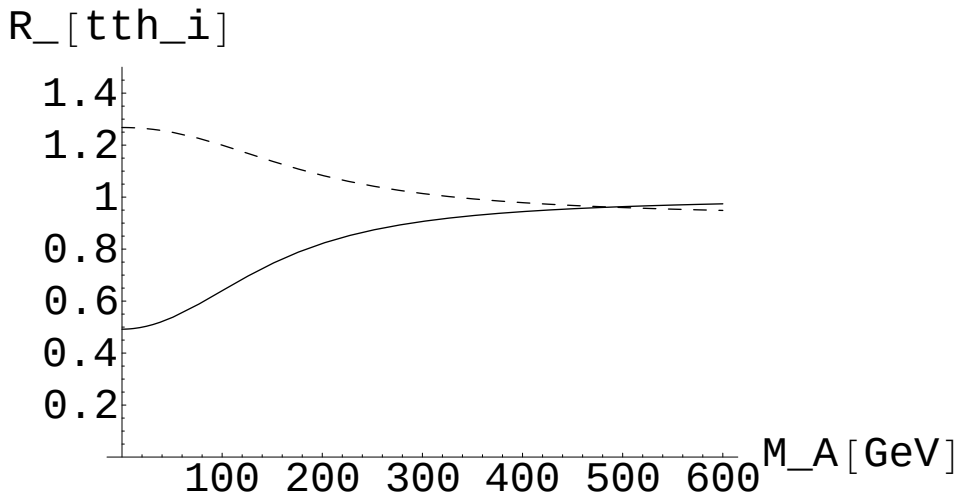

Figure 7.11: The R-factors for the Higgs-top couplings with Λ at the Planck scale and $h_t^2(\Lambda) = 10$. These denote the modification to the coupling of the Higgses to the top quark. The solid line is for the light Higgs and the dashed line is for the heavy Higgs.

the light Higgs to the top quark is strongly suppressed for very low values of m_A, less than about 200 GeV. However it too approaches the SM value for $m_A \gtrsim 300$ GeV.

Low values of m_A are disfavoured by data on $B \to X_s, \gamma$ decays. For example, in model II the charged scalar mass is constrained to be greater than 350 GeV [112]. This means the couplings must be very close to the SM values.

The situation does not change dramatically when $h_t^2(\Lambda)$ is lowered to 2.25 as shown in figures 7.12 and 7.13. This is to be expected since the couplings should still be close to their QFP values.

Data from LEP [113] constrains the mass of the Higgs. The Higgs was searched for in so-called Higgsstrahlung processes, where $e^+e^- \to ZH$. This means the constraints on the Higgs mass depend on the coupling of the Higgs to the Z boson.

As is shown in figures 7.10 and 7.12, the QFP scenario at large MPP scales implies that $R_{ZZh_1} > 0.85$ across the whole range of m_A. Comparing this with Figure 10 of reference [113], this can be seen to lead to a slight relaxation of the constraints on the mass of the Higgs from $M_H > 114.4$ GeV at 95% C.L. in the SM to $M_H \gtrsim 113$ GeV.

Non-observation of the Higgs at LEP thus rules out most of the parameter space for the QFP scenario at large MPP scales, since the mass of the lightest Higgs in this scenario is below the LEP bounds.

The situation changes when low values of the MPP scale are considered, for instance $\Lambda = 10$ TeV. In this case the convergence to the QFP is very weak and represents only an upper bound on $h_t(M_t)$ and correspondingly an upper bound on $\tan\beta$.

The values $R_1 = 0.75$ and $R_2 = 0.883$ are used as a benchmark, with R_3 and R_4 chosen to satisfy the MPP conditions. Using these values along with $h_t^2(\Lambda) = 10$, the scalar mass spectrum can be found. This is shown in figure 7.14. As before, the thick line

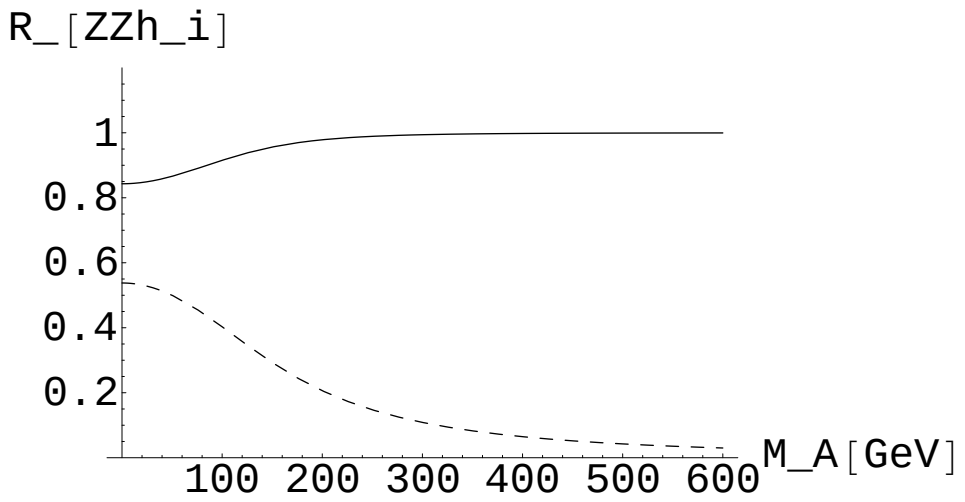

Figure 7.12: The R-factors for the Higgs-gauge boson couplings with Λ at the Planck scale and $h_t^2(\Lambda) = 2.25$. These denote the modification to the coupling of the Higgses to the W and Z gauge bosons. The solid line is for the light Higgs and the dashed line is for the heavy Higgs.

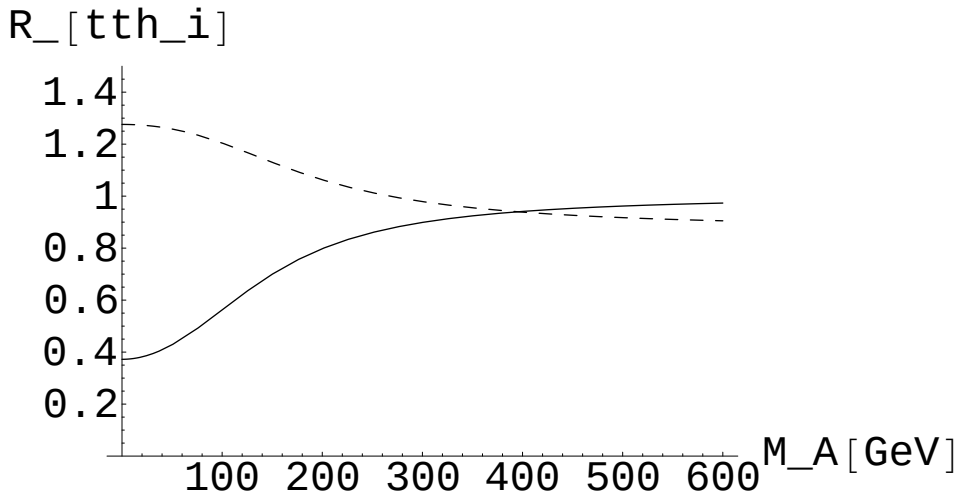

Figure 7.13: The R-factors for the Higgs-top couplings with Λ at the Planck scale and $h_t^2(\Lambda) = 2.25$. These denote the modification to the coupling of the Higgses to the top quark. The solid line is for the light Higgs and the dashed line is for the heavy Higgs.

is the light Higgs, the thin line is the heavy Higgs and the dotted line is the charged Higgs.

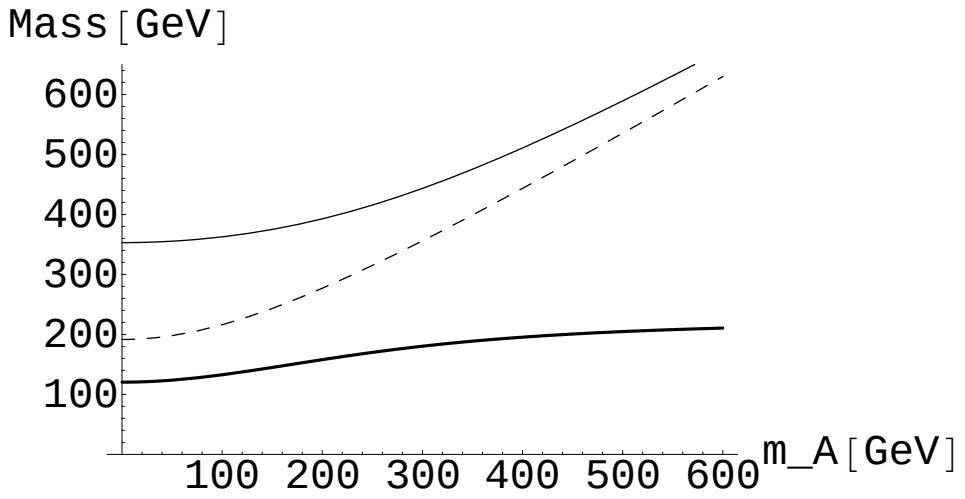

Figure 7.14: Higgs mass spectrum for $\Lambda = 10$ TeV as a function of m_A, the CP odd Higgs mass. The thick solid line is the light CP even Higgs, the thin solid line is the heavy CP even Higgs and the dashed line is the charged Higgs.

The R-factors in the low MPP scale scenario are plotted in figures 7.15 and 7.16. The solid lines denote couplings of h_1 and the dotted lines denote couplings of h_2. It can be seen that $R_{ZZh_1} \gtrsim 0.81$ across the range of m_A which translates into a Higgs mass bound from LEP of $M_H \gtrsim 112$ GeV at 95% C.L..

In this scenario, the mass of the lightest Higgs is comfortably above the LEP limit for all allowed values of m_A, as can be seen in figure 7.14.

In this case the couplings of the light SM-like Higgs to the top quark are enhanced considerably due to the low values of $\sin\beta$. Even for $m_A \gtrsim 600$ GeV the coupling is enhanced by 25% relative to the SM. The cross section is correspondingly boosted by a factor of about 1.5-2.5. This allows the MPP inspired 2HDM with low MPP scale to be distinguished from the SM and supersymemtric extensions of the SM even if the extra scalars are heavy ($\gtrsim 500 - 700$ GeV).

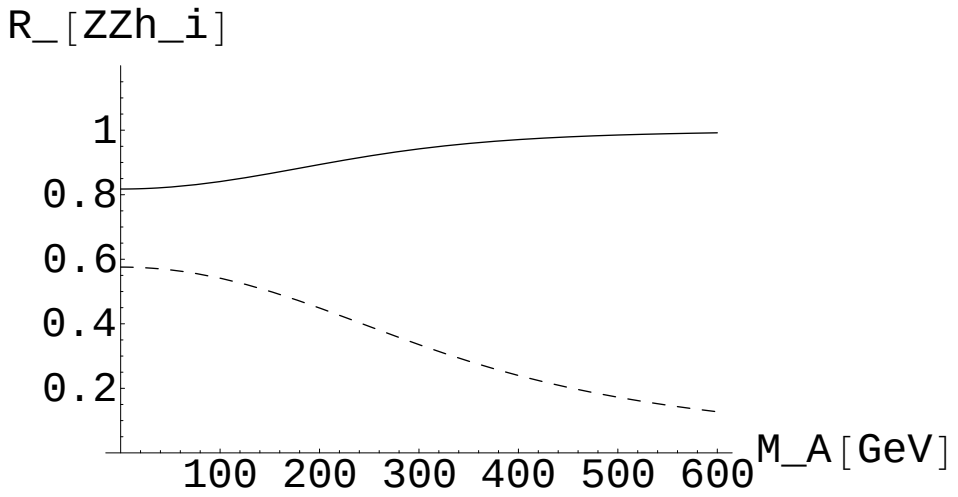

Figure 7.15: R-factors for Higgs-gauge boson couplings with $\Lambda = 10$ TeV. These denote the modification to the coupling of the Higgses to the W and Z gauge bosons. The solid line is for the light Higgs and the dashed line is for the heavy Higgs.

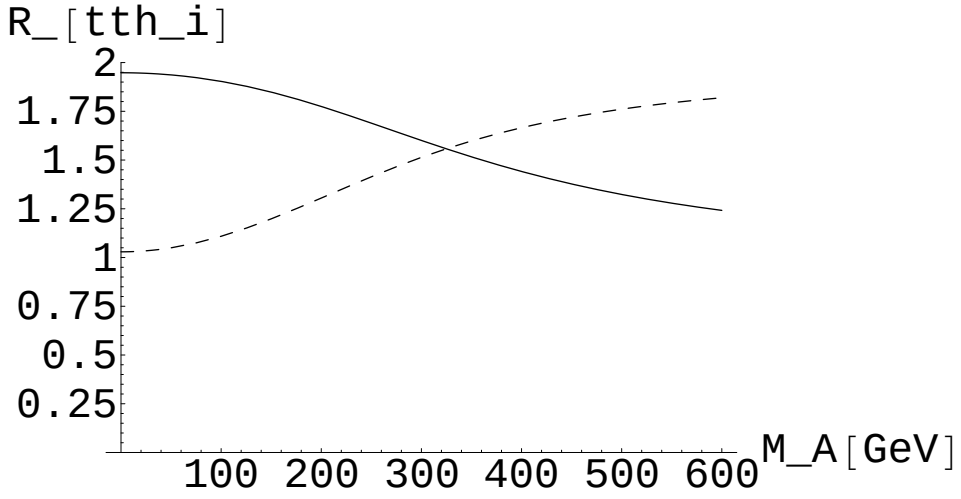

Figure 7.16: R-factors for Higgs-top couplings with $\Lambda = 10$ TeV. These denote the modification to the coupling of the Higgses to the top quark. The solid line is for the light Higgs and the dashed line is for the heavy Higgs.

Chapter 8

Summary and Conclusions

The hierarchy problem motivates the search for new physics beyond the standard model. The Higgs mass suffers from a quadratic instability in its mass term which requires the introduction of new physics to avoid unnatural fine-tuning. However, there is a tension between naturalness, which favours new physics at a low energy scale, and the electroweak precision constraints, which favour a high energy scale for new physics.

Little Higgs models provide an innovative and interesting solution of the hierarchy problem. The Higgs is taken to be a pseudo-Goldstone boson associated with the spontaneous breakdown of some global symmetry at the scale of about 10 TeV. A Higgs mass is generated through radiative corrections, but global symmetries prevent any diagram involving only a single (large) gauge or Yukawa coupling from generating a contribution to the Higgs mass. In particular, no quadratically divergent contribution is present below the two-loop level, with the leading order contribution coming from one-loop logarithmically divergent diagrams. This leads to a naturally light "little Higgs" without violating the electroweak precision constraints.

Two particular Little Higgs models, the Littlest Higgs and the Schmaltz model, were examined in detail as representative of the two broad classes of Little Higgs models, namely the product group and simple group classes respectively.

A detailed exposition of the Littlest Higgs model was performed, resulting in the correction of some mistakes in the literature. In particular, the correct mixing angles of the t and T quarks were found and used to calculate the couplings of these quarks to scalars.

Along the same lines, a detailed analysis of the Schmaltz model was undertaken. The masses, mixing angles and couplings of particles in the weak gauge boson and top sectors were calculated up to terms of order v^4/f^4, which is necessary for detailed phenomenological investigations.

The results of this analysis were applied to calculate corrections to loop induced interactions of the Higgs boson. In the standard model, the Higgs can interact with gluon pairs via top quark loops, and with photon pairs via loops of top quarks or W bosons. Little Higgs models introduce corrections to these processes both due to modification of the standard model couplings and through the introduction of new paricles (such as the T quark and heavy gauge bosons) which can run in the loop.

The Little Higgs corrections to these processes tend to be relatively small, typically no

more than 10-20%. The largest corrections for a given value of f arise in the Schmaltz model if the ratio f_2/f_1 is large.

The prospects for observing this discrepancy are not so good. The best chance is at a photon collider which can measure the coupling of Higgs to photons to within 2 or 3%. However, NLO QCD corrections are expected to be larger than the one-loop Little Higgs corrections calculated meaning that higher order calculations would be required in order to use these processes to distinguish the Little Higgs scenario from the standard model.

Higgs pair production via gluon fusion at the LHC was also examined in both the Littlest Higgs and the Schmaltz models. Due to the complexity of this process it was necessary to use automated techniques to evaluate the cross section. It was found that the corrections are typically less than 20%, but can be significantly higher in certain regions of the parameter space of the Littlest Higgs model where $f \lesssim 2$ TeV and when $x \gtrsim 0.85$, i.e. when the vev of the scalar triplet is comparatively large. However, factorisation scale uncertainty along with prohibitively large QCD backgrounds mean that even in this scenario the Little Higgs model corrections are not observable.

In addition to Little Higgs models, this thesis also investigated the consequences of applying the multiple point principle (MPP) in the two Higgs doublet model (2HDM). The MPP posits that nature tunes the values of the parameters of the theory such that there is a large set of vacua degenerate with our current vacuum. This condition was shown to result in a Peccei-Quinn type symmetry which naturally suppresses flavour changing neutral currents.

Particular attention was paid to the quasi-fixed point (QFP) regime of the MPP inspired 2HDM. For large values of the MPP scale the top quark Yukawa coupling was found to be well approximated by the QFP value at the weak scale for a large range of values at the MPP scale. This allowed the ratio of the doublet vevs, $\tan\beta$, to be calculated from the running mass of the top quark. In addition, the QFP scenario with large b or τ Yukawa couplings was ruled out, because it leads to phenomenologically unacceptable large values of the running top mass.

Numerical solution of the renormalisation group equations, using the MPP conditions as boundary conditions, allowed the Higgs mass spectrum to be calculated as a function of the mass of the pseudo-scalar. The couplings of the lightest Higgs to top quarks and weak bosons were also found. The mass of the lightest Higgs tends to be below the LEP bounds when the MPP scale is taken to be the Planck scale ($\approx 1.22 \times 10^{19}$ GeV) although one-loop corrections to the scalar masses are large so this does not rule out the Planck scale MPP scenario.

The most interesting scenario is if the MPP scale is low. In this case the couplings of the lightest Higgs can be substantially modified. Taking the MPP scale to be 10 TeV the coupling of the light Higgs to the top quark is enhanced by 25% or more.

Appendix A

2 Higgs Doublet Model β Functions

The renormalisation group equations describing the evolution of the Higgs self-couplings in a 2 Higgs doublet model are presented below. Here, the definition of the beta functions are

$$\beta_{\lambda_i} = \frac{d\lambda_i}{dt} \tag{1}$$

where $i = 1..7$ and t is defined to be $\ln \mu$ where μ is the renormalization scale.

All Yukawa couplings other than those of the third generation are neglected. Also, λ_6 and λ_7 are taken to be zero since this will always be the case in this thesis. The renormalization group equations are

$$\begin{aligned}
\beta_{\lambda_1} &= \frac{1}{16\pi^2}[12\lambda_1^2 + 4\lambda_3^2 + 4\lambda_3\lambda_4 + 2\lambda_4^2 + 2|\lambda_5|^2 + \frac{9}{4}g_2^4 + \frac{3}{2}g_2^2g_1^2 + \frac{3}{4}g_1^4 \\
&\quad -\lambda_1(3(3g_2^2 + g_1^2) - 12|h_b|^2 - 4|h_\tau|^2) - 12|h_b|^4 - 4|h_\tau|^4] \\
\beta_{\lambda_2} &= \frac{1}{16\pi^2}[12\lambda_2^2 + 4\lambda_3^2 + 4\lambda_3\lambda_4 + 2\lambda_4^2 + 2|\lambda_5|^2 + \frac{9}{4}g_2^4 + \frac{3}{2}g_2^2g_1^2 + \frac{3}{4}g_1^4 \\
&\quad -\lambda_2(3(3g_2^2 + g_1^2) - 12|h_t|^2 - 12|g_b|^2 - 4|g_\tau|^2) - 12|h_t|^4 - 12|g_b|^4 - 4|g_\tau|^4] \\
\beta_{\lambda_3} &= \frac{1}{16\pi^2}[2(\lambda_1 + \lambda_2)(3\lambda_3 + \lambda_4) + 4\lambda_3^2 + 2\lambda_4^2 + 2|\lambda_5|^2 + \frac{9}{4}g_2^4 + \frac{3}{2}g_2^2g_1^2 + \frac{3}{4}g_1^4 \\
&\quad -\lambda_3(3(3g_2^2 + g_1^2) - 6|h_t|^2 - 6|g_b|^2 - 2|g_\tau|^2 - 6|h_b|^2 - 2|h_\tau|^2) - 12|h_t|^2|h_b|^2 \\
&\quad -12|h_b|^2|g_b|^2 - 4|h_\tau|^2|g_\tau|^2] \\
\beta_{\lambda_4} &= \frac{1}{16\pi^2}[2\lambda_4(\lambda_1 + \lambda_2 + 4\lambda_3 + 2\lambda_4) + 8|\lambda_5|^2 + 3g_2^2g_1^2 - \lambda_4(3(3g_2^2 + g_1^2) \\
&\quad -6|h_t|^2 - 6|g_b|^2 - 2|g_\tau|^2 - 6|h_b|^2 - 2|h_\tau|^2) + 12|h_t|^2|h_b|^2 - 12|h_b|^2|g_b|^2 \\
&\quad -4|h_\tau|^2|g_\tau|^2] \\
\beta_{\lambda_5} &= \frac{1}{16\pi^2}[2\lambda_5(\lambda_1 + \lambda_2 + 4\lambda_3 + 6\lambda_4) - \lambda_5(3(3g_2^2 + g_1^2) - 6|h_t|^2 - 6|g_b|^2 \\
&\quad -2|g_\tau|^2 - 6|h_b|^2 - 2|h_\tau|^2) - 12h_b^2g_b^{*2} - 4h_\tau^2g_\tau^{*2}] \\
\beta_{\lambda_6} &= \frac{1}{16\pi^2}[(\lambda_1 + \lambda_3 + \lambda_4)(3g_b^*h_b + h_\tau g_\tau^*) + \lambda_5(3h_b^*g_b + h_\tau^*g_\tau) - 12|h_b|^2h_bg_b^* \\
&\quad -4|h_\tau|^2h_\tau g_\tau^*] \\
\beta_{\lambda_7} &= \frac{1}{16\pi^2}[(\lambda_1 + \lambda_3 + \lambda_4)(3g_b^*h_b + h_\tau g_\tau^*) + \lambda_5(3h_b^*g_b + h_\tau^*g_\tau) - 12|g_b|^2h_bg_b^* \\
&\quad -4|g_\tau|^2h_\tau g_\tau^*]
\end{aligned} \tag{2}$$

The renormalization group equations for the Yukawa couplings will also be required. These are given by

$$
\begin{aligned}
\frac{dg_t}{dt} &= \frac{1}{16\pi^2}[g_t(\frac{9}{2}|g_t|^2+\frac{9}{2}|h_t|^2+\frac{3}{2}|h_b|^2+\frac{1}{2}|g_b|^2+|h_\tau|^2)+h_t(g_b h_b^*+g_\tau h_\tau^*) \\
&\quad -g_t(8g_3^2+\frac{9}{4}g_2^2+\frac{17}{12}g_1^2)] \\
\frac{dh_t}{dt} &= \frac{1}{16\pi^2}[h_t(\frac{9}{2}|g_t|^2+\frac{9}{2}|h_t|^2+\frac{1}{2}|h_b|^2+\frac{3}{2}|g_b|^2+|g_\tau|^2)+g_t(h_b g_b^*+h_\tau g_\tau^*) \\
&\quad -h_t(8g_3^2+\frac{9}{4}g_2^2+\frac{17}{12}g_1^2)] \\
\frac{dg_b}{dt} &= \frac{1}{16\pi^2}[g_b(\frac{1}{2}|g_t|^2+\frac{3}{2}|h_t|^2+\frac{9}{2}|h_b|^2+\frac{9}{2}|g_b|^2+|g_\tau|^2)+h_b(g_t h_t^*+g_\tau h_\tau^*) \\
&\quad -g_b(8g_3^2+\frac{9}{4}g_2^2+\frac{5}{12}g_1^2)] \qquad (3) \\
\frac{dh_b}{dt} &= \frac{1}{16\pi^2}[h_b(\frac{3}{2}|g_t|^2+\frac{1}{2}|h_t|^2+\frac{9}{2}|h_b|^2+\frac{9}{2}|g_b|^2+|h_\tau|^2)+g_b(h_t g_t^*+h_\tau g_\tau^*) \\
&\quad -h_b(8g_3^2+\frac{9}{4}g_2^2+\frac{5}{12}g_1^2)] \\
\frac{dg_\tau}{dt} &= \frac{1}{16\pi^2}[g_\tau(3|h_t|^2+3|g_b|^2+\frac{5}{2}|h_\tau|^2+\frac{5}{2}|g_\tau|^2)+3h_\tau(g_b h_b^*+g_t h_t^*) \\
&\quad -g_\tau(\frac{9}{4}g_2^2+\frac{15}{4}g_1^2)] \\
\frac{dh_\tau}{dt} &= \frac{1}{16\pi^2}[h_\tau(3|g_t|^2+3|h_b|^2+\frac{5}{2}|h_\tau|^2+\frac{5}{2}|g_\tau|^2)+3g_\tau(h_b g_b^*+h_t g_t^*) \\
&\quad -h_\tau(\frac{9}{4}g_2^2+\frac{15}{4}g_1^2)]
\end{aligned}
$$

Bibliography

[1] C. D. Froggatt, R. Nevzorov, H. B. Nielsen and D. Thompson, Phys. Lett. B **657** (2007) 95 [arXiv:0708.2903 [hep-ph]].

[2] W. M.Yao *et al,* J. Phys. G **33** (2006) and 2007 partial update for the 2008 edition

[3] J. F. Gunion, H. E. Haber, G. L. Kane and S. Dawson,

[4] http://lepewwg.web.cern.ch/LEPEWWG/

[5] G. F. Giudice, Int. J. Mod. Phys. A **19** (2004) 835 [arXiv:hep-ph/0311344].

[6] M. Schmaltz, Nucl. Phys. Proc. Suppl. **117** (2003) 40 [arXiv:hep-ph/0210415].

[7] N. Arkani-Hamed, A. G. Cohen and H. Georgi, Phys. Lett. B **513** (2001) 232 [arXiv:hep-ph/0105239].

[8] N. Arkani-Hamed, A. G. Cohen, E. Katz and A. E. Nelson, JHEP **0207** (2002) 034 [arXiv:hep-ph/0206021].

[9] N. Arkani-Hamed, A. G. Cohen, E. Katz, A. E. Nelson, T. Gregoire and J. G. Wacker, JHEP **0208** (2002) 021 [arXiv:hep-ph/0206020].

[10] N. Arkani-Hamed, A. G. Cohen, T. Gregoire and J. G. Wacker, JHEP **0208** (2002) 020 [arXiv:hep-ph/0202089].

[11] I. Low, W. Skiba and D. Smith, Phys. Rev. D **66** (2002) 072001 [arXiv:hep-ph/0207243].

[12] W. Skiba and J. Terning, Phys. Rev. D **68** (2003) 075001 [arXiv:hep-ph/0305302].

[13] S. Chang and J. G. Wacker, Phys. Rev. D **69** (2004) 035002 [arXiv:hep-ph/0303001].

[14] S. Chang, JHEP **0312** (2003) 057 [arXiv:hep-ph/0306034].

[15] M. Schmaltz, JHEP **0408** (2004) 056 [arXiv:hep-ph/0407143].

[16] D. E. Kaplan and M. Schmaltz, JHEP **0310** (2003) 039 [arXiv:hep-ph/0302049].

[17] H. C. Cheng and I. Low, JHEP **0309** (2003) 051 [arXiv:hep-ph/0308199].

[18] H. C. Cheng and I. Low, JHEP **0408** (2004) 061 [arXiv:hep-ph/0405243].

[19] E. Katz, J. y. Lee, A. E. Nelson and D. G. E. Walker, JHEP **0510** (2005) 088 [arXiv:hep-ph/0312287].

[20] D. E. Kaplan, M. Schmaltz and W. Skiba, Phys. Rev. D **70** (2004) 075009 [arXiv:hep-ph/0405257].

[21] M. Schmaltz and D. Tucker-Smith, Ann. Rev. Nucl. Part. Sci. **55** (2005) 229 [arXiv:hep-ph/0502182].

[22] T. Han, H. E. Logan and L. T. Wang, JHEP **0601** (2006) 099 [arXiv:hep-ph/0506313].

[23] M. Perelstein, Prog. Part. Nucl. Phys. **58** (2007) 247 [arXiv:hep-ph/0512128].

[24] D. L. Bennett, C. D. Froggatt and H. B. Nielsen, arXiv:hep-ph/9504294.

[25] D. L. Bennett, C. D. Froggatt and H. B. Nielsen, 28th International Symposium on Particle Theory, proceedings (1994)

[26] C. D. Froggatt and H. B. Nielsen, arXiv:hep-ph/9607302.

[27] N. Cabibbo, Phys. Rev. Lett. **10** (1963) 531.

[28] M. Kobayashi and T. Maskawa, Prog. Theor. Phys. **49** (1973) 652.

[29] C. Froggatt, L. Laperashvili, R. Nevzorov and H. B. Nielsen, Phys. Atom. Nucl. **67** (2004) 582 [Yad. Fiz. **67** (2004) 601] [arXiv:hep-ph/0310127].

[30] H. Georgi and S. Weinberg, Phys. Rev. D **17** (1978) 275.

[31] M. A. Luty, Phys. Rev. D **57** (1998) 1531 [arXiv:hep-ph/9706235].

[32] S. R. Coleman and E. Weinberg, Phys. Rev. D **7** (1973) 1888.

[33] T. Han, H. E. Logan, B. McElrath and L. T. Wang, Phys. Rev. D **67** (2003) 095004 [arXiv:hep-ph/0301040].

[34] T. Han, H. E. Logan, B. McElrath and L. T. Wang, Phys. Lett. B **563** (2003) 191 [Erratum-ibid. B **603** (2004) 257] [arXiv:hep-ph/0302188].

[35] J. J. Liu, W. G. Ma, G. Li, R. Y. Zhang and H. S. Hou, Phys. Rev. D **70** (2004) 015001 [arXiv:hep-ph/0404171].

[36] G. Marandella, C. Schappacher and A. Strumia, Phys. Rev. D **72** (2005) 035014 [arXiv:hep-ph/0502096].

[37] R. Barbieri, A. Pomarol, R. Rattazzi and A. Strumia, Nucl. Phys. B **703** (2004) 127 [arXiv:hep-ph/0405040].

[38] Z. Han and W. Skiba, Phys. Rev. D **72** (2005) 035005 [arXiv:hep-ph/0506206].

[39] C. Csaki, J. Hubisz, G. D. Kribs, P. Meade and J. Terning, Phys. Rev. D **67** (2003) 115002 [arXiv:hep-ph/0211124].

[40] M. C. Chen and S. Dawson, Phys. Rev. D **70** (2004) 015003 [arXiv:hep-ph/0311032].

[41] M. Perelstein, M. E. Peskin and A. Pierce, Phys. Rev. D **69** (2004) 075002 [arXiv:hep-ph/0310039].

[42] C. Csaki, J. Hubisz, G. D. Kribs, P. Meade and J. Terning, Phys. Rev. D **68** (2003) 035009 [arXiv:hep-ph/0303236].

[43] O. C. W. Kong, arXiv:hep-ph/0307250.

[44] T. Hahn, S. Heinemeyer, F. Maltoni, G. Weiglein and S. Willenbrock, arXiv:hep-ph/0607308.

[45] K. Monig and A. Rosca, arXiv:0705.1259 [hep-ph].

[46] F. Wilczek, Phys. Rev. Lett. **39** (1977) 1304

[47] H. M. Georgi, S. L. Glashow,M. E. Machacek and D. V. Nanopoulos Phys. Rev. Lett. **40** (1978) 692

[48] J. R. Ellis, M. K. Gaillard, D. V. Nanopoulos and C. T. Sachrajda, Phys. Lett. B **83** (1979) 339

[49] T. G. Rizzo, Phys. Rev. D **22** (1980) 178

[50] D. Graudenz, M. Spira, P. M. Zerwas Phys. Rev. Lett. **70** (1993) 1372

[51] R. V. Harlander and W. B. Kilgore, Phys. Rev. Lett. **88** (2002) 201801 [arXiv:hep-ph/0201206].

[52] V. Ravindran, J. Smith and W. L. van Neerven, Nucl. Phys. B **665** (2003) 325 [arXiv:hep-ph/0302135].

[53] S. Moch and A. Vogt, Phys. Lett. B **631** (2005) 48 [arXiv:hep-ph/0508265].

[54] V. Ravindran, Nucl. Phys. B **752** (2006) 173 [arXiv:hep-ph/0603041].

[55] K. G. Chetyrkin, B. A. Kniehl and M. Steinhauser, Phys. Rev. Lett. **79** (1997) 353 [arXiv:hep-ph/9705240].

[56] P. A. Baikov and K. G. Chetyrkin, Phys. Rev. Lett. **97** (2006) 061803 [arXiv:hep-ph/0604194].

[57] M. A. Shifman, A. I. Vainshtein, M. B. Voloshin and V. I. Zakharov, Sov. J. Nucl. Phys. **30**, 711 (1979) [Yad. Fiz. **30**, 1368 (1979)].

[58] L. b. Okun, *Amsterdam, Netherlands: North-holland (1982) 361p*

[59] M. B. Gavela, G. Girardi, C. Malleville and P. Sorba, Nucl. Phys. B **193** (1981) 257.

[60] G. Passarino, C. Sturm and S. Uccirati, Phys. Lett. B **655** (2007) 298 [arXiv:0707.1401 [hep-ph]].

[61] M. Steinhauser, arXiv:hep-ph/9612395.

[62] B. Badelek *et al.* [ECFA/DESY Photon Collider Working Group], Int. J. Mod. Phys. A **19** (2004) 5097 [arXiv:hep-ex/0108012].

[63] U. Aglietti, R. Bonciani, G. Degrassi and A. Vicini, Phys. Lett. B **595** (2004) 432 [arXiv:hep-ph/0404071].

[64] F. Fugel, B. A. Kniehl and M. Steinhauser, Nucl. Phys. B **702** (2004) 333 [arXiv:hep-ph/0405232].

[65] D. Zeppenfeld, R. Kinnunen, A. Nikitenko and E. Richter-Was, Phys. Rev. D **62** (2000) 013009 [arXiv:hep-ph/0002036].

[66] M. Duhrssen, S. Heinemeyer, H. Logan, D. Rainwater, G. Weiglein and D. Zeppenfeld, arXiv:hep-ph/0407190.

[67] A. Belyaev and L. Reina, JHEP **0208** (2002) 041 [arXiv:hep-ph/0205270].

[68] D. Zeppenfeld, in *Proc. of the APS/DPF/DPB Summer Study on the Future of Particle Physics (Snowmass 2001)* ed. N. Graf, *In the Proceedings of APS / DPF / DPB Summer Study on the Future of Particle Physics (Snowmass 2001), Snowmass, Colorado, 30 Jun - 21 Jul 2001, pp P123* [arXiv:hep-ph/0203123].

[69] A. Rosca and K. Monig, arXiv:hep-ph/0310036.

[70] E. Boos, J. C. Brient, D. W. Reid, H. J. Schreiber and R. Shanidze, Eur. Phys. J. C **19** (2001) 455 [arXiv:hep-ph/0011366].

[71] J. A. Aguilar-Saavedra *et al.* [ECFA/DESY LC Physics Working Group], arXiv:hep-ph/0106315.

[72] M. Battaglia, arXiv:hep-ph/9910271.

[73] T. Abe *et al.* [American Linear Collider Working Group], in *Proc. of the APS/DPF/DPB Summer Study on the Future of Particle Physics (Snowmass 2001)* ed. N. Graf, arXiv:hep-ex/0106056.

[74] H. E. Logan, arXiv:hep-ph/0409004.

[75] T. Binoth, S. Karg, N. Kauer and R. Ruckl, Phys. Rev. D **74** (2006) 113008 [arXiv:hep-ph/0608057].

[76] E. W. N. Glover and J. J. van der Bij, Nucl. Phys. B **309** (1988) 282.

[77] S. Dawson, S. Dittmaier and M. Spira, Phys. Rev. D **58** (1998) 115012 [arXiv:hep-ph/9805244].

[78] P. Nogueira, J. Comput. Phys. **105** (1993) 279.

[79] J. A. M. Vermaseren, arXiv:math-ph/0010025.

[80] R. Kleiss and W. J. Stirling, Nucl. Phys. B **262** (1985) 235.

[81] Z. Xu, D. H. Zhang and L. Chang, Nucl. Phys. B **291** (1987) 392.

[82] T. Hahn, Nucl. Phys. Proc. Suppl. **89** (2000) 231 [arXiv:hep-ph/0005029].

[83] A. D. Martin, R. G. Roberts, W. J. Stirling and R. S. Thorne, Eur. Phys. J. C **28** (2003) 455 [arXiv:hep-ph/0211080].

[84] http://hepforge.cedar.ac.uk/lhapdf/

[85] http://minami-home.kek.jp/

[86] G. Passarino and M. J. G. Veltman, Nucl. Phys. B **160** (1979) 151.

[87] D. Miller, PhD Thesis, University of Durham.

[88] T. Binoth, J. P. Guillet, G. Heinrich, E. Pilon and C. Schubert, JHEP **0510** (2005) 015 [arXiv:hep-ph/0504267].

[89] M. Spira, arXiv:hep-ph/9703355.

[90] F. Jegerlehner, Eur. Phys. J. C **18** (2001) 673 [arXiv:hep-th/0005255].

[91] C. O. Dib, R. Rosenfeld and A. Zerwekh, AIP Conf. Proc. **815** (2006) 296 [arXiv:hep-ph/0509013].

[92] C. O. Dib, R. Rosenfeld and A. Zerwekh, JHEP **0605** (2006) 074 [arXiv:hep-ph/0509179].

[93] U. Baur, T. Plehn and D. L. Rainwater, Phys. Rev. D **68** (2003) 033001 [arXiv:hep-ph/0304015].

[94] U. Baur, T. Plehn and D. L. Rainwater, Phys. Rev. D **69** (2004) 053004 [arXiv:hep-ph/0310056].

[95] A. Pierce, J. Thaler and L. T. Wang, JHEP **0705** (2007) 070 [arXiv:hep-ph/0609049].

[96] U. Baur, T. Plehn and D. L. Rainwater, Phys. Rev. D **67** (2003) 033003 [arXiv:hep-ph/0211224].

[97] F. Gianotti *et al.*, Eur. Phys. J. C **39** (2005) 293 [arXiv:hep-ph/0204087].

[98] M. Sher, Phys. Rept. **179** (1989) 273.

[99] S. Weinberg, Phys. Rev. Lett. **40** (1978) 223.

[100] F. Wilczek, Phys. Rev. Lett. **40** (1978) 279.

[101] G. 't Hooft, Phys. Rev. Lett. **37** (1976) 8.

[102] R. Jackiw and C. Rebbi, Phys. Rev. Lett. **37** (1976) 172.

[103] C. G. . Callan, R. F. Dashen and D. J. Gross, Phys. Lett. B **63** (1976) 334.

[104] R. Tarrach, Nucl. Phys. B **183** (1981) 384.

[105] N. Gray, D. J. Broadhurst, W. Grafe and K. Schilcher, Z. Phys. C **48** (1990) 673.

[106] E. Brubaker *et al.* [Tevatron Electroweak Working Group], arXiv:hep-ex/0608032.

[107] R. B. Nevzorov and M. A. Trusov, Phys. Atom. Nucl. **64** (2001) 1299 [Yad. Fiz. **64** (2001) 1375] [arXiv:hep-ph/0110363].

[108] R. B. Nevzorov and M. A. Trusov, Phys. Atom. Nucl. **65** (2002) 335 [Yad. Fiz. **65** (2002) 359] [arXiv:hep-ph/0301179].

[109] R. B. Nevzorov, K. A. Ter-Martirosyan and M. A. Trusov, arXiv:hep-ph/0301068.

[110] R. Nevzorov and D. J. Miller, arXiv:hep-ph/0411275.

[111] M. S. Carena and H. E. Haber, Prog. Part. Nucl. Phys. **50** (2003) 63 [arXiv:hep-ph/0208209].

[112] P. Gambino and M. Misiak, Nucl. Phys. B **611** (2001) 338 [arXiv:hep-ph/0104034].

[113] R. Barate *et al.* [LEP Working Group for Higgs boson searches], Phys. Lett. B **565** (2003) 61 [arXiv:hep-ex/0306033].